THE EFFECT OF OBESITY AND HIGH FAT DIET ON CARDIOVASCULAR RISK AND INTESTINAL DRUG METABOLISM

A DISSERTATION
SUBMITTED TO THE FACULTY OF
UNIVERSITY OF MINNESOTA
BY

Harrison Kin Chi Tam

IN PARTIAL FULFILLMENT OF THE REQUIREMENTS
FOR THE DEGREE OF
DOCTOR OF PHILOSOPHY

Adviser: L'Aurelle Johnson PhD

January 2015

Acknowledgements

This thesis would not have been possible without the support and work of a multitude of people both within the College of Pharmacy at the University of Minnesota and collaborators outside of the college. I am particularly grateful for my advisor, Dr. L'Aurelle Johnson. The constructive suggestions and time dedicated to all phases of the research presented in this thesis was invaluable and is very much appreciated. I would also like to thank my committee members, Dr. Rory Remmel, Dr. Aaron Kelly, and Dr. Robert Straka for all of the support, knowledge, and mentorship that they have provided me. I would also like to extend my thanks to everyone that contributed to my research and my growth as an academic and as an individual. Finally, I wish to thank all of my friends and family for their support and encouragement throughout my time working on this thesis.

Dedication

This thesis is dedicated my family, my friends, and everyone in the Department of Experimental and Clinical Pharmacology in the College of Pharmacy at the University of Minnesota.

Abstract

Introduction: Childhood obesity is a major epidemic for many industrialized countries, especially in countries where a high fat diet is prevalent. The purpose of this thesis was to examine the effect of obesity and high fat diet on cardiovascular risk factors (e.g. xanthine oxidase activity and uric acid formation) and on small intestinal drug metabolism.

Methods: An assay measuring the production of 7-hydroxy-lumazine was developed as a probe for xanthine oxidase activity. This lumazine assay was used to study xanthine oxidase as a risk factor for cardiovascular disease in obese children compared to normal-weight children, and this assay was also utilized to study xanthine oxidase activity in obese adolescents before and after weight loss to determine xanthine oxidase's role in mediating changes in blood pressure due to weight loss. In order to study the effects of obesity and high fat diet on small intestinal drug metabolism, UGT activity was assessed in a rat model of diet-induced obesity using in vitro phenotyping methodologies.

Results: Plasma xanthine oxidase activity was increased in obese children and was associated with BMI z-score and waist circumference, but was not associated with blood pressure. Weight loss via meal replacement therapy led to decreases in both uric acid production and excretion, but no significant change in plasma levels. Increases in UGT activity were observed in both obesity resistant and obesity prone rats when they were fed a high fat diet, even though the obesity resistant rats didn't gain a significant amount of weight when fed a high fat diet.

Conclusions: Changes in xanthine oxidase activity and intestinal UGT activity may be due to changes to diets and gut microbiota. High fat diets have been shown to alter the gut microbiota and increase plasma LPS levels. Therefore, a high fat diet and not obesity may be responsible for both the changes in xanthine oxidase and UGT activities, and future studies on obesity and CVD risk or alterations in drug metabolizing enzymes should focus on monitoring diets and changes to the gut microbiota.

Table of Contents

List of Tables

List of Figures

Chapter I

Literature Review

1.1 Childhood Obesity

1.1.1 Prevalence and definition of childhood obesity:

Childhood obesity is a major epidemic for many industrialized countries. As shown in **Figure 1.1,** childhood obesity in the United States has tripled over the last 3 decades to a rate of 18%.[1] In children, obesity is defined differently as compared to obesity in adults. In adults, cut-off values for body mass index (BMI), a ratio of the weight (kg) to the height (m^2), are used to define obesity. Using these cut-off values, adults are classified as normal weight, overweight, or obese (class I-III) according to cut-off values shown in **Table 1.1**. On the other hand, obesity in children is defined by the percentile of a child's BMI. A child or adolescent (ages 2-18 years old) is considered overweight if they are between the 85^{th} and 95^{th} percentile for children of the same age and sex, and a child is considered obese if they are at or above the 95^{th} percentile for children of the same age and sex. A chart that is used to calculate the percentile in boys is shown in **Figure 1.2**.

Table 1.1 Classification of Obesity in Adults:

BMI	Obesity Classification
19 - 24.9	Normal
25 – 29.9	Overweight
30 – 34.9	Class I Obesity
35 – 39.9	Class II Obesity
40 +	Class III Obesity

Figure 1.1 Trends in Obesity Among Children and Adolescents: United States, 1963-2008

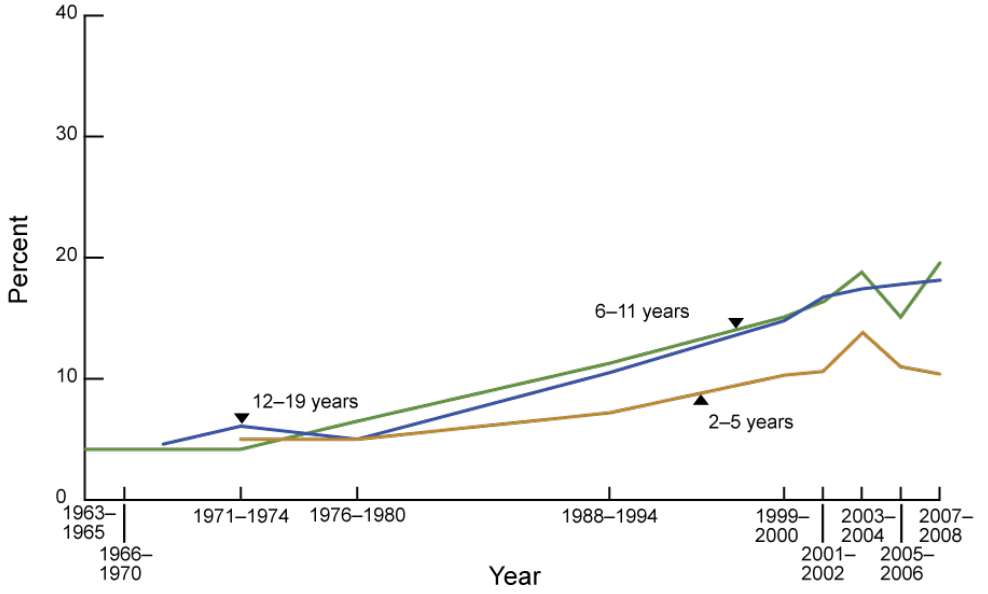

NOTE: Obesity is defined as body mass index (BMI) greater than or equal to sex- and age-specific 95th percentile from the 2000 CDC Growth Charts.
SOURCES: CDC/NCHS, National Health Examination Surveys II (ages 6–11), III (ages 12–17), and National Health and Nutrition Examination Surveys (NHANES) I–III, and NHANES 1999–2000, 2001–2002, 2003–2004, 2005–2006, and 2007–2008.

Figure 1.2 BMI-for-Age Percentiles in Boys Ages 2-20 Years Old

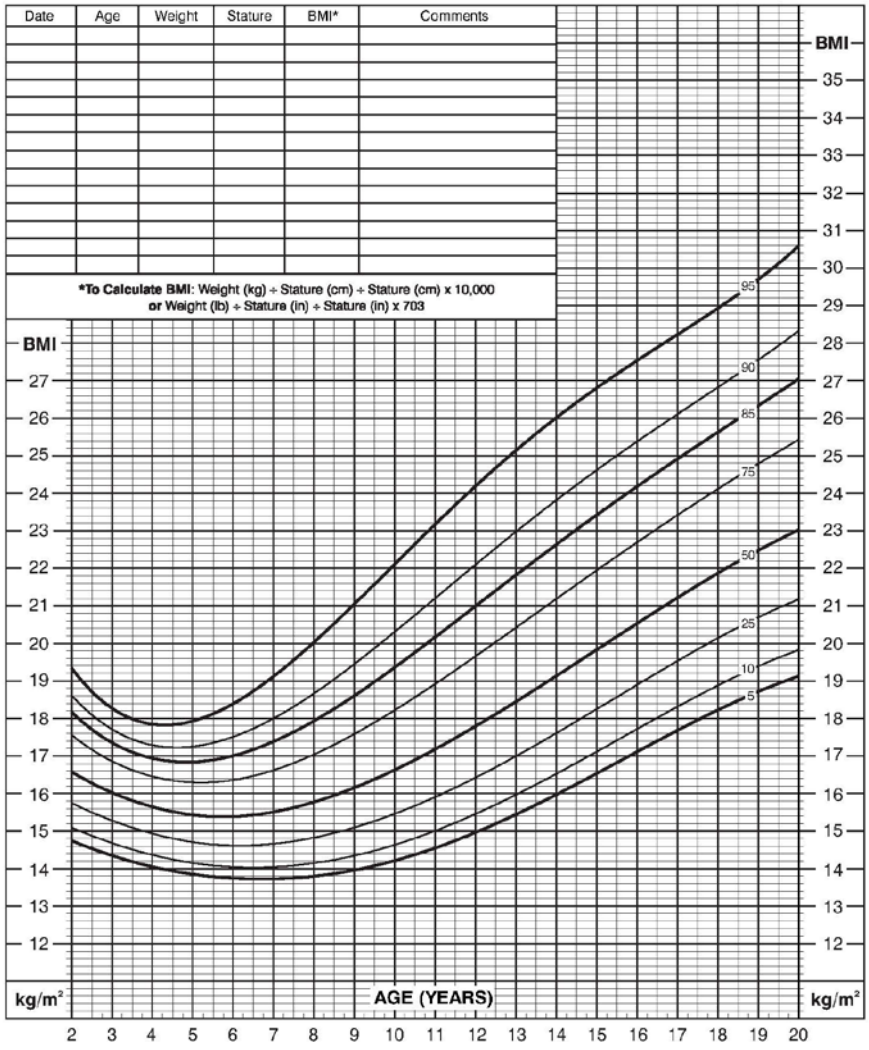

Published May 30, 2000 (modified 10/16/00).
SOURCE: Developed by the National Center for Health Statistics in collaboration with the National Center for Chronic Disease Prevention and Health Promotion (2000).
http://www.cdc.gov/growthcharts

SAFER • HEALTHIER • PEOPLE™

1.1.2 Environmental causes of obesity:

In general terms, the cause of obesity childhood obesity is an imbalance in caloric consumption and insufficient amount of energy expenditure; which ultimately leads to increased accumulation of fat or white adipose tissue. Even though the cause of obesity is relatively simple, many factors influence the accumulation of body fat including various environmental and genetic factors. Schools, communities, and homes are all environments that influence what children eat and the amount of physical activity they participate in. Schools have a major influence on what children eat because most students drink beverages and eat meals and snacks while in school, and over half of middle and high schools in the U.S. offer less healthy foods that are high in fat or calories and beverages that are high in sugar for purchase in vending machines, at school canteens, and at events.[2] Schools also impact a child's physical activity via their physical education classes, which are important for providing physical activity to children and adolescents. However, reports on the physical activity habits of children and adolescents in 2007 and 2009 (from the Centers for Disease Control and Prevention and the Department of Health and Human Services) reported that only 33% of students in the U.S. attended daily physical education classes and more than 80% of students in grades 9-12 had less than 60 minutes of physical activity each day. [3,4] In addition to schools as a factor influencing childhood obesity, modern technology and social media negatively impact the obesity epidemic by specifically targeting children and adolescents with advertisements and marketing of unhealthy foods that are low in nutrients and high in calories, fat, sugar, and salt.[5] Television viewing not only increases exposure to advertisements of unhealthy

foods, it also contributes as a factor for childhood obesity by decreasing the amount of time a child can spend doing physical activities and increasing food intake through snacking and eating meals in front of the television.[6,7] Lastly, geographical communities have a large influence on childhood obesity; for example a community with access to a supermarket has reduced risk for obesity as compared to communities without access. Specifically, families that live in rural, minority, or low-income communities have little to no access to supermarkets that sell fruits, vegetables, and other affordable and healthy foods which results in increased risk of obesity in these communities.[8] The aforementioned environmental factors influence obesity to varying degrees and these factors may be very hard to target to improve the health of children, but nonetheless these factors must be taken into consideration when conducting research on childhood obesity.

1.1.3 Genetic causes of obesity:

In addition to the multiple environmental factors that affect obesity, genetics also play a role in childhood obesity. Single nucleotide polymorphisms (SNPs) have been found by genome-wide association studies to increase an individual's risk for obesity and are associated with either monogenic or polygenic obesity via satiety signaling pathways; the most significant SNPs include those found in fat mass and obesity associated gene (*FTO*) and melanocortin 4 receptor (*MC4R*).[9] These two genes are involved in hormonal regulation of appetite (**Figure 1.3)**. The arcuate nucleus of the hypothalamus is the major site for neuronal signaling for appetite regulating hormones and it is composed of two types of neurons. The neurons that express proopiomelanocortin (POMC) and cocaine- and amphetamine-regulated transcript (CART) are responsible for the anorexigenic

signaling. POMC is precursor protein that is processed in to alpha, beta, and gamma melanocortins (also known as melanocyte stimulating hormones or MSH) and lipotropins. These anorexic neurons are activated by peptides leptin and glucagon-like peptide-1 (GLP-1) which leads to the release of alpha-melanocyte stimulating hormone (α-MSH). α-MSH then binds to and activates MC4R on downstream secondary neurons in the paraventricular nucleus (PVN) that express thyrotropin-releasing hormone (TRH) and corticotropin-releasing hormone (CRH) which mediate the downstream anorexigenic effect. In addition to modulating the anorexigenic signaling, leptin and GLP-1 also inhibit orexigenic (increases appetite) signaling by inhibiting neurons in the lateral hypothalamic area (LHA) of the hypothalamus. The neurons responsible for the orexigenic signaling are the neurons that express neuropeptide Y (NPY) and agouti-related peptide (AgRP). These orexigenic neurons are stimulated by ghrelin which leads to the release of neuropeptide-Y (NPY) and the activation of neuropeptide-Y receptors (Y1R). Activation of Y1Rs on neurons in the LHA that express orexin A/B (ORX) and melanin concentrating hormone (MCH) mediates the downstream orexigenic effect. NPY also activates Y1Rs on neurons that express POMC/CART and neurons in the PVN which leads to inhibition of anorexigenic signaling.

The *FTO* gene encodes a 2-oxoglutarate-dependent nucleic acid demethylase that has an uncertain cellular function, but a SNP within the first intron of *FTO* (rs9939609) is strongly associated with BMI in both children and adults.[10-12] The risk allele (A allele) for the SNP in *FTO* is very common and it was found to have an allele frequency of 54 percent.[13] According to Frayling et al., individuals that were homozygous for the A allele

of *FTO* had 1.7-fold increased odds of obesity compared to individuals that were homozygous for the low risk T allele.[11] One possible mechanism of action of this *FTO* SNP's obesity risk is regulation of ghrelin, an orexigenic hormone.[13] The obesity risk allele in *FTO* has been shown to increase ghrelin mRNA and peptide levels which lead to both the inhibition of anorexic signaling and activation of orexigenic signaling.[13]

SNPs in *MC4R* also increase risk for obesity via changes in the hormonal regulation of appetite, and loss of function mutations in *MC4R* are responsible for the majority of monogenic obesity cases.[14] Hyperphagia is a key feature of MC4R deficiency, and this is due to MC4Rs being expressed on neurons in both the PVN and the LHA of the hypothalamus. Subsequent stimulation of these receptors leads to activation of anorexic signaling and inhibition of orexigenic signaling pathways. Even though MC4R plays a major role in appetite suppression, loss of function mutations in *MC4R* do not necessarily lead to obesity. As shown in a longitudinal study by Stutzmann et al., the penetrance of obesity in carriers of *MC4R* mutations is 37% in subjects at 20 year olds, which increases to 60% in subjects as they reach ages >40 years old.[14] This change in penetrance of obesity in *MC4R* mutation carriers over time shows that environmental factors contribute greatly to the development of obesity even in those predisposed to it.

Figure 1.3 Hormonal Regulation of Appetite

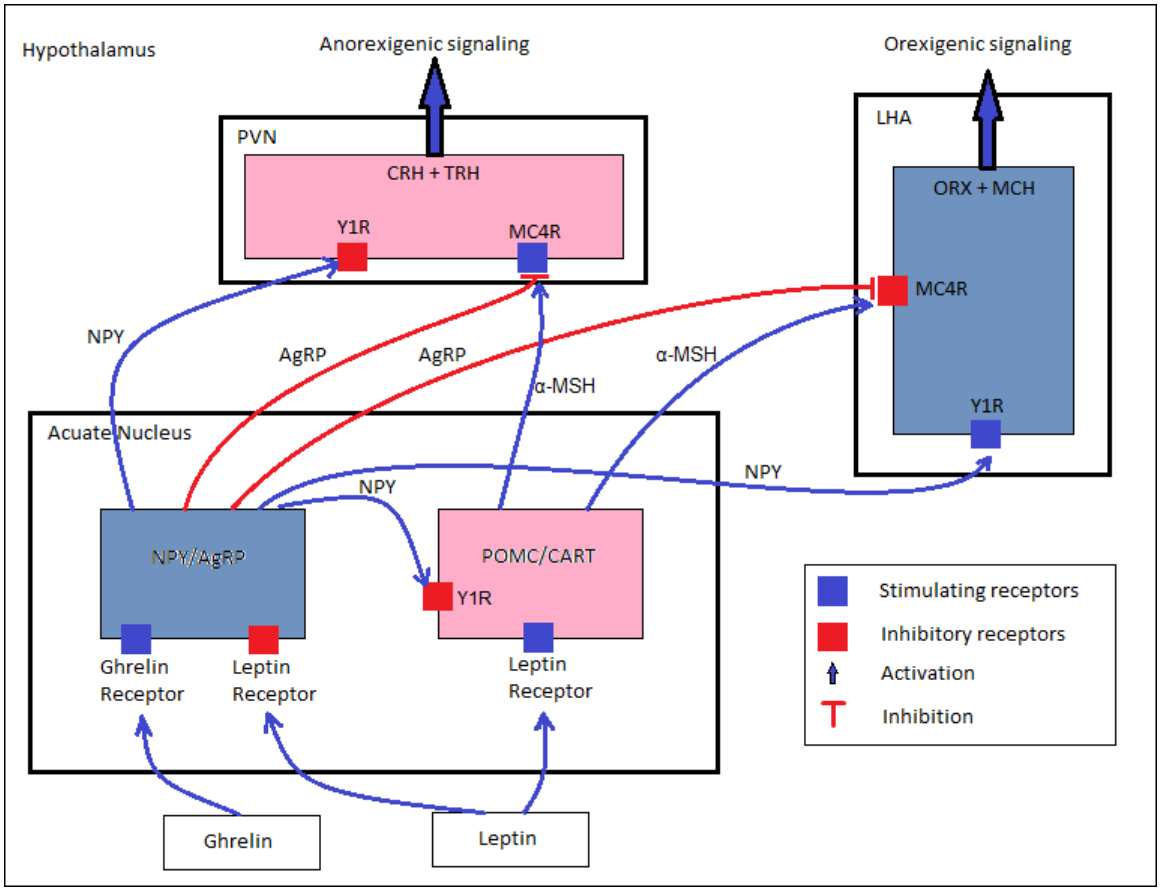

1.1.4 Chronic inflammatory state that occurs in obesity:

Although there are a multitude of factors that influence the cause of obesity, the biological and physical consequences of obesity are relatively consistent. For example, obesity is characterized by an abundance of adipose tissue, increased oxidative stress, and a low-grade systemic inflammation. These changes in biophysical characteristics are due to adipocytes secreting various inflammatory cytokines and adipokines. There are two major types of adipose tissue: white adipose tissue (WAT) and brown adipose tissue, however, obesity is characterized only by the increase in the former. WAT is the major depot for energy storage and it is made up of adipocytes, endothelial cells, fibroblasts, leukocytes, and macrophages. Adipocytes are the major secretory cells of WAT and the adipokines and inflammatory cytokines that are secreted by WAT include leptin, adiponectin, resistin, interleukin-6 (IL-6), tumor necrosis factor-alpha (TNF-α), and monocyte chemoattractant protein-1 (MCP-1). Because obesity often results in increased amounts of WAT, obese adults and children often have higher levels of adipokines and cytokines (Table 1.2). [15,16]

Adipokines are proteins that are mainly produced by adipocytes. Leptin and adiponectin are examples of adipokines that have been extensively studied in obesity. Leptin's primary role is to suppress appetite via the signaling pathway shown in **Figure 1.3**, and it is positively correlated with adipose tissue mass.[17] Leptin has also been shown to upregulate adhesion molecules and the production of various cytokines such as TNF-α and MCP-1.[15] Leptin is so important in the development of obesity that mutations in the leptin gene or its receptors in animals serve as obesity models for obesity related

research. Adiponectin is primarily produced by adipocytes, but paradoxically its levels do not increase in obesity as compared to leptin. Adiponectin is decreased in obesity and increased in patients with anorexia nervosa.[18,19] Adiponectin has an important role in the regulation of cytokines released by adipocytes. For example, there is feedback inhibition in which TNF-α levels and activity are reduced by adiponectin, but TNF-α also downregulates adiponectin; which would explain why we see both decreased levels of adiponectin and increased TNF-α levels in obesity.[20,21] Adiponectin is also considered to be an anti-inflammatory adipokine due to its inhibition of IL-6 production via inhibition of nuclear factor κB (upstream regulator of inflammation), which would partly explain why the decrease in adiponectin seen in obesity leads to a chronic inflammatory state.[22]

Table 1.2: Plasma levels of Adipokines and Cytokines in obese individuals.[15,16]

Variable	Pediatric		Adult	
	Control (n = 63)	**Obese (n = 63)**	**Control (n = 16)**	**Obese (n = 9)**
Leptin (ng/ml)	7.9 ± 5.1	19.9* ± 7.4	7 ± 3	17 ± 2*
IL - 6 (pg/ml)	13.1 ± 3.9	45.2* ± 11.8	1.2 ± 0.3	2.8 ± 0.5*
TNF - α (pg/ml)	3.9 ± 1	9.2* ± 2.3	8 ± 1	9.2 ± 1.4
Resistin (ng/mL)	12.8 ± 8.3	24.6* ±12.9	6.3 ± 0.8	7.8 ± 0.5*
Adiponectin (μg/mL)	13.3 ± 1.8	8.6* ± 0.8	11 ± 1.8	8.8 ± 1.3

*p-value ≤ 0.05

1.1.5 Physiological changes due to obesity:

In conjunction with inflammation, many physical changes also occur in obesity. The most obvious physical sign of obesity is size; of which, body surface area (BSA) is a unit that is a useful measure to assess size as it increases with weight. The increase in BSA with weight has been accurately estimated in obese individuals using multiple published formulas (with r^2 values between 0.971 and 0.999).[23] It has been observed that obese individuals have increased cardiac output as compared to non-obese individuals. Cardiac output is increased in obesity due to increases in stroke volume and higher heart rates, and cardiac output has been accurately predicted in obese populations when BSA is factored into calculations.[24-26] Cardiac output is an important factor in the renal clearance of drugs because an increase in cardiac output also results in a change in kidney function due to hyperfiltration. This increase in glomerular filtration due to obesity can be accurately predicted in obese adults by various methods such as the modified Cockcroft-Gault method or the Modification of Diet in Renal Disease method; although currently, there are no good prediction equations for estimating kidney function in obese children or adolescents.[27,28] Surprisingly, even though the obese population has increased cardiac output, hepatic and intestinal blood flow have not been shown to differ between lean and obese populations.[28-30]

1.1.6 The effect of obesity on drug metabolism:

The major sites of drug metabolism are the liver and the small intestine, and although blood flow to the liver and intestine are unchanged, obesity has been shown to impact drug metabolism in obese populations.[31] Therefore, changes in the expression or

activity of drug metabolizing enzymes are attributed to these changes in drug metabolism. There is a need to understand the expression and activity of drug metabolizing enzymes in the obese population in order to better predict potential adverse drug reactions, drug clearance, and drug efficacy. The major families of drug metabolizing enzymes are the oxidative cytochrome P450s (CYPs) and the conjugative uridine diphosphate glucuronosyltransferases (UGTs). The minor families of drug metabolizing enzymes are other oxidative enzymes such as xanthine oxidase, (XO), flavin monoxogenases (FMOs), and aldehyde oxidase (AO), and conjugative enzymes such as sulphotransferases, N-acetyltransferases and glutathione S-transferases. The primary role of these enzymes in drug metabolism is to convert xenobiotics to a more polar form so that they can be more easily excreted. In regards to obesity, the expression and activity of CYPs in obese populations has been studied extensively. CYPs catalyze the oxidation of substrates to make substrates more polar and more readily conjugated. The major CYPs that were studied in obese populations are the isoforms CYP1A2, CYP2B6, CYP2C9, CYP2C19, CYP2D6, CYP2E1 and CYP3A4/5. The effect of obesity on CYPs is specific to individual isoforms, with a decrease in CYP3A4 activity, an increase in CYP2E1 activity, and the effect of obesity on isoforms CYP1A2, CYP2B6, CYP2C9, CYP2C19, and CYP2D6 being inconclusive.[31] Various probe substrates have been used to test for changes in CYP3A4 activity in obese individuals and decreases of 10-40% have been reported, while increases of 10-140% have been reported for CYP2E1.[28] The effect of obesity on drug metabolism by CYPs in obese children has not been studied as extensively as adults, but one study comparing obese children and non-

obese children by Chiney et al. reported that there were no differences in the activities of CYP1A2, CYP2D6, or CYP3A4 as determined by the metabolism of caffeine and dextromethorphan.[32]

1.1.7 Drug metabolism by UGTs:

While the effect of obesity on CYPs has been studied extensively, the effects of obesity and high fat diet (HFD) on UGTs and intestinal drug metabolism have been neglected. UGTs catalyze the conjugation of glucuronic acid to substrates from uridine diphosphate in order to make substrates more polar and more readily excreted. In humans, the UGTs are classified into four families: UGT1, UGT2, UGT3 and UGT8, with UGT1 and UGT2 being the most important families in drug metabolism. The UGT1 family consists of UGT1A1, UGT1A3, UGT1A4, UGT1A5, UGT1A6, UGT1A7, UGT1A8, UGT1A9, and UGT1A10. The UGT2 family consists of UGT2A1, UGT 2A2, UGT2A3, UGT2B4, UGT2B7, UGT2B10, UGT2B11, UGT2B15, UGT2B17, and UGT2B28. Transcriptional regulators of UGT expression include the ligand activated nuclear receptors Farsenoid X receptor (FXR), peroxisome proliferator-activated receptor (PPARα), and nuclear factor (erythroid-derived 2)-like 2 (Nrf2). All three of these nuclear receptors have endogenous ligands whose levels are altered in obesity which may lead to changes to expression and activity levels. FXR activation is possibly increased in obesity as unsaturated fatty acids are ligands for FXR, and obesity due to a high fat diet (HFD) may lead to increases in unsaturated fatty acids. Fatty acids are also ligands for PPARα, which may have increased activation due to obesity and a HFD increasing fatty acid levels in the blood. Increases in oxidative stress due to obesity or a HFD also

increases Nrf2 activation, which may lead to changes in the expression of UGTs. Of the various UGT1A and UGT2B family members, the following isoforms are expressed in the small intestine and play an important role on first-pass drug metabolism: UGT1A1, 1A3, 1A4, 1A6, 1A8, 1A9, 1A10, 2B4, 2B7, 2B10, and 2B15. First-pass metabolism of drugs by UGTs in the intestine has been shown to significantly affect drug bioavailability and toxicity, and potential changes in intestinal UGT expression or activity due to obesity or HFD may contribute to the large inter-individual variability that is seen in UGT activity.[33]

1.1.8 Disease and hypertension risk associated with childhood obesity:

Unfortunately, the rise in childhood obesity results in the elevation of concomitant disease risk. Obese children have been shown to have increased risk for high blood pressure, high cholesterol, impaired glucose tolerance, insulin resistance, type II diabetes, breathing problems (eg. sleep apnea and asthma), joint problems, musculokeletal discomfort, fatty liver disease, gallstones, gastro-esophageal reflux, and social and psychological problems when compared to non-obese children.[34-40] Specifically, cardiovascular disease (CVD) is a major health problem associated with obesity. CVD is a class of diseases that involve the vasculature and the heart, such as coronary artery disease, heart disease, or cerebrovascular disease. The majority of CVD is caused by hypertension, atherosclerosis, and/or hyperlipidemia. Freedman and others have demonstrated that obese children have a 70% chance of having at least 1 CVD risk factor and a 39% chance to have 2 CVD risk factors (**Figure 1.4**).[35] These CVD risk factors included elevated triglyceride levels, increased low-density lipoprotein (LDL) cholesterol

levels, decreased high-density lipoprotein (HDL) cholesterol levels, elevated fasting insulin levels, elevated systolic blood pressure (SBP) and diastolic blood pressure (DBP). CVD risk in children and adolescents are also defined differently than adults. For example, adult hypertension or high blood pressure is defined as a having a SBP ≥ 140mm Hg or DBP ≥ 90mm Hg, whereas childhood hypertension is defined as being at ≥95^{th} blood pressure percentiles for a child of the same age, sex, and height. **Table 1.3** defines the cut-off values of pediatric hypertension in children of various ages and height percentiles. Hypertension, in both adults and adolescents, is associated with increased uric acid, and there have been debates over the last few decades about the role uric acid plays in the development of CVD in obesity.

Figure 1.4 Prevalence of CVD Risk Factors Across BMI-for-Age Percentiles[41]

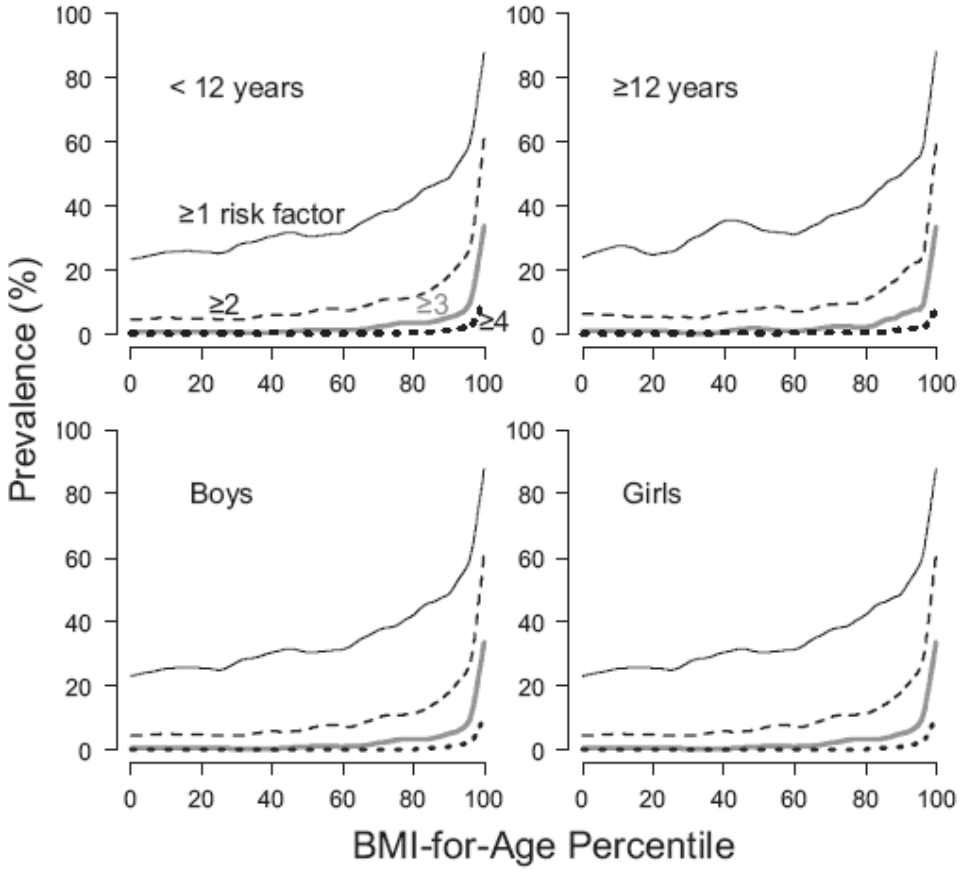

Table 1.3 Cut-off Values for Hypertension in Children and Adolescents

Age, y	95th BP Percentile for Girls, mm Hg		95th BP Percentile for Boys, mm Hg	
	50th Height Percentile	75th Height Percentile	50th Height Percentile	75th Height Percentile
1	104/58	105/59	103/56	104/58
6	111/74	113/74	114/74	115/75
12	123/80	124/81	123/81	125/82
17	129/84	130/85	136/87	138/87

1.1.9 Uric Acid's history as a CVD risk factor:

In addition to the six previously mentioned CVD risk factors, uric acid has long been debated as a CVD risk factor. Uric acid is the final catabolism product of purines in humans, and it is produced from the sequential oxidation of hypoxanthine to xanthine and from xanthine to uric acid. The enzyme responsible for the oxidation of both hypoxanthine and xanthine is xanthine oxidoreductase (XOR). There are two forms of XOR: xanthine oxidase and xanthine dehydrogenase (further information on XOR will be presented in **section 1.2.1 Xanthine oxidoreductase**).[42] Uric acid, which is not further metabolized in humans, is excreted primarily via the kidneys. Uric acid was first hypothesized to be associated with hypertension in the late 1800's, and an increase in the prevalence of hypertension and CVD in obesity could be due to increases in xanthine oxidase activity and plasma uric acid, as it has been shown that uric acid levels increase with obesity. During the past 50 years, over 50 epidemiologic studies have shown that uric acid levels were associated with, hypertension, or CVD risk[43], but most investigators concluded that uric acid was just a surrogate marker for obesity, diabetes, or chronic

kidney disease (CKD) due to two major factors. The first factor was that the link between uric acid and CVD was not always independent of confounding factors such as hypertension, diabetes, or renal disease, and the second factor was that there was no clear physiological mechanism to link uric acid with CVD or hypertension. Many of the confounding factors listed previously develop with age; therefore a way to minimize these confounders is to study the uric acid-CVD relationship in younger populations. The link between uric acid and CVD is particularly strong in young populations; for example, in an evaluation of young adults in the Israeli armed forces, it was shown that those in the highest tertile of uric acid levels had a two-fold increased risk for developing hypertension within five years.[44] Similar results were found across several racial groups, including African Americans[45] and Japanese[46], and a strong link between uric acid and hypertension was also found in children/adolescents[47]. However, in older populations, the uric acid-CVD relationship is more variable and conflicting.[48,49] The decrease in the strength of the uric acid-CVD relationship with age would indicate that a physiological mechanism that links uric acid and CVD likely changes over time in an individual.

1.1.10 Physiological mechanism linking uric acid and hypertension via animal models of mild hyperuricemia:

In order to determine the mechanism linking uric acid to CVD and hypertension, investigators studied hyperuricemia in rats. Unlike humans, where uric acid is the final catabolism product of purines; rats, mice, and other animals have the enzyme uricase, which further metabolizes uric acid to allantoin. Many researchers have induced severe hyperuricemia in animals by feeding them uric acid supplements along with the uricase

inhibitor oxonic acid. For example, Stavric et al. found that supplementing rats with both uric acid and oxonic acid increased serum uric acid levels by 6- to 10-fold, which led to acute renal failure due to obstruction of renal tubules by urate crystals.[50] This model of severe hyperuricemia was useful for studying acute urate nephropathy syndrome observed in cancer patients experiencing tumor lysis syndrome, but this model was inappropriate for studying the chronic damage of milder hyperuricemia seen in the obese population or those with CVD. Mazzali et al. developed a mild hyperuricemia model in rats by feeding them a diet supplemented with 2% oxonic acid without adding any uric acid.[51,52] Mild hyperuricemia (no urate crystal formation in renal tubules) was achieved with a 40-100% increase in serum uric acid in their rats. Mazzali et al. recorded a significant increase in blood pressure after their rats were fed oxonic acid for seven weeks (>30 mm Hg increase) and they also found that there was a significant positive correlation between uric acid levels and systolic blood pressure (SBP), with r=0.75, which was due to the induction of the renin-angiotensin system (RAS) and the inhibition of intrarenal nitric oxide synthase (NOS).[51] The same research group also found that mild hyperuricemia induced renal arteriolopathy by inducing the renin-angiotensin system (RAS), along with interstitial fibrosis, macrophage infiltration, and afferent arteriolar thickening.[51,52]

1.1.11 Drugs used to lower uric acid:

Increases in uric acid levels in obesity may be associated with CVD risk, which makes uric acid a target for pharmacotherapy to reduce an obese individual's risk. Currently, there are three major drugs in the United States that are primarily used to

lower uric acid levels: allopurinol, febuxostat, and probenecid (**Figure 1.5**). Allopurinol is a purine analog that competitively inhibits XO, but the major inhibitory effect can be attributed to allopurinol's active metabolite, oxypurinol. Allopurinol is also metabolized by XO to produce oxypurinol, which acts as an irreversible inhibitor by binding to the molybdopterin active site of XO. Febuxostat is a non-purine selective inhibitor of both XO and XDH. And lastly, probenecid is a uricosuric drug that competitively blocks the reabsorption of uric acid by inhibiting organic anion transporters, including solute carrier family 22 member 12 (SLC22A12 or URAT1).

Figure 1.5 Structures of Urate Reducing Drugs

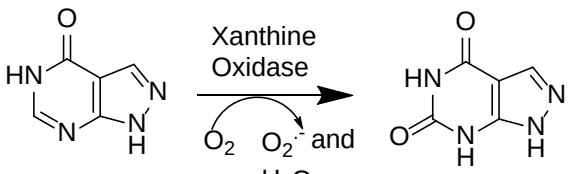

A. Allopurinol Oxipurinol

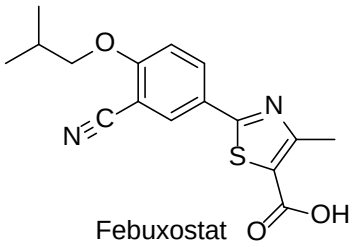

B. Febuxostat

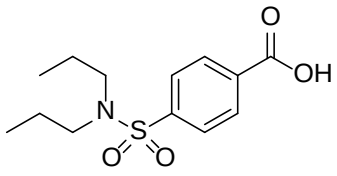

C. Probenecid

1.1.12 Pharmacological interventions in animal models to reverse hypertension and kidney damage due to hyperuricemia:

One method to demonstrate that uric acid is mechanistically linked to CVD and hypertension is to reverse these cardiovascular effects by lowering uric acid using various pharmacological interventions. For example, pharmacological interventions were tested to reverse both hypertension and kidney damage by Mazzali et al. caused by hyperuricemia in their rat model of hyperuricemia.[51,52] Mazzalie et al. reported that reducing uric acid via the inhibition of uric acid production due to the addition of allopurinol (xanthine oxidase inhibitor), or increasing uric acid clearance via the addition of benziodarone (uricosuric agent no longer used in humans) led to normalization of blood pressure in their mild hyperuricemic rat model. Blocking the production of uric acid or increasing its clearance both negated the effect of oxonic acid on blood pressure, which indicates that increased plasma uric acid levels are responsible for the increase in blood pressure seen in hyperuricemic rat models. In addition to modifying uric acid levels, Mazzali et al. also determined the effect of administering enalapril (an angiotensin-converting-enzyme (ACE) inhibitor) or losartan (an angiotensin II receptor blocker). Both enalapril and losartan prevented the increase in blood pressure and damage to the kidneys due to the addition of oxonic acid to the diet; and it can be concluded that the increase in blood pressure and kidney damage from mild hyperuricemia is attributed to the induction of the renin-angiotensin system (RAS).[52] The link between uric acid and hypertension and kidney damage lead to a two-phase mechanism for the modulation of blood pressure.[43] The first phase of blood pressure

modulation is uric acid dependent, whereby uric acid induces the RAS, which leads to acute vasoconstriction and ultimately renal arteriolopathy. The second phase, due to the kidney damage, results in chronic hypertension and is uric acid independent and sodium dependent. This two-phase mechanism explains the discrepancy between uric acid and blood pressure that is observed in a young population versus an older population, and it also explains why uric acid could not be shown to be independent of hypertension or chronic kidney disease (CKD). With a plausible mechanism linking uric acid levels with hypertension, uric acid must be reevaluated as a CVD risk factor.

1.2 Xanthine Oxidoreductase as a Risk Factor for CVD in Obesity

1.2.1 Xanthine oxidoreductase:

With uric acid reestablished as a CVD risk factor, the production of uric acid may be responsible for the increased uric acid levels seen in obesity. Therefore, xanthine oxidoreductase (XOR), the source of uric acid production, must be evaluated as a CVD risk factor in obesity. As stated previously, XOR is an enzyme which produces uric acid via the subsequent oxidation of hypoxanthine to xanthine and xanthine to uric acid. In addition to the production of uric acid, XOR is responsible for a variety of roles in the body. In the regulation of nucleic acid turnover, XOR produces irreversible metabolites from purines which block the recovery of nucleotides through the purine salvage pathway. Another role that XOR is involved in is the production of reactive oxygen species (ROS), which may contribute to cardiovascular risk. When oxygen is the electron acceptor for a reaction involving XOR, the reactive oxygen species superoxide and hydrogen peroxide are formed as byproducts of the XOR catalyzed reaction.[53,54] These

ROS are responsible for the oxidative damage that is seen in ischemia-reperfusion injury and they may contribute to CVD risk in obesity. Lastly XOR catalyzes the metabolism of multiple xenobiotics, which include antivirals and anti-cancer agents.[55] The numerous effects XOR has on CVD risk, drug metabolism, and on other pathways makes XOR a pertinent enzyme to study in relation to obesity.

1.2.2 Expression and organ distribution of xanthine oxidoreductase:

In humans, XOR can be found in multiple organs, but the liver and intestine have the highest transcription levels and activity of XOR.[42] XOR is present in two inter-convertible forms: xanthine dehydrogenase (XDH) and xanthine oxidase (XO).[56] XOR is expressed as XDH, which can then be converted to XO via oxidation (reversible) or proteolysis (irreversible). XOR is considered as a cytosolic enzyme and is highly abundant in the cytosol, but it has also been to be associated with the cellular membrane and intracellular organelles, such as peroxisomes.[57] In addition to being expressed in organs, XOR can also be found in biological fluids including blood and milk.[56,58] Circulating XOR in the blood is quickly converted to its XO form, which then attaches to and is endocytosed by the vasculature and organs that have low or no expression of XOR.[59] The circulating XO is able to attach to vascular cells and insert into organs due to its ability to bind to sulphated glycosaminoglycans expressed on the endothelial cell surface of the vasculature and various organs.[60] Circulating XO would explain why XOR activity can be found in some organs that show no expression of XOR. The activity of circulating XO is particularly intriguing to study in obesity as XO activity in the

blood/plasma is much easier to measure clinically, than measuring XO activity in the liver.

1.2.3 Molecular and catalytic structure of xanthine oxidoreductase:

As mentioned previously, XOR has two forms in XO and XDH, but the components that make up XOR are the same in both forms. The XOR enzyme is a homodimer (approximately 145 kDa), and each subunit consists of a molybdopterin domain, a flavin adenine dinucleotide (FAD) binding domain, and two iron-sulphur redox centers. For a substrate to be oxidized by XOR, the enzyme goes through a two-step reaction (**Figure 1.6**). During the reductive half reaction, substrates bind to the molybdopterin domain of XOR, where XOR oxidizes the substrate and XOR consequently gets reduced. In the oxidative half reaction, XOR reduces an electron acceptor bound to the FAD-binding domain and the XOR itself gets oxidized. The electron acceptors for the XDH form can be either NAD^+ or O_2, but for the XO form, O_2 is the only electron acceptor. During the oxidative half reaction, the ROS superoxide anion and hydrogen peroxide are formed from the reduction of O_2. Superoxide anion produced from circulating XO will react with and reduce the levels of nitric oxide (a potent vasodilator) by forming peroxynitrite. Therefore, circulating XO in the plasma may lead to endothelial dysfunction and may be a risk factor for CVD risk in obesity.

Figure 1.6: Catalysis of Hypoxanthine to Xanthine and Xanthine to Uric Acid by XO

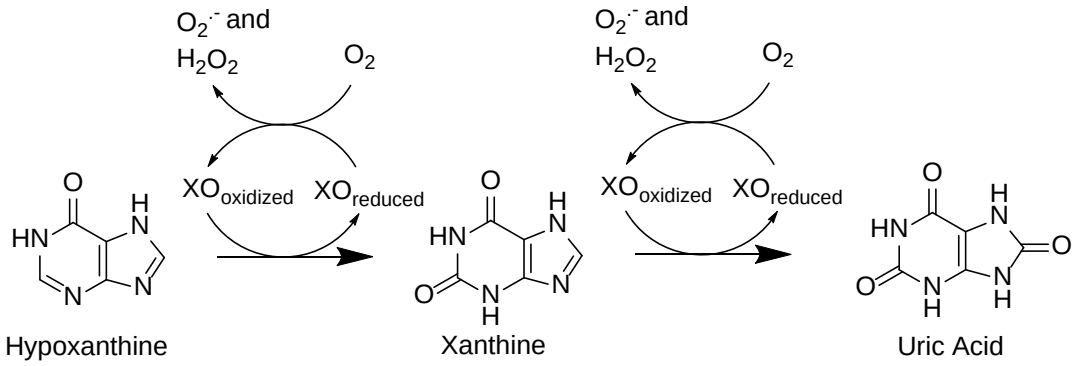

1.2.4 Regulation of xanthine oxidoreductase:

The gene for XOR spans 60kB and is encoded by 36 exons in humans to produce an mRNA transcript of 1333 amino acids.[61,62] The gene is located on the short arm of chromosome 2 p22.[61,62] Human XOR has 91% homology to mouse and rat XOR and 50% homology to aldehyde oxidase which has a very similar gene structure and is also located on chromosome 2.[61] XOR is extensively regulated by both transcriptional and post-transcriptional methods. It should be noted that the expression of XOR in organs such as liver and kidney is >100-fold lower in humans compared to mice and rats indicating significantly different regulation between species.[63] The gene expression of XOR is modulated by multiple factors which include diet,[64] cytokines,[65] lipopolysaccharide (LPS),[66,67] and oxygen tension.[68,69] Schröder et al. reported that in mice fed a high fat diet, XOR mRNA and protein expression were increased; although no mechanism was proposed as the cause of this increase. A second factor that influences XOR expression are cytokines, and the inflammatory markers and cytokines IL-6 and TNF-α have been shown to induce XOR mRNA expression as well as increase XOR activity in bovine renal epithelial cells and in human bronchial epithelial cells.[62,65] This increase in XOR expression is likely due to a decrease in the repression of XOR by the tumor suppressing protein scaffold attachment factor B1 (SAFB1) due to the IL-6 phosphorylating SAFB1, which leads to increases in XOR expression and activity.[62,70] Another factor that regulates XOR expression is plasma LPS levels (generated by bacteria in the gut). Kurosaki et al. reported that in mice exposed to LPS, XOR expression in various organs and tissues was induced.[67] A high fat diet, which is common in childhood obesity, has

been shown to increase LPS levels by altering the gut microbiota to express more gram negative bacteria.[71,72] Lastly, changes in oxygen tension signaling also alter XOR expression or activity in obesity. Lanzillo et al. and Terada et al. have reported that XO is regulated by oxygen tension by studying XO activity and messenger RNA expression in hypoxic and hyperoxic environments.[68,69] Terada et al. reported increases in XO activity after 24 hours of exposure to hypoxia and a decrease in in XO activity after 24 hours of hyperoxia, but they noted that mRNA expression of xanthine oxidoreductase was unchanged until 48 hours of exposure to either hypoxia or hyperoxia.[68] Those changes in XO activity before changes in protein expression occur suggests that XO is regulated both pre- and post-translationally by oxygen tension. As mentioned before, obesity is characterized by inflammation and oxidative stress, which increases the amount of ROS in obesity. ROS are important mediators of oxygen tension signaling (involved in hypoxia inducible factor 1-alpha stabilization, plasminogen activator inhibitor-1 induction, and others), which may lead to changes in the expression and activity of XOR due to the fact that XOR has a hypoxia inducible factor binding site in its promoter region.[62,73]

1.2.5 Uric acid excretion:

In addition to the production of uric acid by XOR, uric acid excretion by the kidneys plays a major role in the regulation of plasma uric acid levels. Uric acid excretion is via the kidneys is modulated by three factors: glomerular filtration rate, secretion, and reabsorption. Glomerular filtration rates (GFR) are known to scale with body size descriptors such as weight, BMI, and BSA, which leads to increased GFR in obesity.

Secretion of uric acid is mediated mainly by the adenosine triphosphate-binding cassette transporter 2, ABCG2, and the sodium-phosphate co-transporters NPT1 and NPT4.[74,75] Lastly, reabsorption of uric acid is mediated by the organic anion transporter URAT1 and the solute carrier family 2, GLUT9. Both secretion and reabsorption of uric acid occurs at the proximal tube of the nephron, and the dominant mode of urate transport is reabsorption; with an average of only 5-10% of filtered urate actually being excreted into the urine.[74] However, the renal proximal tube tubule can dramatically increase its reabsorption capacity such that the fractional excretion of urate is nearly constant even with dramatic changes in urate concentrations; for example, when compared to healthy individuals, gout patients with nearly twice the concentration of urate in the blood had similar fractional excretion rates of urate between 5% and 7%.[75] Therefore, changes in uric acid excretion must be accounted for when examining the relationship between obesity, uric acid, and hypertension.

1.3 Methods to Study Obesity and its Consequences

1.3.1 Treatments and weight loss methods to study obesity's effect on XO activity and uric acid levels:

Weight loss has always been the recommendation to obese populations to reduce CVD risk associated with obesity, and studying the effect of weight loss on XO activity, uric acid, and blood pressure will give us greater insight into the mechanism of how obesity increases cardiovascular risk. Weight loss can be achieved in a variety of ways; including diet modification, pharmacological intervention, or bariatric surgery. Diet intervention via meal replacement therapy (MRT) has been shown to be effective at

moderately reducing weight in both obese adolescents and adults in a short period of time leading to reductions in weight varying from 5-10% after 2-4 months.[76,77] Orlistat is the only approved pharmacological intervention for weight loss in adolescents. Orlistat works by inhibiting intestinal lipases which blocks the digestion of triglycerides into free fatty acids. Only digested triglycerides can be absorbed by the intestine, which leads to a calorie deficit. Orlistat does however have notable side effects and its limited efficacy impedes its use clinically in children. Bariatric surgery, such as Roux-En-Y gastric bypass (RYGB) surgery has been shown to be safe and it has been shown to reduce weight in severely obese adolescents by an average of 70% at one year post surgery.[78] RYGB is a common bariatric surgery that is effective at reducing weight that also has a good safety record.[79,80] RYGB is a procedure that is defined as both restrictive and metabolic. RYGB involves separating the stomach into a small pocket in the upper stomach that is connected to a roux jejunal limb (restrictive change) and the rest of the stomach is still attached to the biliary limb (metabolic change). Restrictive surgeries limit the rate of food intake to aid in weight loss; while metabolic procedures alter bile flow which leads to less absorption of fatty acids. Changes in the bile flow after RYGB has been shown to alter the gut microbiota, and this change is likely due to changes in the amount of free bile acids in the intestinal tract. In the normal enterohepatic circulation, conjugated bile acids are secreted into the duodenum to mix with fatty acids to aid in their digestion, and any free bile acids are then reabsorbed in the ileum. After RYGB serum bile acids increase and this is attributed to the fact that bile acids and food have less time to mix and more free bile acids are reabsorbed at the ileum.[81] More free bile

acids will select for bile-tolerant bacteria such as the gram negative proteobacteria,[82] which may lead to alterations on LPS levels, XOR expression, and drug metabolism.

1.3.2 Animal models of obesity to study changes in drug metabolism:

Initial studies on the effect of obesity and HFD on liver-mediated drug metabolism were done in animal models of obesity. In the case of intestinal drug metabolism by UGTs, animal models would also be ideal for initial studies as many of the confounding factors from human studies of obesity are eliminated. There are two major types of animal models of obesity: genetic models of obesity and diet-induced models of obesity. These models of obesity are from mice and rats, which have neurotransmitters and peptides that regulate food intake and satiety that are similar to a human's hormonal control of appetite that was previously described.[83] The genetic models of obesity that are most prevalent are due to single point mutations leading to a loss of leptin or loss of leptin receptor activity; which leads animals to overeat and become overweight within weeks after birth. The major concern with studying obesity in models which lack leptin activity is that obesity in humans is rarely caused a loss in leptin activity, and in fact an increase in leptin is characteristic of human obesity.[84]

Diet induced models of obesity are more similar to human obesity than genetic models of obesity, and they lead to clinical symptoms that are also present in human obesity such as insulin resistance, elevated cholesterol, elevated triglycerides, and elevated plasma leptin levels when compared with controls on a standard diet. Diet-induced models of obesity are achieved by allowing normal-weight animals free access to high fat diets (HFDs), which contain similar amounts of fat content contained in modern western diets. Diet

induced models of obesity also take longer to develop than genetic models; usually 12-16 weeks of a HFD before significant weight gain is achieved in rats.[83] HFDs have also been shown to increase LPS production and penetration into the body due to changes in the gut microbiota, which may ultimately lead to changes in XOR and UGT expression or activity via an increase in oxidative stress.[71,72]

1.4 Summary:

Obesity and a high fat diet are associated with increases in various CVD risk factors, such as hypertension. Hypertension in obesity may be caused by increases in uric acid and XO activity, as a plausible mechanism linking uric acid and blood pressure has been discovered. Alterations in obese populations in the production of uric acid by XO or changes in uric acid excretion may be underlying changes in uric acid levels and ultimately blood pressure. In addition to increased risk for CVD risk factors, drug metabolism may be altered in the small intestine of obese individuals. Therefore, the following research objectives are presented to study XO and uric acid as CVD risk factors in childhood obesity and changes to intestinal UGT activity in obesity.

1.5 Research Objectives:

1. Develop a sensitive assay to quantitate plasma xanthine oxidase activity

An assay capable of measuring XO activity in plasma would allow for easy measurement of uric acid production in children.

2. Determine if obesity is associated with plasma xanthine oxidase activity and if plasma xanthine oxidase activity is correlated with cardiovascular disease risk factors.

Uric acid has long been considered as a CVD risk factor, but XO activity has not been studied as a possible risk factor for CVD in obesity. Therefore, the purpose of this study was to determine if the production of uric acid via XO activity is associated with obesity.

3. Evaluate the effects of weight loss on plasma xanthine oxidase activity, uric acid clearance, traditional CVD risk factors, cytokine levels, and creatinine clearance.

The purpose of this study was to determine the mechanism(s) of how obesity and weight loss alters cardiovascular risk.

4. Develop assays to probe for UGT inhibition.

Specific inhibitors of UGTs are needed in order to determine substrate specificity for UGT isoforms, which will allow for more detailed studies on UGTs in areas such as obesity.

5. Determine alterations in intestinal UGT activity by obesity and high fat diet in animal models of obesity.

The purpose of this study was to evaluate the changes in drug metabolism enzyme activity in rat models of obesity with a purpose of identifying the feasibility of using these animal models of obesity as predictors of changes in clearance in obese humans.

Chapter II

Lumazine as a Highly Sensitive and Specific Probe for Plasma Xanthine Oxidase

2.1 Introduction:

Xanthine oxidase (XO) is an oxidative enzyme that is responsible for purine catabolism, oxidizing hypoxanthine to xanthine and xanthine to uric acid. [85] XO has been extensively studied due to its role in producing uric acid and reactive oxygen and nitrogen species (RONS).[86,87] Both uric acid and RONS have been shown to be important regulators of vascular function and dysfunction. Specifically high levels of uric acid (hyperuricemia) has been implicated as a risk factor for hypertension [43], cardiovascular disease (CVD) [88,89], and chronic kidney disease (CKD). [90] RONS play an important role in ischemia-reperfusion injury and regulation of redox-sensitive transcription factors that can affect angiogenesis.[91,92] Because XO is a key component to vascular health, it is an attractive biomarker candidate for vascular health and disease. An accurate method to measure XO activity that is both fast and easy would be essential to determining if XO would serve as an ideal candidate biomarker for vascular health and disease. XO is found in the epithelium of many tissues, but more highly expressed in the liver and intestines.[93-95] Therefore, measuring XO activity from the liver cytosol is an option, as activity would be high. Chiney et al. and others have measured xanthine oxidase activity with caffeine as a probe substrate for in vivo phenotyping.[96,97] Despite the robustness of in vivo phenotyping, these methodologies are difficult, costly, and time consuming; and therefore, would not be an appropriate methodology to measure XO activity rapidly. Alternatively, XO is also present in plasma.[58,98] Measuring XO activity from the plasma may be a better option, however there are still some challenges as plasma XO activity is not as robust as XO activity in the liver.[58,99,100].

The gold standard or conventional method to measure XO activity is to quantify the conversion of hypoxanthine to xanthine or xanthine to uric acid (Scheme 2.1). However, measuring uric acid production in human plasma is challenging because; 1) human plasma contains varying amounts of endogenous uric acid, 2) uric acid has poor solubility in water which leads to precipitation of analytical standards, and 3) analytical analysis of uric acid via HPLC+UV detection are not sensitive enough to quantify XO activity in human plasma. Thus an alternative method of measuring XO activity is with a commercially available XO kit. Commercial XO fluorometric assay kits are available (e.g. Cayman 10010895). According to the manufacturer's description, "The assay is based on a multistep enzymatic reaction whose end product resorufin, a highly fluorescent compound, can be easily analyzed using an excitation wavelength of 520-550 nm and an emission wavelength of 585-595 nm". XO activity assay kits indirectly measure XO activity by measuring the hydrogen peroxide byproduct of XO metabolism. Unfortunately, many kits are not sensitive enough to detect plasma XO activity in most healthy individuals, but could potentially detect plasma XO activity when it is increased in certain disease states. However, during an initial evaluation of this kit for measuring XO activity in plasma, we observed lack of inhibition by allopurinol, a selective XO inhibitor, indicating that the assay was not selective for XO. Therefore, the aim of this study was to develop a highly sensitive and specific method to measure plasma XO activity in humans and to compare this method to conventional and alternative methods of measuring plasma XO activity.

To alleviate some of the challenges to measuring XO activity in plasma, we utilized lumazine, a fluorescent pteridine that is a highly selective substrate for XO, and measured the conversion of lumazine to 7-OH lumazine [101,102] (Scheme 2.1.). The advantages of measuring 7-OH-lumazine production instead of uric acid production are 1) 7-OH-lumazine is not found in plasma endogenously, 2) the high water solubility of 7-OH-lumazine, and 3) 7-OH-lumazine is a highly fluorescent compound resulting in more sensitive method than a xanthine-based assay with a UV detector. Therefore we now describe an accurate, sensitive and specific methodology for quantifying XO activity in plasma to determine if plasma activity is a biomarker for vascular health and oxidative stress.

2.2 Methods:

Supplies and Chemicals

Lumazine, xanthine, uric acid, chromatographically purified xanthine oxidase from bovine milk (Grade I, suspension in 2.3M $(NH_4)_2SO_4$, containing 1 mM Na salicylate, Cat # X1875) , allopurinol, and pooled human liver cytosol were obtained from Sigma (St. Louis, MO, USA). Oxypurinol was obtained from Toronto Research Chemicals (North York, ON, Canada). Strata-X 33µ polymeric reversed phase filters were obtained from Phenomenex (Torrance, CA, USA). Nanosep 30k Omega filters were from Pall Life Sciences (Port Washington, NY, USA). Xanthine Oxidase Assay Kit (Cat # 10010895, Cayman Chemical Company, Ann Arbor, MI, USA). Rat plasma was obtained from BioreclamationIVT (New York, USA). This study was approved by the

University of Minnesota IRB Board (IRB no. 1204M12582) for the assay and method development.

7-OH-lumazine purification method

To purify 7-OH lumazine, 100mL of 3.3mM lumazine in 5mM potassium phosphate buffer pH 7.4 were incubated with 100 Units (~2.2mL) of purified xanthine oxidase (XO) from bovine buttermilk for 5.5h at 37°C to produce 7-OH-lumazine. The reaction was stopped by addition of 200mL ice-cold methanol. Incubation mixture was then centrifuged at 10,000 x g for 10 min at 4°C. Supernatant was then saved and dried. Subsequently the sample was reconstituted in mobile phase (99:1 25mM ammonium acetate pH 4.7:acetonitrile) and injected into the preparatory HPLC system to separate 7-OH-lumazine from lumazine. The preparatory HPLC system used to purify 7-OH-lumazine consisted of a SCL-10A HPLC controller, a SIL-10A autosampler, LC-10AD pumps, (Shimadzu, Columbia, MD), a SpectraFOCUS forward optical scanning UV detector (Spectra-Physics, Santa Clara, CA, USA), and a HAISIL HL C18 5uM 100x20mm column (Higgins Analytical Inc., Mountain View, CA, USA). The isocratic gradient used was 99:1 25mM ammonium acetate pH 4.7 acetonitrile at 5 mL/min. 7-OH-lumazine was collected and lyophilized after separation. 7-OH-lumazine metabolite was confirmed via mass spectrometry and NMR spectroscopy (Supplemental Figure 2.1).

Measuring XO Activity With and Without Inhibitors Using Xanthine Oxidase Assay Kit

XO activity in plasma and liver cytosol was measured per manufacturers' directions; in short, 50 µL of assay cocktail was mixed with 40 µL of human/rat plasma

(undiluted) or liver cytosol (100x/1000x diluted with kit's sample buffer) with the addition of 10 µL of sample buffer or inhibitor. Only plasma samples with detectable XO activity were used and incubated with inhibitors. Final inhibitor concentrations of 50µM allopurinol and oxypurinol were used in these experiments. Boiled samples were also used as a negative control (boiled plasma samples were reconstituted with an equal volume of sample buffer provided in the kit). Samples were incubated for 45 minutes at 37°C and then fluorescence was measured at the following wavelengths: Excitation=530nm and Emission=590nm. All samples were run in triplicate.

Production of 7-OH lumazine compared to uric acid production

Partially-purified XO (0.28, 0.56, 1.13, 2.25, 4.5, 9, 18 mUnits/mL final concentration) was incubated with 25mM xanthine in 50mM potassium phosphate buffer pH 7.4 for 20 minutes (100 µL total incubation volume) in triplicate. Incubations were flash frozen to terminate the incubation. 200 µL of 250µM caffeine (internal standard) in water was added to the incubations and incubations were then thawed on ice. Samples were then filtered using 30K MWCO filters. Uric acid production was measured with the following HPLC system: Waters 2695 HPLC (Milford, MA, USA), Waters 2487 dual absorbance detector (Milford, MA, USA), and a Synergi 4u 200x4.6mm Polar-RP 80A column (Phenomenex, Torrance, CA, USA). The protein-free samples were then injected into the analytical HPLC system and absorbance was measured at a wavelength of 292nm. The gradient used is listed in Supplemental Table 2.1. Purified XO (0.28, 0.56, 1.13, 2.25, 4.5, 9, 18 mUnits/mL final concentration) was also incubated in triplicate with 40µM lumazine in 50mM potassium phosphate buffer, pH 7.4 for 10 min (200 µL total

incubation volume). Uric acid production (ng/min) was then plotted against 7-OH-lumazine production (ng/min).

Kinetics of Lumazine Metabolism

The enzyme kinetics for lumazine metabolism were determined by incubating 1.8mUnits/mL of partially-purified bovine XO with 45, 15, 5, 1.67, 0.556, 0.185, and 0.062 µM of lumazine with and without the addition of allopurinol (50µM final concentration) or uric acid (80µM final concentration)in 50mM phosphate buffer, pH 7.4. Reaction mixtures (200 µL total volume) were incubated at 37°C for 5 min.

Measuring XO Activity With or Without Inhibitors Using Lumazine as a Probe Substrate

XO activity was determined by incubating lumazine (40µM final concentration) with 100 µL of human/rat plasma (undiluted) or liver cytosol (100x/1000x diluted with 50mM potassium phosphate buffer, pH 7.4) with the addition of 20 µL of buffer or inhibitor in triplicate. Final inhibitor concentrations of 50µM were used for allopurinol and oxypurinol, and 80µM of uric acid was also tested for inhibition. Reaction mixtures (200 µL total volume) were incubated at 37°C for 3 hours (plasma) or 5 minutes (cytosol).

Sample Preparation and HPLC Method for 7-OH-lumazine Quantification

Reactions were stopped and proteins were precipitated by the addition of 2x incubation volume (400 µL) of 771nM umbelliferone in ice-cold methanol (internal standard). After centrifugation at 10000g for 10 min at 4°C, the supernatants were passed through Strata-X 33µ polymeric solid-phase extraction cartridges. The flow-through was

saved for HPLC analysis of 7-OH-lumazine. The analytical HPLC system consisted of an Agilent 1100 HPLC (Agilent, Santa Clara, CA, USA), a Jasco FP-920 fluorescence detector (Jasco, Easton, MD, USA), and a Synergi 4u 200x4.6mm Polar-RP 80A column (Phenomenex, Torrance, CA, USA). 50µL of flow-through was injected into the analytical HPLC system and fluorescence was measured at the following wavelengths: Excitation=340nm and Emission=400nm. The gradient used is listed in Supplemental Table 2.2.

Statistics

A Student's t-test was used to determine significance of differences in xanthine oxidase activity between control and incubations with inhibitors. P-values < 0.05 were considered statistically significant. All values are expressed as mean ± SD unless stated otherwise.

2.3 Results:

Inhibition of Cytosolic and Plasma XO Determined by Xanthine Oxidase Assay Kit

The XO specific inhibitors allopurinol and oxypurinol were both effective at inhibiting XO activity in rat liver cytosol, showing >80% inhibition. However, little allopurinol and oxypurinol inhibition was observed in human liver cytosol, with 11% (p-value=0.01) and 15% (p-value<0.01) inhibition, respectively (Figure 2.1). Boiling the cytosolic samples had similar effects in inhibiting XO activity in both human and rat cytosol, resulting in only 65% (p-value<0.01) and 71% (p-value<0.01) inhibition, respectively. As shown in Figure 2.2, allopurinol and oxypurinol inhibited XO activity in rat plasma by 49% (p-value<0.01) and 50% (p-value<0.01) respectively; whereas

allopurinol and oxypurinol were ineffective at inhibiting XO activity in human plasma (0-35% inhibition). Boiling plasma samples had varying effects ranging from 85% inhibition in rat plasma (p-value<0.01) to no change in human plasma 1 (p-value=0.16) and 49% activation in human plasma 2 (p-value<0.01).

Lumazine as a Substrate for Bovine Milk Xanthine Oxidase

7-OH lumazine formation from lumazine, as shown in Figure 2.3, followed Michaelis-Menten kinetics with partially purified bovine milk XO with a V_{max}= 532 pmol/min and k_m= 1.05µM. Allopurinol strongly inhibits lumazine intrinsic clearance (V_{max}/K_m) by 97.8% resulting in a decrease in V_{max} to 60 pmol/min (p-value< 0.01) and an increase in k_m 5.36µM (p-value< 0.01). Uric acid slightly inhibits lumazine turnover resulting in a decrease in V_{max} to 353 pmol/min (p-value= 0.02) but no change to k_m (1.27µM, p-value= 0.36). XO mediated conversion of lumazine to the 7-OH-lumazine correlated with XO-mediated conversion of xanthine to uric acid r^2 value = 0.99 (Figure 2.4).

Inhibition of Cytosolic and Plasma XO Determined by Lumazine Metabolism

Allopurinol (50 µM) inhibited XO activity in human liver cytosol by 74% (p-value<0.01) and rat liver cytosol by 95% (p-value<0.01). (Figure 2.5) Oxypurinol (50 µM) inhibited XO activity in human liver cytosol by 65% (p-value<0.01) and rat liver cytosol by 93% (p-value<0.01).). Boiling samples inhibited XO activity in human liver cytosol by 83% (p-value<0.01) and rat liver cytosol by 95% (p-value<0.01). Uric acid increased XO activity in human liver cytosol by 59% (p-value<0.01) and rat liver cytosol by 22% (p-value=0.04). However, as shown in Figure 2.6, allopurinol inhibited XO

activity in human plasma sample 1 by 87% (p-value<0.01), human plasma sample 2 by 46% (p-value<0.01), and rat plasma by 98% (p-value<0.01). Oxypurinol inhibited XO activity in human plasma sample 1 by 84% (p-value<0.01), human plasma sample 2 by 48% (p-value=0.02), and rat plasma by 69% (p-value<0.01).). Boiling samples inhibited XO activity in human plasma sample 1 by 91% (p-value<0.01) human plasma sample 2 by 45% (p-value=0.02) and rat plasma by 99% (p-value<0.01). Uric acid had no significant effect on lumazine metabolism by XO in human plasma or rat plasma.

2.4 Discussion:

Xanthine oxidase is an important contributor to hyperuricemia and oxidative stress, and may have a role as a risk factor for hypertension, CVD, and CKD. [43,88-90] Accurate measurement of XO activity is important in determining its role as a possible biomarker for vascular health. There are few tools available to easily and accurately assess XO activity in human plasma. Therefore, we developed an assay using lumazine as a probe substrate and compared it to commercialized XO kits and an assay using xanthine as the prototypical substrate for XO. In addition, we also compared the effects of specific and non-specific inhibition methods for XO on the metabolism of lumazine and in the commercialized kits in order to confirm the specificity of these methods for XO.

We observed that xanthine oxidase activity was not inhibited in human plasma or liver cytosol samples by the selective XO inhibitors allopurinol or oxypurinol when using the commercial XO assay (figures 2.1 and 2.2), which would indicate that other enzymes besides XO are being measured. Because there is a differential effectiveness of xanthine oxidase inhibitors in rat when compared to human samples, these results demonstrate that

the commercialized XO kit is not specific for accurate determination of XO in human samples. One explanation for differential results between species is that the commercialized kits use an indirect method of measuring XO activity in multi-step enzymatic assay by measuring the production of resorufin from the hydrogen peroxide produced by XO. The production of hydrogen peroxide is not specific to XO and other enzymes such as semicarbazide-sensitive amine oxidases (SSAO) could be responsible for the production of hydrogen peroxide which would interfere with XO assay kits.[103] SSAO activity is higher in humans than in rats, which could explain why this assay was more responsive to XO inhibitors in rat samples than compared to human samples.[103,104] The ineffectiveness of XO inhibitors in human samples suggests that the commercialized kit may not be measuring XO activity, but instead, it could be measuring the activity of other enzymes such as SSAOs. Therefore, kits using hydrogen peroxide as a surrogate for XO activity is not an accurate method to quantify XO activity in humans.

To show that lumazine metabolism is actually due to XO, multiple specific and non-specific inhibition methods were tested. The inhibitors allopurinol and oxypurinol and boiling samples were almost equally effective at inhibiting XO activity in both human and rat liver cytosol or plasma. The specific XO inhibitors inhibiting lumazine metabolism to a similar extent as the non-specific method of boiling samples shows that lumazine is not metabolized by other enzymes and that it is a specific substrate for XO. Recently, Barr et al. found that human liver cytosol usually contains residual oxipurinol and sometimes allopurinol, because allopurinol (1 mM) is present in the University of Wisconsin cryopreservation solution to prevent reperfusion injury from reactive oxygen

species produced by XO (Barr, DMD 2014).[105] 6-Mercaptopurine, 6-nitroquinazolinone, and N-[(2-dimethylamino)ethyl]acridine-4-carboxamide (DACA) were used a probe substrates and their metabolites determined by LC-MS/MS. Their studies confirmed that XO activity in human liver cytosol is often not measurable, except in cases when allopurinol was not present in the perfusate. This may be why we did not observe complete inhibition of XO activity in human liver cytosol.

In order to use lumazine metabolism as a surrogate for xanthine oxidase activity, we needed to determine if 7-OH-lumazine production correlated well with the gold standard of uric acid production. The linear relationship between lumazine production and uric acid production with bovine milk XO indicates that lumazine is a good surrogate to measure xanthine oxidase activity instead of measuring overall uric acid production (a much less sensitive HPLC-UV method) or with a commercial XO assay kit. Lumazine is a more sensitive probe substrate than xanthine, as 2.25 mUnits/mL of XO was producing the lowest detectable amounts of uric acid, but 0.28 mUnits/mL of XO was still producing detectable amounts of 7-OH-lumazine. The sensitivity of our assay was also very high with a limit of detection of 32pg/mL and a limit of quantification of 53pg/mL. This higher sensitivity with lumazine allows us to measure XO activity in plasma samples or in small samples of human liver (e.g. biopsies) where we could not detect any activity using xanthine as a probe substrate.

The effect of uric acid on lumazine metabolism is something that needs to be considered because plasma samples will have endogenous uric acid present at varying levels. We see varying effects of uric acid on the metabolism of lumazine based on the

matrix and species the XO is derived from. In purified XO from buttermilk, uric acid inhibited lumazine metabolism by 34%. This inhibition of bovine XO could be related to the inhibition by purines that has previously been reported in bovine XO. [106,107] However, in human and rat liver cytosol, we see that the addition of uric acid actually increases lumazine metabolism by 59% and 22%. (Figure 2.5) This increase in lumazine metabolism could be related to the substrate activation of XO from chicken liver that has been previously reported with xanthine as a substrate, in which XO was proposed to have multiple substrate binding sites. [108,109] It could be possible that uric acid binds to one substrate binding site of XO which leads to changes in xanthine metabolism. In contrast to the substrate activation seen in chicken liver XO, a previous study by Tan et al. showed that bovine XO added to human plasma is inhibited by uric acid. [110] In our study, XO activity in both human and rat plasma showed that uric acid had no effect on lumazine metabolism, but endogenous uric acid in human plasma could be masking any potential effects of adding uric acid. Human XO has not yet been fully investigated for activation or inhibition by purines and the effect of purines on human XO needs further investigation.

In order to show that our lumazine assay is reliable and accurate, we validated our assay in four ways: accuracy, precision, linearity, and stability of metabolite. Accuracy is the measure of how close a measurement is to its true value and precision is the measure of how much variability is in a measurement. Our assay for 7-OH-lumazine is both accurate (inter-day and intra-day relative errors of 0-12%) and precise (inter-day and intra-day coefficients of variation of 1-12%) as shown in Supplemental Table 2.3. Time

linearity of incubations is needed in order to show that the enzyme being investigated is not degrading during an incubation, and the metabolism of lumazine to 7-OH-lumazine in plasma is linear up to four hours as shown in Supplemental Figure 2.2. Stability of the metabolite is needed in order to determine the true activity of an enzyme, as degradation or further metabolism of the metabolite will lead to underestimations of enzyme activity. 7-OH-lumazine is stable in plasma for at least 24 hours at 37°C as shown in Supplemental Table 2.4.

In conclusion, lumazine is a specific and sensitive probe substrate that correlates well with xanthine metabolism which makes it a good substrate to determine plasma XO activity. We also show that commercialized XO kits are not accurate for measuring XO activity in humans because they use hydrogen peroxide production as a surrogate for XO activity, but hydrogen peroxide can be made by enzymes other than XO. With a sensitive and specific method to measure plasma XO activity, we can now use this method to determine if plasma XO activity would be a good biomarker for cardiovascular health or as a risk factor for hypertension, CVD, or CKD.

Scheme 2.1 Reactions Used to Measure Xanthine Oxidase Activity

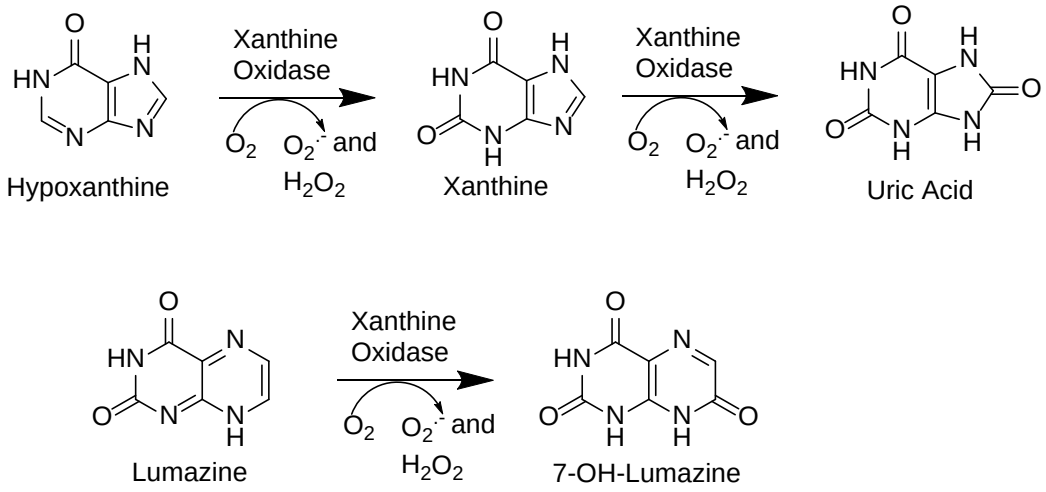

Figure 2.1 Cytosolic Xanthine Oxidase Activity Using Xanthine Oxidase Activity Kit
Human/rat liver cytosol (100x/1000x diluted with sample buffer) was mixed with sample buffer or inhibitors (concentrations of 50µM for allopurinol and oxypurinol) and xanthine oxidase activity was determined using a xanthine oxidase activity kit. Boiled samples were also used as a negative control. All samples were run in triplicate.
*p-value ≤ 0.05, **p-value ≤ 0.01
ND = Not Detectable

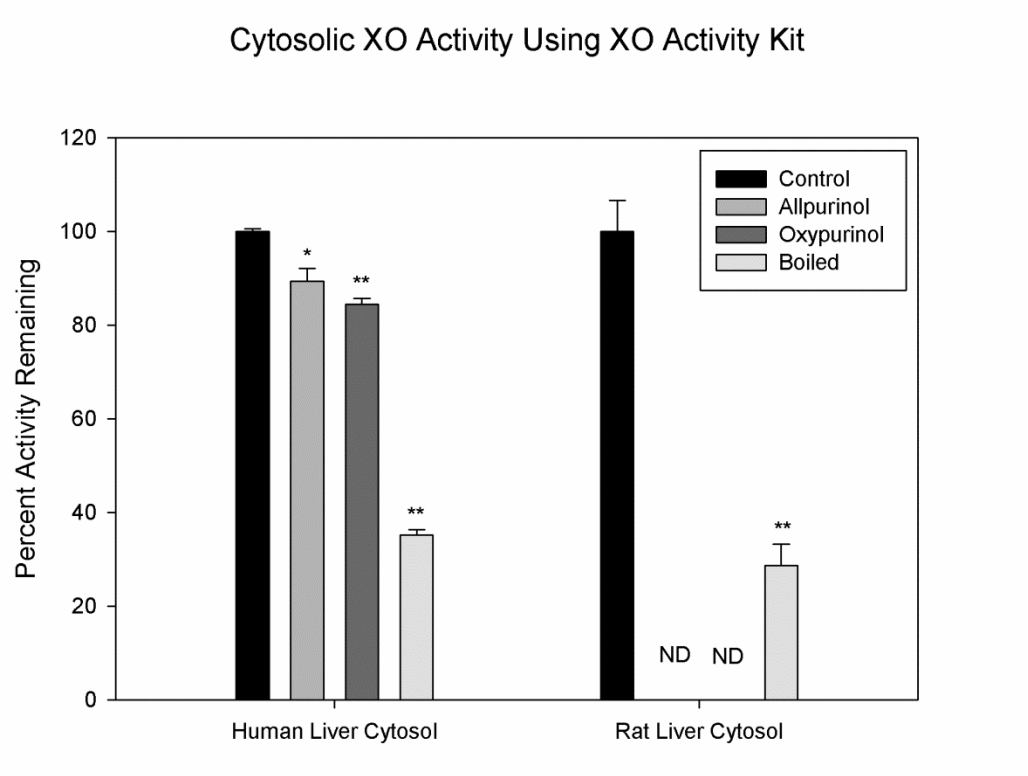

Figure 2.2 Plasma Xanthine Oxidase Activity Using Xanthine Oxidase Activity Kit
Human/rat plasma was mixed with sample buffer or inhibitors (concentrations of 50µM for allopurinol and oxypurinol) and xanthine oxidase activity was determined using a xanthine oxidase activity kit. Boiled samples were also used as a negative control (boiled samples were reconstituted with an equal volume of sample buffer). All samples were run in triplicate.
*p-value ≤ 0.05, **p-value ≤ 0.01

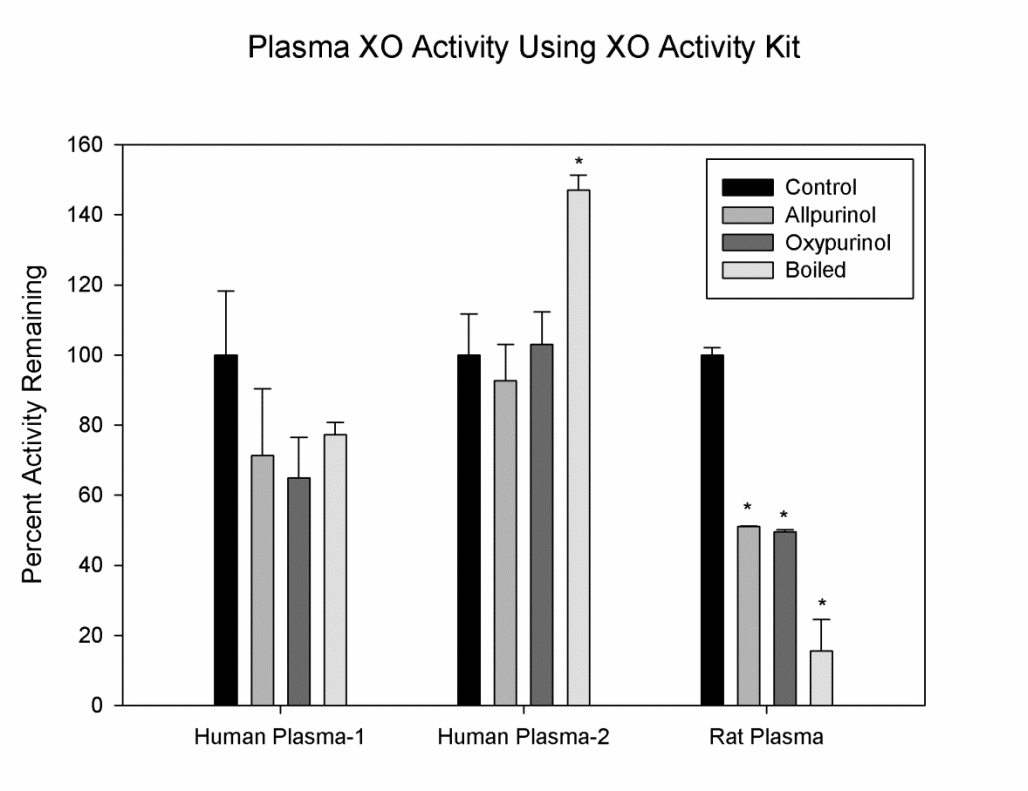

Figure 2.3 Lumazine Kinetics in Purified Bovine Xanthine Oxidase With Allopurinol or Uric Acid

Kinetics of lumazine metabolism was determined by incubating 1.8mUnits/mL purified xanthine oxidase with 45, 15, 5, 1.67, 0.556, 0.185, and 0.062 µM of lumazine with and without the addition of allopurinol (50µM final concentration) or uric acid (80µM final concentration). Compared to control (V_{max}= 532 pmol/min and k_m= 1.05µM) allopurinol significantly inhibits lumazine turnover resulting in a decrease in V_{max} to 60 pmol/min (p-value< 0.01) and an increase in k_m 5.36µM (p-value< 0.01). Uric acid slightly inhibits lumazine turnover resulting in a decrease in V_{max} to 353 pmol/min (p-value= 0.02) but no change to k_m (1.27µM, p-value= 0.36).

*significant difference in V_{max} (p-value=0.02)

**significant difference in V_{max} and k_m (p-value<0.01)

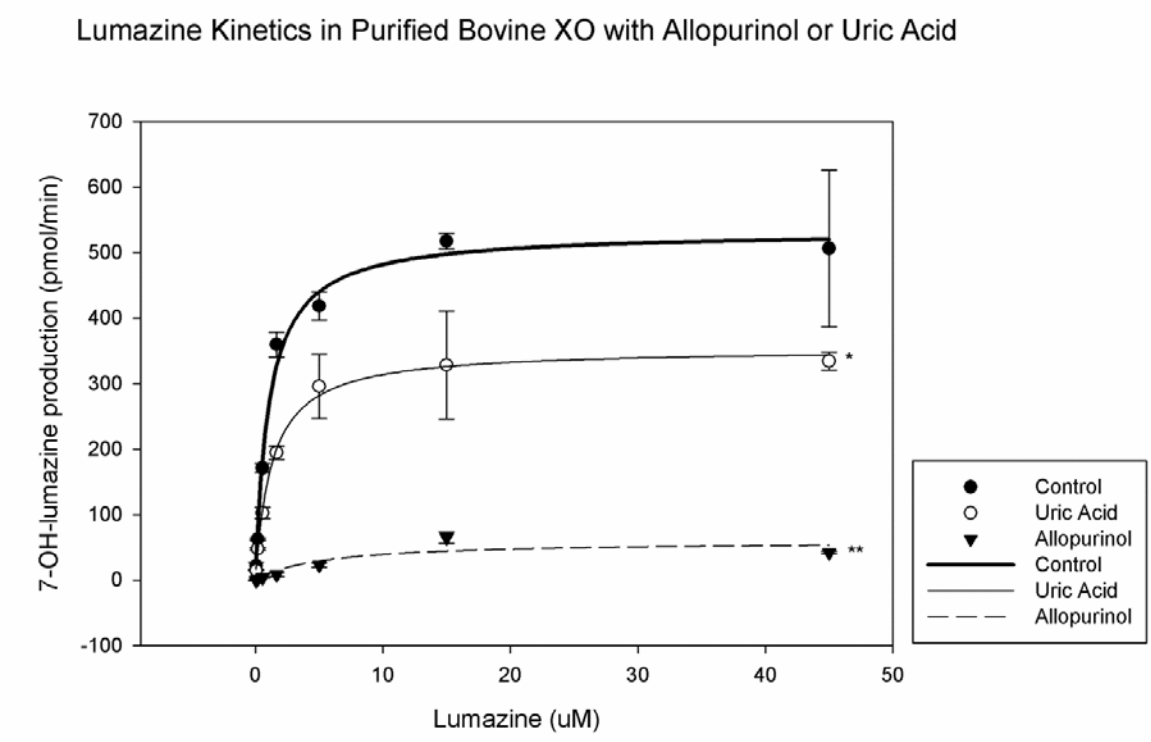

Figure 2.4 Comparison Between XO Activities as Measured by 7-OH-Lumazine vs. Uric Acid Production

Purified xanthine oxidase (0.28, 0.56, 1.13, 2.25, 4.5, 9, 18 mUnits/mL final concentration) was incubated with 25mM xanthine or 40µM lumazine in triplicate. Uric acid production (ng/min) was then plotted against 7-OH-lumazine production (ng/min). The three lowest concentrations of XO did not produce enough uric acid to be detected and were not included in the linear fitting. r^2 value = 0.99

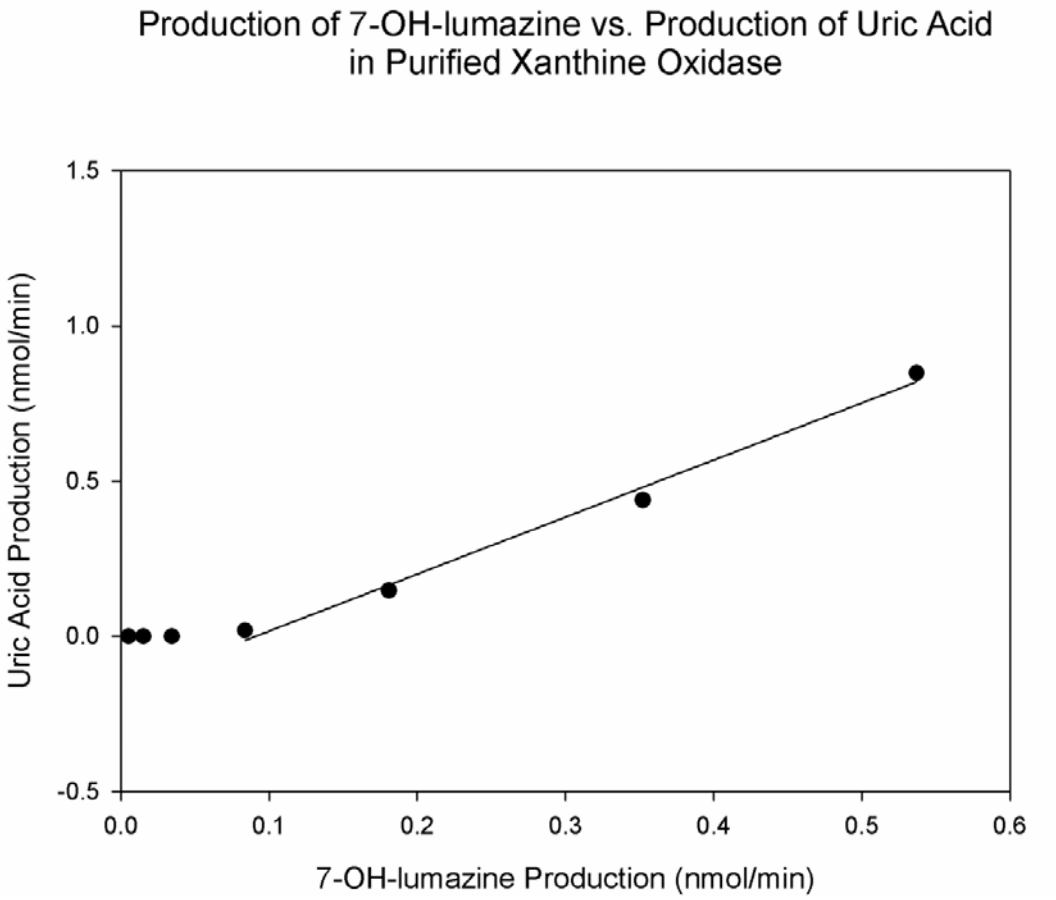

Figure 2.5 Cytosolic Xanthine Oxidase Activity Using Lumazine as a Probe Substrate

Human/rat liver cytosol (100x/1000x diluted with sample buffer) was mixed with sample buffer or inhibitors (concentrations of 50µM for allopurinol and oxypurinol) and xanthine oxidase activity was determined using lumazine as a probe substrate. Boiled samples were also used as a negative control. All samples were run in triplicate.
*p-value ≤ 0.05, **p-value ≤ 0.01

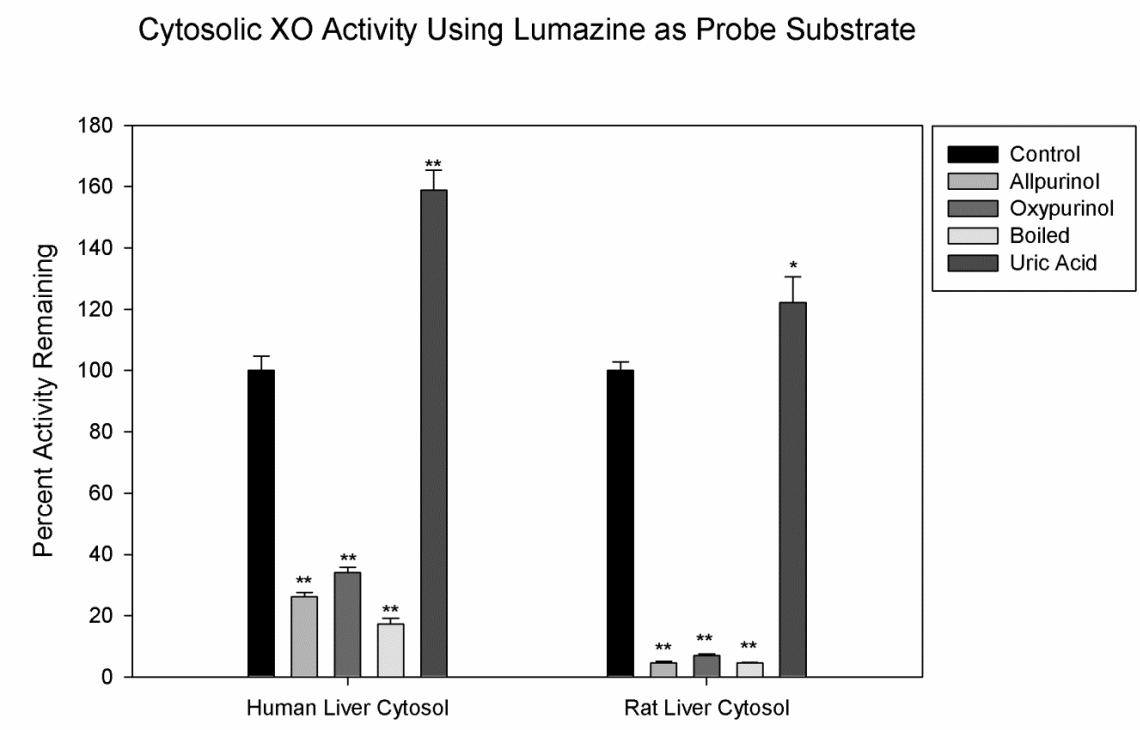

Figure 2.6 Plasma Xanthine Oxidase Activity Using Lumazine as a Probe Substrate
Human/rat plasma was mixed with sample buffer or inhibitors (concentrations of 50µM for allopurinol and oxypurinol) and xanthine oxidase activity was determined using lumazine as a probe substrate. Boiled samples were also used as a negative control (boiled samples were reconstituted with an equal volume of sample buffer). All samples were run in triplicate.
*p-value ≤ 0.05, **p-value ≤ 0.01

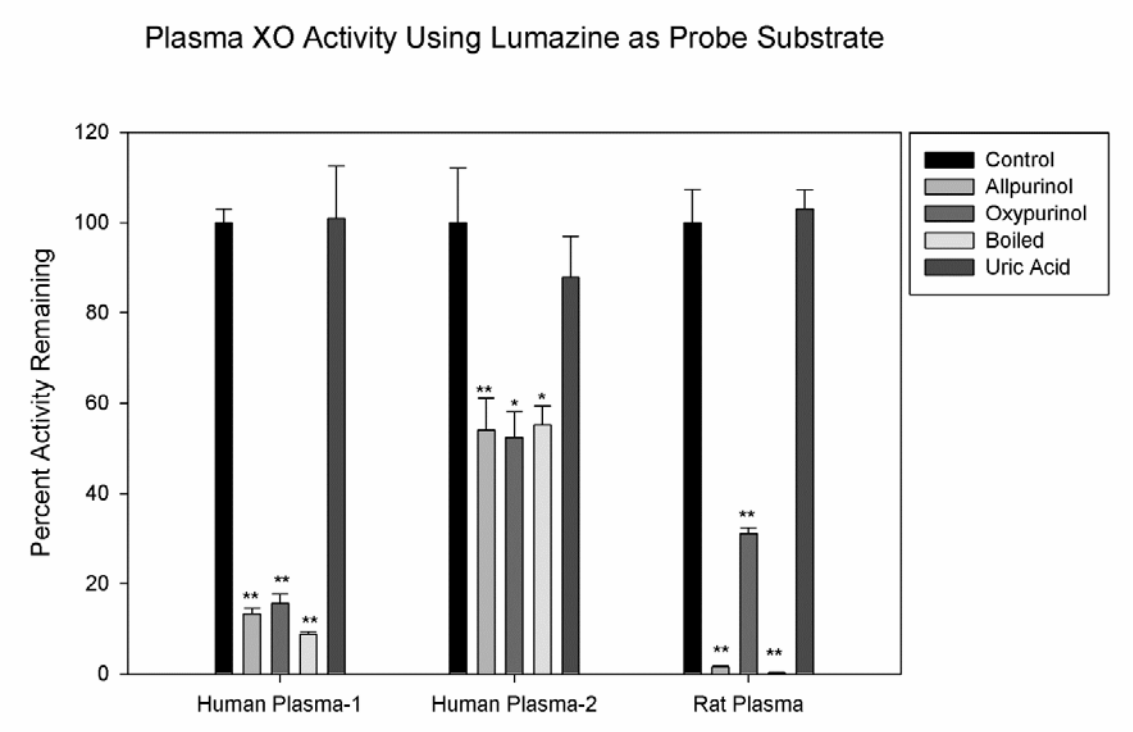

Supplemental material:

Supplemental Figure 2.1 LC/MS chromatogram of 7-OH-lumazine using electrospray ionization in negative mode.

The most abundant peak shows a mass of 179 g/mol which shows that our compound is indeed 7-OH-lumazine.

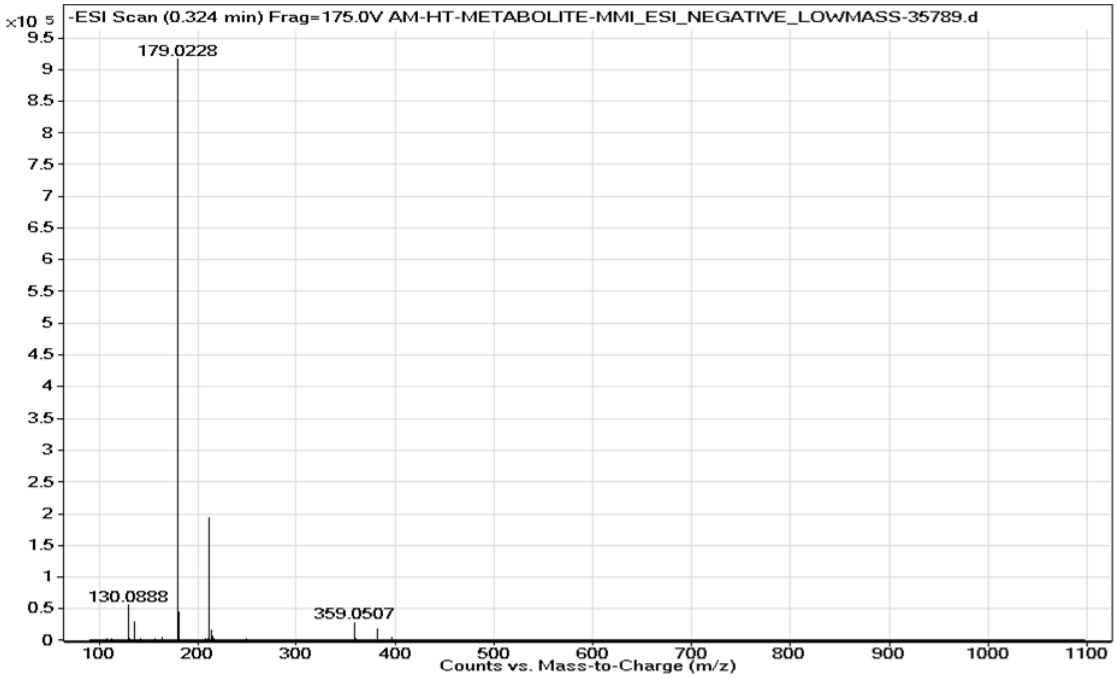

Supplemental Table 2.1 Gradient used for uric acid HPLC assay

Time	A (%)	B(%)
0	0	100
6.5	0	100
7	30	70
14	30	70
14.5	0	100
18	0	100

A = Acetonitrile
B = 97:3 5mM Potassium Phosphate Buffer: Acetonitrile pH=3.0

Supplemental Table 2.2 Gradient used for 7-OH-lumazine HPLC assay

Time	A (%)	B(%)
0	95	5
6.5	95	5
6.51	50	50
15.5	50	50
15.51	95	5
19	95	5

A = 25mM Ammonium Actetate pH=4.8
B = Acetonitrile

Supplemental Table 2.3
Inter-day and intra-day variability for quantification of 7-OH-lumazine in plasma.

Added Concentration (pg/ml)	Intra-day			
	Mean Measured (pg/ml)	Intra-day Precision (CV %)	Accuracy (%)	Relative Error %
156.25	137.42 ±5.2	3.75	87.95	12.05
625.00	612.45 ±7.1	1.16	97.99	2.01
2500.00	2496.62 ±118.4	4.74	99.86	0.14
Added Concentration (pg/ml)	**Inter-day**			
	Mean Measured (pg/ml)	**Inter-day Precision (CV %)**	**Accuracy (%)**	**Relative Error %**
156.25	152.00 ±18.8	12.42	97.28	2.72
625.00	586.67 ±46.7	7.96	93.87	6.13
2500.00	2252.63 ±199.3	8.85	90.11	9.89

Supplemental Figure 2.2 Time Linearity of 7-OH-Lumazine Production in Plasma
Two plasma samples were incubated with 40µM lumazine at 37°C for 1, 2, 3, or 4 hours in duplicate and the data was linearly fitted. R^2=0.98 for both fits below.

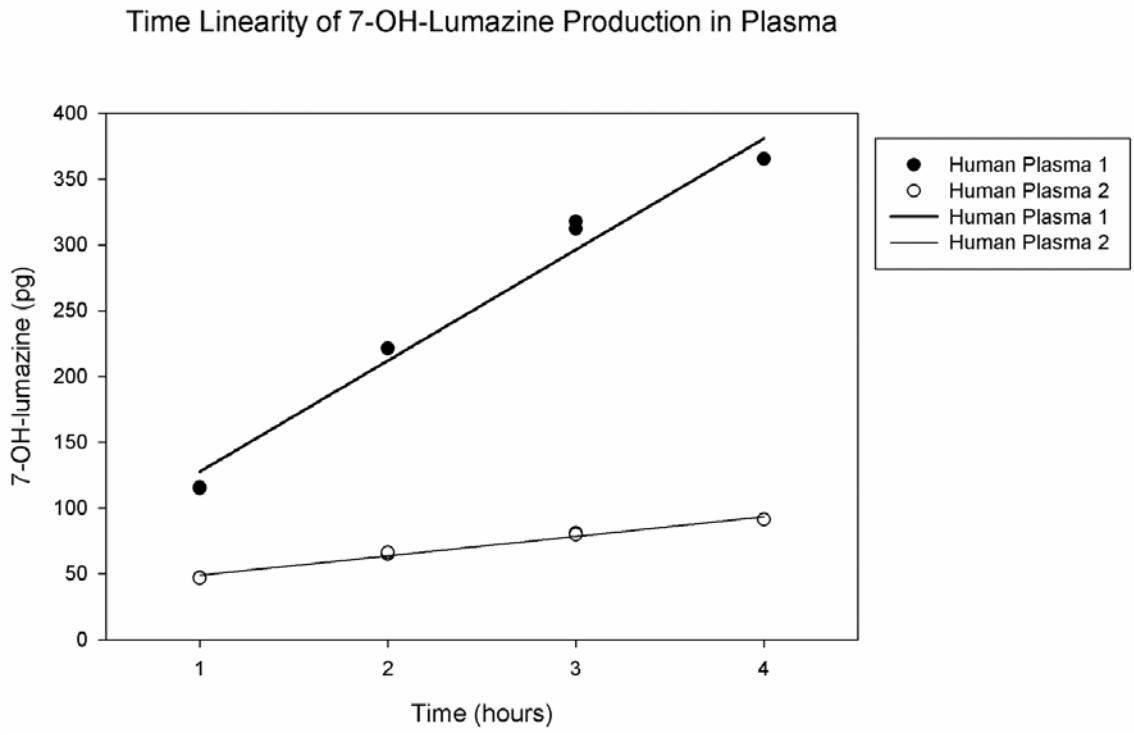

Supplemental Table 2.4 Stability of 7-OH-lumazine

Stability of 7-OH-lumazine was tested by incubating standard solutions at 37°C in buffer (control), human plasma, or rat plasma for up to 24 hours. Samples were compared to standard solution in buffer for zero hours as a control.

	0 hr	1 hr	2 hr	3 hr	20 hr	24 hr
Control	100.0%	102.1%	111.6%	101.4%	96.1%	103.8%
Human plasma	93.9%	98.5%	106.4%	105.6%	103.4%	114.6%
Rat Plasma	98.0%	108.6%	100.1%	107.2%	103.2%	104.1%

Chapter III

Xanthine Oxidase and Cardiovascular Risk in Obese Children

3.1 Introduction:

Obesity rates in the United States among children and adolescents ages 2-19 years old have risen nearly 3-fold since 1980; to a rate of nearly 17% in 2010.[111] A high rate of obesity in children has led to an increased cardiovascular disease (CVD) risk, for example, a population based study showed that nearly 70 percent of obese children had at least one risk factor for cardiovascular disease.[35] The pathological mechanisms of how childhood obesity leads to increased risk of CVD are not fully characterized. Oxidative stress is one factor that plays an important role in the cardiovascular system and controls endothelial function, vascular tone and cardiac function. The major sources of vascular oxidative stress occur through the generation of reactive oxygen species (ROS) by the enzymes nicotinamide adenine dinucleotide phosphate oxidase (NADPH oxidase), uncoupled nitric oxide synthase (NOS), and xanthine oxidase (XO).[112,113] ROS generated from XO, such as superoxide anion, are known to affect endothelial function by sequestering the endogenous vasodilator nitric oxide (NO). For example, NO-stimulated blood flow was increased and endothelial dysfunction was reversed when XO was inhibited by allopurinol in adult smokers[114] and patients with diabetes[115], which shows that XO plays a role in CVD in adults. However, little is known about how oxidative stress pathways, such as XO, influence cardiovascular risk factors in children.[116] The primary objective of this study was to determine if plasma XO activity is increased in obese children compared to normal weight children. The secondary objective was to evaluate if XO activity is associated with CVD risk factors in children by studying the correlations between XO activity and CVD risk factors and cytokine levels.

3.2 Methods:

This was a cross-sectional study of 42 children and adolescents (mean age = 12 ± 3 years) from the Minneapolis-St. Paul metropolitan area who were categorized into two groups, normal weight and obese, based on age- and sex-specific BMI percentiles.[117] Data were collected between 2007 and 2012. Normal weight subjects were age- and gender-matched, were classified as having a BMI >5th and <85th BMI percentile (n=22), and participated in a study evaluating cardiovascular risk factors among families. Obese subjects were classified as having a BMI ≥95th BMI percentile (n=20) and were recruited from the University of Minnesota Amplatz Children's Hospital Pediatric Weight Management Clinic. The protocol was approved by the University of Minnesota Institutional Review Board and consent and assent was obtained from parents and participants, respectively.

Height and weight were obtained using a standard stadiometer and electronic scale, respectively, with participants wearing light clothes and no shoes. BMI was calculated as weight in kilograms divided by height in meters squared. Waist circumference was measured midway between the base of the ribs and the superior iliac crest, to the nearest 0.5 cm, taken in duplicate and the mean values were used in the analyses. Seated blood pressure was obtained after 5 min of quiet rest, on the right arm using an automatic sphygmomanometer. Three consecutive blood pressure measurements were taken with a 3 minute rest between. Blood pressure was then averaged. Blood samples were collected after a minimum 8-hour fast. Lipids, glucose, and insulin assays were conducted with standard procedures at the Fairview Diagnostic Laboratories,

Fairview-University Medical Center (Minneapolis, MN), a Centers for Disease Control and Prevention–certified laboratory. Homeostasis model assessment-insulin resistance (HOMA-IR) was calculated using methods previously described.[118] Flow-mediated dilation of the brachial artery (FMD) was measured in a subset of the participants (n=16) as described previously.[119]

Cytokine and oxidative stress markers were measured using a Luminex multiplex bead array assay. Measurement of oxidative stress and inflammation blood markers in plasma included oxidized LDL (Mercodia, Winston-Salem, NC), C-reactive protein (CRP) (Immundiagnostik AG, Bensheim, Germany), interleukin-6 (IL-6) (Quantikine HS; R&D Systems, Minneapolis, MN), leptin, monocyte chemotactic protein-1 (MCP-1), serpin E1, adiponectin, resistin, and factor D. Plasma was stored frozen at −70 °C until assayed at the University of Minnesota Cytokine Reference Laboratory (Clinical Laboratory Improvement Amendments licensed) using enzyme-linked immunosorbent assay. Oxidized LDL, measured in this fashion, is a reflection of both minimally and fully oxidized LDL particles. The intra- and inter-assay coefficients of variation were as follows: oxidized LDL 5.5–7.3 and 4.0–6.2, respectively; CRP 5.5–6 and 11.6–13.8, respectively; IL-6 6.9–7.8 and 6.5–9.6, respectively.

Plasma XO activity was determined by measuring the XO-specific conversion of lumazine to isoxantholumazine. Briefly, reaction mixtures containing 100µL plasma and 100 µL of 20µM lumazine in 50mM potassium phosphate buffer (pH=7.4) were incubated at 37°C for one hour followed by addition of 200µL methanol (with umbelliferone as internal standard) to stop the reaction and remove the proteins. After

centrifugation and filtration, the supernatants were saved for HPLC analysis of isoxantholumazine. 100 µL of the supernatant was injected onto a 250mm YMC-Pack Phenyl column and fluorescence was measured on a Waters 474 Scanning Fluorescence Detector set at Excitation wavelength=340nm and Emission wavelength=400nm. One Unit of XO activity is defined as the production of one micromole of uric acid per minute at 25°C. Xanthine oxidase activity was normalized for total protein in the plasma samples.

Statistical Analyses: Student's t-test was used to determine the differences between obese and normal weight children in regards to plasma XO activity and baseline characteristics. Linear regression analysis was used to determine the association between plasma XO activity and cardiovascular risk factors, cytokine levels, and oxidative stress levels. Data are presented as mean ± standard deviation unless stated otherwise. Statistical significance was set at a p-value ≤ 0.05.

3.3 Results:

Baseline characteristics are shown in Table 3.1 Compared to normal weight children, obese children had higher systolic blood pressure (116±12 vs. 104±10 mmHg, $p<0.001$), total cholesterol (168±25 and 150±27 mg/dL, $p=0.03$) LDL cholesterol (104±20 vs. 85±21 mg/dL, $p=0.004$), triglycerides (113±57 vs. 62±21 mg/dL, $p<0.001$) and insulin (13±8 vs. 6±1 mU/L, $p=0.002$), and lower HDL cholesterol (41±9 vs. 53±11 mg/dL, $p<0.001$).

XO was 3.8 fold higher in obese when compared to normal weight children as shown in figure 3.1 (118±21 vs. 31±9 nU/mg protein, $p<0.001$, data is shown in mean ±

SEM). FMD was not different between the obese and normal weight children (9.2±2.6 vs. 10.5±5 %). In a subset of subjects (n=16), plasma cytokine and adipokine levels were measured (Table 3.2). Compared to normal weight children, obese children had higher leptin (53.3±25 vs. 6.5±5 ng/mL, $p<0.01$), and lower MCP-1 (80±42 vs. 289±86 pg/mL, $p<0.01$) and serpin E1 (16±20 vs. 103±22 ng/mL, $p<0.01$), and a trend toward lower adiponectin (11.2±3 vs. 16.5±5 μg/mL, $p=0.05$)(Table 3.2). Cardiovascular risk factors that were positively associated with XO activity were BMI Z-score ($R=0.41$, $p<0.01$), waist circumference ($R=0.41$, $p<0.01$), and oxidized LDL ($R=0.57$, $p=0.05$). CVD risk factors/adipokines that were negatively associated with XO activity were HDL ($R=-0.32$, $p=0.04$), adiponectin ($R=-0.53$, $p=0.04$), and MCP-1 ($R=-0.59$, $p=0.02$)(Table 3.3).

3.4 Discussion:

Childhood obesity is associated with cardiovascular disease risk factors such as elevated systolic blood pressure, LDL, triglycerides, and insulin, and low HDL levels. In addition, obese children have adverse levels of cytokines/adipokines (i.e. elevated leptin, CRP, IL-6, and a reduction in adiponectin).[120] In this study we examined the association of childhood obesity and cardiovascular risk factors on XO activity as a marker of oxidative stress. We directly measured XO activity in the plasma by measuring the conversion of lumazine to isoxantholumazine instead of measuring plasma uric acid levels as an indirect method of quantitating XO activity. Using a direct method to measure XO is preferable because there are less conflicting variables as compared to using uric acid levels, which can change based on differences in diet and the ability to eliminate uric acid via the kidneys. The results show that XO activity was significantly

increased in obese children and adolescents (3.8 fold increase in XO activity) and that this XO activity was significantly associated with CVD risk factors such as BMI Z-score, waist circumference, HDL, and oxidized LDL and with the cytokines adiponectin and MCP-1.

These findings are consistent with previous studies in an obese pediatric population whereby in vivo xanthine oxidase activity was increased, as assessed by in vivo caffeine phenotyping strategies;[32] and high serum uric acid concentrations were associated with metabolic syndrome and cardiovascular risks in similar pediatric populations. (Kong and Ford and Pacifico) We observed that adiponectin was inversely associated with XO activity. This finding is similar to previous studies whereby plasma uric acid concentration (a surrogate for XO activity) was inversely proportional to adiponectin concentrations.[121-124] Surprisingly we observed that MCP-1 activity was inversely associated with XO activity (Table 3). In vitro studies in whole blood and in mononuclear cells demonstrated that MCP-1 is up-regulated in the presence of reactive oxidative intermediates that are produced by xanthine oxidase.[125] Thus one would anticipate that higher xanthine oxidase enzyme activity would lead to more reactive oxygen species available to increase MCP-1 expression. A limitation of our study is that we were unable to determine in vivo plasma nitric oxide concentrations due to its instability. Nitric oxide, unlike XO, is a negative regulator of MCP-1 expression. Codoner et al. observed that nitric oxide production is increased in obese children, which is contrary to what is observed in obese adults.[126] It is plausible that the obese children in our population have elevated NO levels which would serve as a better surrogate for

MCP-1 expression. There was no correlation of FMD or systolic blood pressure (SBP) with XO activity, and this could be due to an elevated NO level seen in the obese children. An elevated NO level in the obese group would counteract the increase in ROS due to increased XO activity and lead to no net change in dilation of the arteries.

In our study, we observed that HDL concentrations were inversely associated with XO activity. In vitro studies by Chander and Kapoor, demonstrated that HDL can inhibit xanthine oxidase activity by 43% in an in vitro rat liver microsomal system. Thus the higher the HDL the lower the xanthine oxidase activity, which would decrease the generation of reactive oxygen species associated with this enzyme.[127] This inhibitory effect of HDL on XO activity could mean that future studies looking at XO activity should control for HDL levels. A positive correlation was observed between XO activity and oxidized LDL in our study, and this was expected because ROS produced by XO are known to be sources of oxidation for LDLs. Oxidized LDL is elevated in severe pediatric obesity[128] (Nyberg) and is associated with cardiovascular risk factors and insulin resistance in children and adolescents.[129] (Huang and Nyberg) This positive correlation between XO activity and oxidized LDL indicates that XO may play a role in atherosclerosis risk in childhood obesity because oxidized LDLs penetrate the endothelium and form plaques.[130,131]

In conclusion, plasma XO activity in the obese group was increased by 3.8-fold as compared to the normal weight group and was correlated with the CVD risk factors waist circumference, HDL, oxidized LDL and with the cytokines adiponectin and MCP-1. Results of this study provide evidence of a substantial increase in plasma XO activity in

obese children, which could be a factor contributing to increased CVD risk in the context of pediatric obesity. The results of this study could provide a basis for targeting and inhibiting XO as a measure for preventing CVD in obese children and adolescents. Further studies are needed to confirm these findings and to see if inhibiting XO in childhood obesity decreases CVD risk.

Table 3.1 Baseline Characteristics

	Weight Classification		
	Lean (n=22)	**Obese (n=20)**	**p-value**
Gender (% females)	36	35	0.93
Age (years)	12 ± 3	12 ± 3	0.6
Height (cm)	155 ± 16	155 ± 15	0.92
Weight (kg)	48 ± 16	85 ± 32	<0.001
Body mass index (kg/m^2)	19 ± 3	33 ± 8	<0.001
Body mass index Z-score	0.28 ± 0.7	2.4 ± 0.4	<0.001
Waist circumference (cm)	69 ± 10	108 ± 19	<0.001
Systolic blood pressure (mm Hg)	104 ± 10	116 ± 12	<0.001
Diastolic blood pressure (mm Hg)	57 ± 10	61 ± 10	0.07
Heart rate (beats/min)	74 ± 9	76 ± 11	0.67
Total cholesterol (mg/dl)	150 ± 27	168 ± 25	0.03
High-density lipoproteins (mg/dl)	53 ± 11	41 ± 9	<0.001
Low-density lipoproteins (mg/dl)	85 ± 21	104 ± 20	0.004
Triglycerides (mg/dl)	62 ± 21	113 ± 57	<0.001
Glucose (mg/dl)	86 ± 7	85 ± 6	0.24
Insulin (mU/l)	6 ± 5	13 ± 8	0.002
Homeostasis model of assessment - insulin resistance	1.4 ± 1.1	2.8 ± 1.8	0.004
Baseline Brachial Diameter (mm)	3.6 ± 0.8	3.2 ± 0.3	0.24
Flow-mediated dilation (%)	10.5±5	9.2±2.6	0.587

Data are presented as mean ± standard deviation

Table 3.2 Baseline Cytokine and Oxidative Stress Marker Levels

	Weight Classification		
	Lean (n=7)	**Obese (n=9)**	**p-value**
Leptin (ng/mL)	6.5 ± 5	53.3 ± 25	<0.01
Monocyte chemotactic protein-1 (pg/mL)	289 ± 86	80 ± 42	<0.01
Serpin E1 (ng/mL)	103 ± 22	16 ± 20	<0.01
Adiponectin (µg/mL)	16.5 ± 5	11.2 ± 3	0.05
C-reactive protein (mg/L)	0.4 ± 0.55	4.89 ± 6.12	0.06
Oxidized low density lipoproteins* (U/L)	76 ± 19	97 ± 30	0.18
Resistin (ng/mL)	8.0 ± 4	6.8 ± 3	0.51
Factor D (ng/mL)	2.4 ± 0.5	2.3 ± 0.4	0.94

*lean(n=5) and for obese(n=7)

Data are presented as mean ± standard deviation

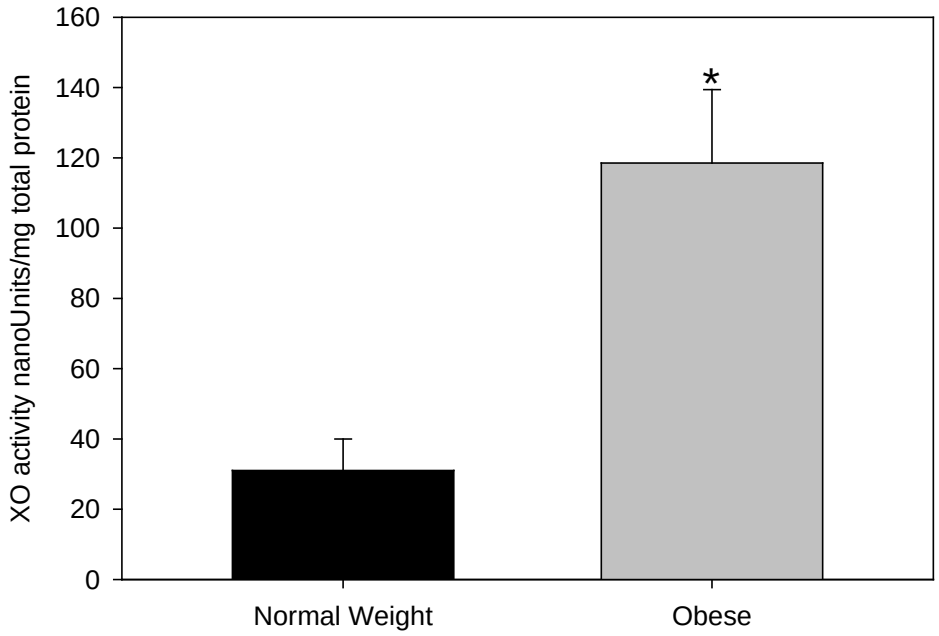

Figure 3.1 Plasma xanthine oxidase (XO) activity in normal weight and obese children.

Isoxantholumazine production from normal weight (n=22) and obese (n=20) plasma samples standardized to purified XO standards of known activity. One Unit of XO activity is defined as the production of one micromole of uric acid per minute at 25°C. Data are means ± SEM. *, $p < 0.001$ compared to the normal weight group.

Table 3.3 Correlations Between Xanthine Oxidase Activity and Oxidative Stress Makers and Cytokines

Cardiovascular disease risk factor or cytokine	R	p-value
Body mass index (n=42)	0.26	0.10
Body mass index Z-score (n=42)	0.41	<0.01
Waist circumference (n=42)	0.41	<0.01
Systolic blood pressure (n=42)	0.13	0.41
Diastolic blood pressure (n=42)	0.02	0.88
Heart rate (n=17)	0.45	0.07
Total cholesterol (n=41)	0.04	0.82
High-density lipoproteins (n=41)	-0.32	0.04
Low-density lipoproteins (n=41)	0.08	0.60
Triglycerides (n=41)	0.29	0.07
Glucose (n=41)	-0.18	0.27
Insulin (n=39)	-0.04	0.78
Homeostatis model assessment - insulin resistance (n=39)	0.06	0.71
Baseline Brachial Diameter (n=17)	-0.18	0.49
Flow-mediated dilation (n=16)	-0.14	0.61
Oxidized low-density lipoproteins (n=12)	0.57	0.05
C-reactive protein (n=16)	0.07	0.78
Adiponectin (n=16)	-0.53	0.04
Factor D (n=16)	0.27	0.31
Leptin (n=16)	0.29	0.27
Monocyte chemotactic protein-1 (n=16)	-0.59	0.02
Serpin E1 (n=16)	-0.47	0.06
Resistin (n=16)	-0.31	0.25

Chapter IV
Changes in Xanthine Oxidase Activity and Uric Acid Clearance with Modest and Massive Weight Loss in Adolescents with Severe Obesity

4.1 Introduction:

Obesity rates in the United States among children and adolescents ages 2-19 years old have risen nearly 3-fold since 1980; to a rate of nearly 17% in 2010.[132] Childhood obesity is known to increase xanthine oxidase (XO) activity and blood pressure, which can modulate the cardiovascular risk in these children.[41,96,133] Subsequently, elevated XO activity leads to increased production of uric acid, which has been shown to modulate blood pressure in a two-phase mechanism. [43] The first phase of blood pressure modulation is uric acid dependent, whereby uric acid induces the renin-angiotensin system (RAS), which leads to acute vasoconstriction and ultimately atherosclerosis. This second phase results in chronic hypertension and is uric acid independent and sodium dependent. Therefore, studying the effects of uric acid and xanthine oxidase before the uric acid independent second phase of hyperuricemic hypertension is crucial to determining whether treatment of hyperuricemia is beneficial to treating obesity-mediated hypertension.

Elevated XO activity and uric acid levels are known to be correlated with obesity, but it is not known whether obesity actually causes increases in XO and uric acid. Studying the effect of weight loss on XO activity, uric acid, and blood pressure will give us greater insight into the mechanism of how obesity increases cardiovascular risk. Additionally, studying these effects in a pediatric population allows for the examination of the effect of weight loss on uric acid-mediated changes in blood pressure before chronic hypertension has developed. Weight loss can be achieved in a variety of ways; including diet modification, pharmacological intervention, or bariatric surgery. Diet

intervention via meal replacement therapy (MRT) has been shown to be effective at moderately reducing weight in both obese adolescents and adults in a short period of time leading to reductions in weight varying from 5-10% after 2-4 months.[76,77] Bariatric surgery, such as Roux-En-Y gastric bypass (RYGB) surgery has been shown to be safe and effective, with 2-3 year BMI reductions ranging from 25-87% in adolescents with severe obesity.[134] Owing to the large difference in the amount of weight lost between MRT and RYGB, evaluating these treatments together represents a unique opportunity to determine if a greater degree of weight loss would have a larger effect size on uric acid-mediated changes in blood pressure. Weight loss has also been shown to reduce the elevated cytokine levels and inflammation seen in obese adolescents.[135] Cytokines, including interleukin-6 and tumor necrosis factor-alpha, have been shown to regulate XO expression. [65] Therefore, changes in the levels of cytokines after weight loss may lead to changes in XO activity and blood pressure, which makes these cytokines a factor to measure to account for any changes in XO activity that may occur after weight loss.

The primary objective of this study was to determine if modest and/or massive weight loss in youth with severe obesity would reduce blood pressure via changes in xanthine oxidase activity and plasma uric acid levels. In addition to its production, uric acid's elimination via the kidneys is also a key contributor to changes in plasma uric acid levels; therefore, we also measured uric acid clearance. Creatinine clearance was also measured to estimate kidney function and glomerular filtration rate (GFR) before and after weight loss after MRT to account for any changes in uric acid clearance.

4.2 Methods:

This was an ancillary study within the context of two larger clinical trials in which 16 adolescents (mean age = 15 ± 2 years) received meal replacement therapy over a period of four weeks and 11 adolescents (mean age = 17 ± 2 years) received RYGB. Subjects that received MRT were recruited from the Pediatric Weight Management Clinic at the University of Minnesota Masonic Children's Hospital. Subjects that received RYGB were recruited from Cincinnati Children's Hospital Medical Center. Outcomes measured at baseline and four weeks after MRT or one year after RYGB included weight loss, blood pressure, plasma xanthine oxidase activity, plasma uric acid (MRT only), uric acid clearance (MRT only), and creatinine clearance (MRT only). Meal replacement therapy consisted of 2 frozen entrees (Weight Watchers, Smart Ones®), 3 Slim-Fast® shakes per day, and subjects were allowed to have 2 servings of fruit and 3 servings of vegetables per day (other than peas, corn or potatoes) that they provide themselves (equating to approximately 1370 kcals per day).

Parental consent and child assent were obtained from participants in both studies and the respective protocols were approved by each sites' Institutional Review Board. Height and weight were obtained using a standard stadiometer and electronic scale, respectively, with participants wearing light clothes and no shoes. BMI was calculated as weight in kilograms divided by height in meters squared. Waist circumference was measured midway between the base of the ribs and the superior iliac crest, to the nearest 0.5 cm, taken in duplicate and the mean values were used in the analyses. Seated blood pressure was obtained after 5 min of quiet rest, on the right arm using an automatic sphygmomanometer. Three consecutive blood pressure measurements were taken with a

3 minute rest between. Blood pressure was then averaged. Blood samples were collected after a minimum 8-hour fast. In the subjects that received MRT, lipids, glucose, and insulin assays were conducted with standard procedures at the Fairview Diagnostic Laboratories, Fairview-University Medical Center (Minneapolis, MN), Centers for Disease Control and Prevention–certified laboratory. Cytokine and oxidative stress markers were measured using a Luminex multiplex bead array assay. Measurement of oxidative stress and inflammation blood markers in plasma included tumor necrosis factor-alpha (TNF-α) and interleukin-6 (IL-6). Plasma was stored frozen at −70 °C until assayed at the University of Minnesota Cytokine Reference Laboratory (Clinical Laboratory Improvement Amendments licensed) using enzyme-linked immunosorbent assay.

Plasma XO activity was determined by measuring the XO-specific conversion of lumazine to isoxantholumazine. Briefly, reaction mixtures contained 100µL plasma and 100 µL of 80µM lumazine in 50mM potassium phosphate buffer (pH=7.4) and were incubated at 37°C for three hours followed by addition of 400µL methanol (with umbelliferone as internal standard) to stop the reaction. After centrifugation and filtration, the supernatants were saved for HPLC analysis of isoxantholumazine. 100 µL of the supernatant was injected onto a 250mm YMC-Pack Phenyl column and fluorescence was measured on a Waters 474 Scanning Fluorescence Detector set at Excitation wavelength=340nm and Emission wavelength=400nm.

Statistical Analyses:

Paired t-tests were used to compare the changes before and after intervention for variables of interest including plasma XO activity. Linear regression analysis was used to determine the associations between changes in uric acid vs. changes in blood pressure and uric acid clearance vs. creatinine clearance. Data are presented as mean ± standard error unless stated otherwise. Statistical significance was set at a p-value ≤ 0.05.

4.3 Results:

Meal Replacement: Baseline and post-intervention characteristics are shown for MRT in Table 4.1A. After the meal replacement intervention, participants had a decrease in body weight (3.7% decrease, 109±16 vs. 105±14 kg, p<0.0001) and BMI (3.4% decrease, 38.7±4 vs. 37.4±3 kg, p<0.0001), total cholesterol (169±34 and 155±33 mg/dL, p=0.0066), HDL cholesterol (43±12 vs. 39±11 mg/dL, p=0.0009), and LDL cholesterol (103±31 vs. 94±28 mg/dL, p=0.023). Systolic blood pressure (SBP) was reduced but did not achieve statistical significance (122±10 vs. 119±10 mm Hg, p=0.34); whereas diastolic blood pressure (DBP) was unchanged (69±8 vs. 69±10, p=0.86). As shown in Figure 4.1 plasma XO activity was significantly reduced by 9.8% after four weeks of MRT (0.045±0.007 vs. 0.040±0.007 pmol/hour, p-value= 0.0159). Creatinine clearance was reduced but did not achieve statistical significance (199±17 vs. 160±17 mL/min, p-value= 0.10, Figure 4.2), uric acid clearance was significantly decreased by 39% (8.9±1.4 vs. 5.4±0.7 mL/min, p-value= 0.006, Figure 4.3), and plasma uric acid was reduced but did not achieve statistical significance (8.5±0.5 vs. 8.1±0.6 mg/dL, p-value= 0.38, Figure 4.4). Changes in plasma uric acid levels between baseline and after intervention were compared to changes in SBP and DBP, but no significant relationships were found

(Figure 4.5). Plasma IL-6 and TNF-α levels were measured (Table 4.1A) at baseline and after MRT. IL-6 decreased by 19% (2.2±1.2 vs. 1.8±0.7 pg/mL, p=0.03) and tumor necrosis factor-alpha was unchanged (2.6±0.8 vs. 2.6±0.6 pg/mL, p-value= 0.69).

Bariatric Surgery: Baseline and post-intervention characteristics are shown for RYGB in Table 1B. BMI decreased by 37% (58.2±2.3 vs. 36.5±2.1 kg/m^2, p-value= <0.0001), systolic blood pressure decreased by 10% (124±2.7 vs. 111±2.8 mm Hg, p-value= 0.0005), and diastolic blood pressure decreased by 13% (76±3.0 vs. 66±1.7 mm Hg, p-value= 0.029). As shown in Figure 4.1, plasma XO activity was unchanged after bariatric surgery (0.035±0.002 vs. 0.033±0.002 pmol/hour, p-value= 0.12). Plasma IL-6 and TNF-α levels were measured (Table 4.1B) at baseline and after RYGB. Interleukin-6 decreased by 69% (1.1±0.3 vs. 0.34±0.3 pg/mL, p-value= 0.0316) and tumor necrosis factor-alpha was unchanged (1.0±0.2 vs. 0.89±0.3 pg/mL, p-value= 0.52).

4.4 Discussion:

It has been demonstrated that childhood obesity elevates xanthine oxidase activity, and that XO activity is correlated with pediatric cardiovascular risk factors.[96,133] In obese children, elevated XO activity often results in the subsequent increase in plasma uric acid concentrations which may modify cardiovascular disease risk by modifying blood pressure through activation of the renin angiotensin system. [43,96,133,136] Because obesity causes an elevation in XO activity and is a risk factor for cardiovascular disease in children, we hypothesized that weight loss would reverse the increase in XO activity that is seen in obesity, ultimately lowering both plasma uric acid concentrations and blood pressure. In this study we report that modest weight loss with MRT results in

reduction of XO activity, while massive weight loss with RYGB did not significantly alter XO activity.

It was not surprising to observe that weight loss via MRT resulted in the lowering of xanthine oxidase activity. There are multiple factors that regulate XO activity such as cytokines[65] and lipopolysaccharide (LPS)[66,67]. The cytokine IL-6 plays an important regulatory role in the expression of xanthine oxidase, due the presence of IL-6 binding sites in the promoter region of the xanthine oxidoreductase gene.[62] Therefore the 19% decrease in plasma IL-6 concentrations may be partially responsible for the lowering in overall XO activity due to a reduction in XO expression, but the correlation between the changes in IL-6 were not significantly associated with the changes in XO activity (data not shown). Contrary to other studies, we observed weight loss mediated changes only in IL-6 and not in TNF- α concentrations (Table 4.1A). Jung et al. and Ziccardi et al. both reported significant decreases in multiple inflammatory cytokines including IL-6 and TNF-α after weight loss of at least 10% of baseline weight, but our MRT population averaged a weight loss of only 3.7%.[137,138] Therefore, TNF-α may not have been as sensitive to weight loss as IL-6 and/or our MRT subjects may not have lost enough weight to observe TNF-α changes. Another possible factor that may regulate plasma XO activity is plasma LPS concentration generated by bacteria. Kurosaki et al. reported that mice exposed to LPS induced XO expression in various organs and tissues, therefore changes in the gut microbiota and LPS exposure from this source may contribute to changes in XO activity in our study.[67] For example, a high fat diet or high consumption of dietary fats, which are common in subjects with extreme obesity, may also increase

LPS levels by altering the gut microbiota to express more gram negative bacteria.[71,72] MRT may be partially responsible for changes in XO activity by altering the gut microbiota to decrease LPS production because the MRT used in our study has less fat than an average diet (19% fat in MRT vs. 33% in an average U.S. diet), and MRT has been shown in previous studies to lower LPS levels in obese adolescents.[139]

Modest weight loss via diet replacement therapy lowered plasma XO activity by 9.8%, but XO activity was surprisingly unchanged after a substantial amount of weight was lost via bariatric surgery. The primary explanation for the dissimilar results on the impact on weight loss on xanthine oxidase activity may be due to the surgery induced changes in the gut microbiota. While MRT may lead to decreases in LPS, RYGB surgery has been shown to increase LPS expression by altering the gut microbiota to a population which has more LPS-expressing gram negative bacteria.[82] This change in gut microbiota is likely due to changes in the amount of free bile acids in the intestinal tract. In the normal enterohepatic circulation, conjugated bile acids are secreted into the duodenum to mix with fatty acids to aid in their digestion, and any free bile acids are then reabsorbed in the ileum. After RYGB serum bile acids increase and this is attributed to the fact that bile acids and food have less time to mix and more free bile acids are reabsorbed at the ileum.[81] More free bile acids will select for bile-tolerant bacteria, such as the gram negative proteobacteria, which will lead to increased LPS and XO expression. [82] Therefore, opposing changes in the gut microbiota between the different weight loss methods led to differing effects on xanthine oxidase activity.

Uric acid has been shown to be important in regulating blood pressure in children with hypertension.[136] Plasma uric acid levels depend on its production rate via XO and its elimination rate primarily via the kidneys. We observed that XO activity is reduced after weight loss (Figure 4.1). However both plasma uric acid and blood pressure were unchanged after MRT intervention (Table 4.1A and Figure 4.4). Therefore, we measured creatinine clearance and uric acid clearance before and after weight loss to determine if weight loss is affecting plasma uric acid levels via changes in kidney function and the elimination of uric acid. Uric acid clearance decreased by 39% with weight loss (Figure 4.3) and it is mirrored by a reduction in creatinine clearance (Figure 4.2). These decreases are likely due to reversion of renal hemodynamic overload with glomerular hyperfiltration that is seen with obesity. For example, it has been previously shown that weight loss decreases creatinine clearance in obese adults with metabolic syndrome and diabetic nephropathy.[140,141] The decrease in uric acid clearance that we observe may be due to changes in the filtration rate of uric acid, as creatinine clearance (a common surrogate for glomerular filtration rate) is related uric acid clearance ($r^2 = 0.47$, Figure 4.6); or there may be changes in the reabsorption of uric acid, as the change in uric acid clearance is greater than the change in creatinine clearance uric acid (39% decrease vs. 19% decrease) and uric acid is known to be highly reabsorbed by multiple transporters. The discrepancy between the decreases in creatinine clearance and uric acid clearance indicate that there is an increase in uric acid reabsorption. If uric acid reabsorption was saturated before weight loss, decreasing the filtration rate of uric acid would effectively increase the percentage of uric acid that is reabsorbed, and this would compound the

change in GFR to generate a greater change in uric acid clearance. Therefore, future studies should continue to measure uric acid clearance as changes in creatinine clearance underestimate the changes in uric acid clearance due to the reabsorption of uric acid.

Overall, the opposing changes in uric acid production and elimination resulted in no net change in plasma uric acid levels, which would explain why there was no change in blood pressure after weight loss. Having no net change in plasma uric acid was surprising, as our subjects had very high levels of plasma uric acid (mean of 8.5mg/dL at baseline) that would be considered as hyperuricemic even in adults (cutoff values of hyperuricemia are 5.8mg/dL in women and 6.8mg/dL in men). Hyperuricemia persisted in our subjects even after weight loss, which would indicate that the mean decrease of BMI by 1.3 was not sufficient to lower cardiovascular risk by affecting either plasma uric acid or blood pressure. This high level of uric acid in our subjects may lead to damage to the kidneys via RAS activation and lead to sodium dependent hypertension in the future. Therefore, the decrease in XO activity due to weight loss was not sufficient to lower plasma uric acid, and administration of ace inhibitors or angiotensin receptor blockers to counter-act the effects of uric acid mediated RAS activation should be considered to lower the cardiovascular risk of uric acid. Early intervention and treatment of hyperuricemia before sodium dependent hypertension is established is crucial, as treatment of hyperuricemia in adults has been shown to not be as effective of a measure to treat hypertension compared to children (3.3 mm Hg decrease in SBP vs. 6.9 mm Hg decrease in SBP).[136,142]

A limitation of this study was the fact that blood pressure did not significantly change in the MRT cohort due to several factors. The amount of weight lost was relatively low (3.7%) and it is unknown if further weight loss via this method would lead to significant changes in plasma uric acid and blood pressure. Blood pressure in our MRT cohort were also slightly elevated, but most were not considered as hypertensive ($\geq 95^{th}$ percentile) and this may have been a contributing factor to why we did not see a significant change in blood pressure with MRT. In our RYGB cohort, decreases in blood pressure were observed after one year, but plasma uric acid levels and uric acid clearance were not measured in this cohort. Therefore, uric acid's effect on blood pressure in this cohort could not be ascertained. Including uric acid levels from plasma and urine in future studies would enable us to determine how RYGB alters uric acid levels and its effects on blood pressure after weight loss. Future studies should include an evaluation of LPS levels with XO activity in future weight loss studies to determine if decreased LPS could be responsible for changes in XO activity due to MRT or RYGP.

In conclusion, the relationship between uric acid and blood pressure in obesity remains inconclusive, as changes in XO activity and uric acid levels did not correlate with changes in blood pressure after weight loss. However, weight loss via MRT in an obese pediatric population did lead to decreases in uric acid production by lowering xanthine oxidase activity and decreases in uric acid clearance via a decrease in GFR and a likely increase in reabsorption. The opposing changes of lower production and elimination may explain why we did not find significant changes in plasma uric acid levels or blood pressure. In our RYGB cohort, XO activity did not decrease and blood

pressure was significantly reduced, but without uric acid levels and clearance, the relationship between XO, uric acid, and blood pressure could not be determined. Differences in the changes to XO activity between the methods of weight loss may be due to opposing changes in the gut microbiota between the different weight loss methods, but the ultimate role this plays in uric acid levels and its effect on blood pressure has yet to be determined.

Table 4.1A Baseline and Post-MRT Characteristics

	Baseline (n=16)	After MRT (n=16)	p-value
Gender (% females)	69	N/A	-
Age (years)	14.6 ± 2	14.8 ± 2	-
Height (cm)	168 ± 8	167 ± 8	-
Weight (kg)	109.2 ± 16	105.2 ± 14	**<0.0001***
Body mass index (kg/m^2)	38.7 ± 4	37.4 ± 3	**<0.0001***
Waist circumference (cm)	110 ± 12	108 ± 12	0.36
Systolic blood pressure (mm Hg)	122 ± 10	119 ± 10	0.34
Systolic blood pressure percentile (%)	73 ± 18	70 ± 23	0.53
Diastolic blood pressure (mm Hg)	69 ± 8	69 ± 10	0.86
Diastolic blood pressure percentile (%)	59 ± 22	64 ± 25	0.39
Heart rate (beats/min)	76 ± 7	74 ± 10	0.37
Total cholesterol (mg/dl)	169 ± 34	155 ± 33	**0.0066***
High-density lipoproteins (mg/dl)	43 ± 12	39 ± 11	**0.0009***
Low-density lipoproteins (mg/dl)	103 ± 31	94 ± 28	**0.023***
Triglycerides (mg/dl)	119 ± 58	114 ± 56	0.68
Glucose (mg/dl)	84 ± 8	81 ± 7	0.30
Insulin (mU/l)	24 ± 12	23 ± 9	0.60
IL-6 (pg/mL)	2.2 ± 1.2	1.8 ± 0.7	**0.03***
TNF-alpha (pg/mL)	2.6 ± 0.8	2.6 ± 0.6	0.69

Data are presented as mean ± standard deviation
*p-value<0.05

Table 4.1B Baseline and Post-RYGB Characteristics

	Baseline (n=11)	After RYGB (n=11)	p-value
Gender (% females)	73	N/A	-
Age (years)	16.7 ± 0.5	17.7 ± 0.5	-
Body mass index (kg/m^2)	58.2 ± 2	36.5 ± 2	**<0.0001**
Systolic blood pressure (mm Hg)	124 ± 2.7	111 ± 2.8	**0.0005**
Diastolic blood pressure (mm Hg)	76 ± 3.0	66 ± 1.7	**0.0294**
Interleukin-6 (pg/mL)	1.1 ± 0.3	0.34 ± 0.3	**0.0316**
Tumor necrosis factor-alpha (pg/mL)	1.0 ± 0.2	0.89 ± 0.3	0.52

Figure 4.1 Plasma xanthine oxidase activity before and after intervention.

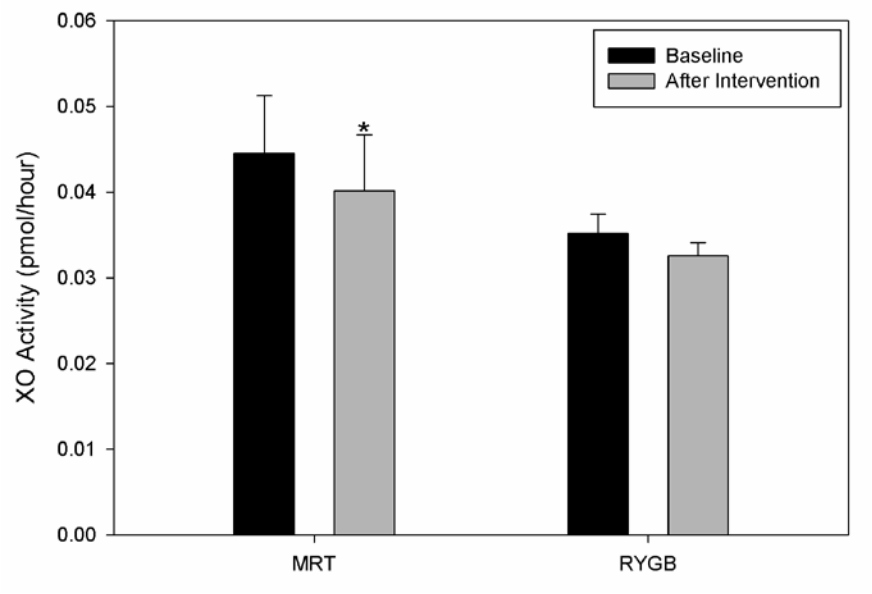

Plasma XO activity was determined by isoxantholumazine production from plasma. A paired t-test was used to determine the differences between subjects at baseline and subjects after intervention for changes in XO activity. n=16 for MRT and n=11 for RYGB. Data are means ± SEM. *p-value= 0.0159 compared to the baseline.

Figure 4.2 Creatinine Clearance at Baseline and After MRT Intervention

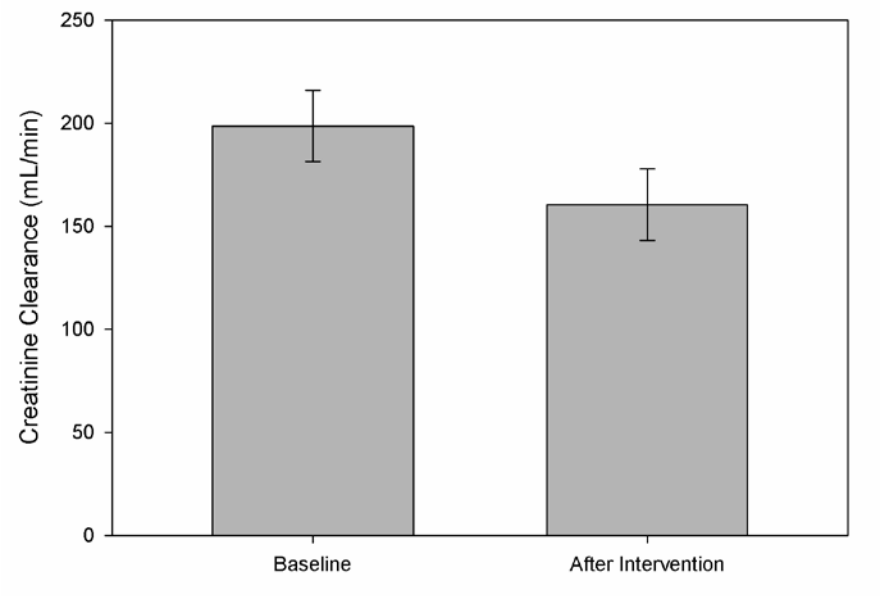

A paired t-test was used to determine the differences between subjects at baseline and subjects after intervention for changes in creatinine clearance. Creatinine clearance was calculated using serum creatinine levels and urine creatinine levels (1-6 hour collection interval) by using the following equation:
(Urine creatinine/plasma creatinine) x (urine volume/collection interval)
n=14
p-value= 0.10

Figure 4.3 Uric Acid Clearance at Baseline and After MRT Intervention

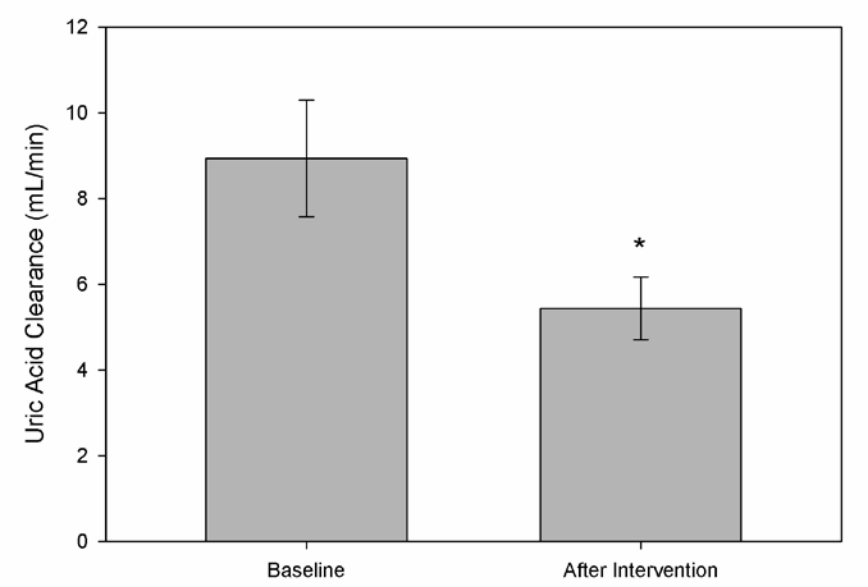

A paired t-test was used to determine the differences between subjects at baseline and subjects after intervention for changes in uric acid clearance. Uric Acid clearance was calculated using serum creatinine levels and urine creatinine levels (1-6 hour collection interval) by using the following equation:
(Urine uric acid/plasma uric acid) x (urine volume/collection interval)
n=14
*p-value= 0.006

Figure 4.4 Plasma Uric Acid Levels at Baseline and After MRT Intervention

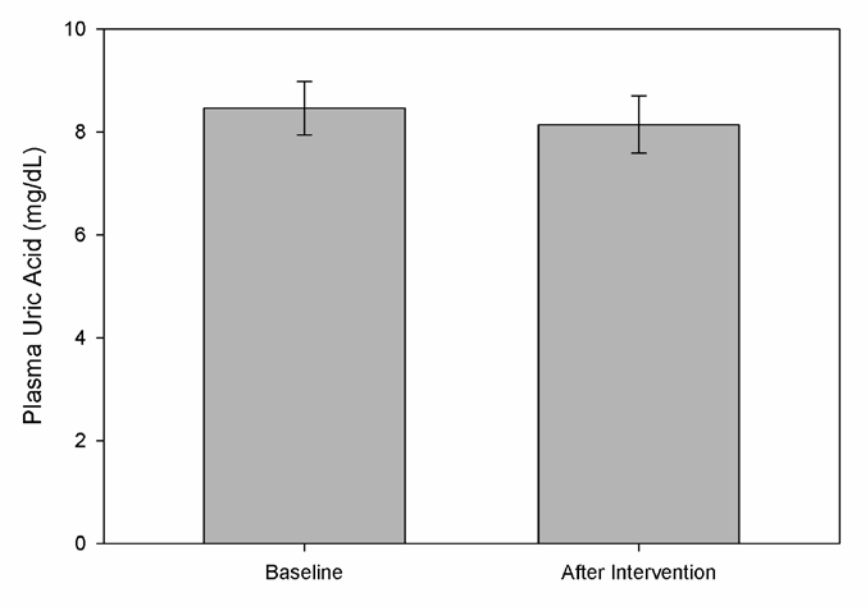

A paired t-test was used to determine the differences between subjects at baseline and subjects after intervention for changes in uric acid.
n=16
p-value= 0.38

Figure 4.5 Linear Regression of the Changes in Uric Acid vs. the Change in Blood Pressure in MRT Subjects

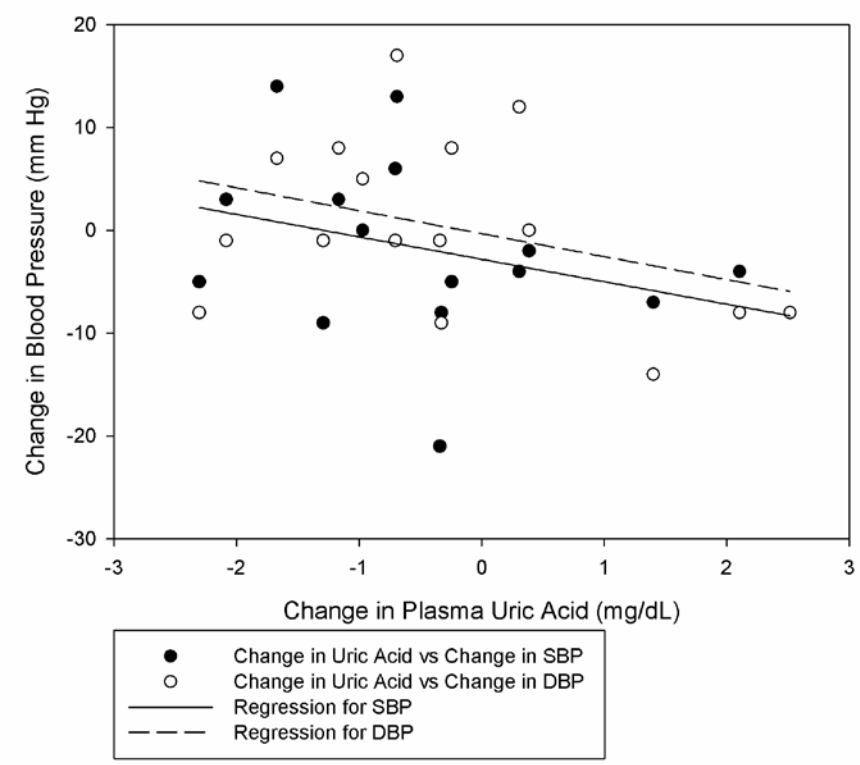

Linear regression analysis was used to determine the association between the change in uric acid clearance vs. systolic blood pressure (r^2= 0.12) and vs. diastolic blood pressure (r^2= 0.13).

Figure 4.6 Creatinine vs. Uric Acid Clearance in MRT Subjects

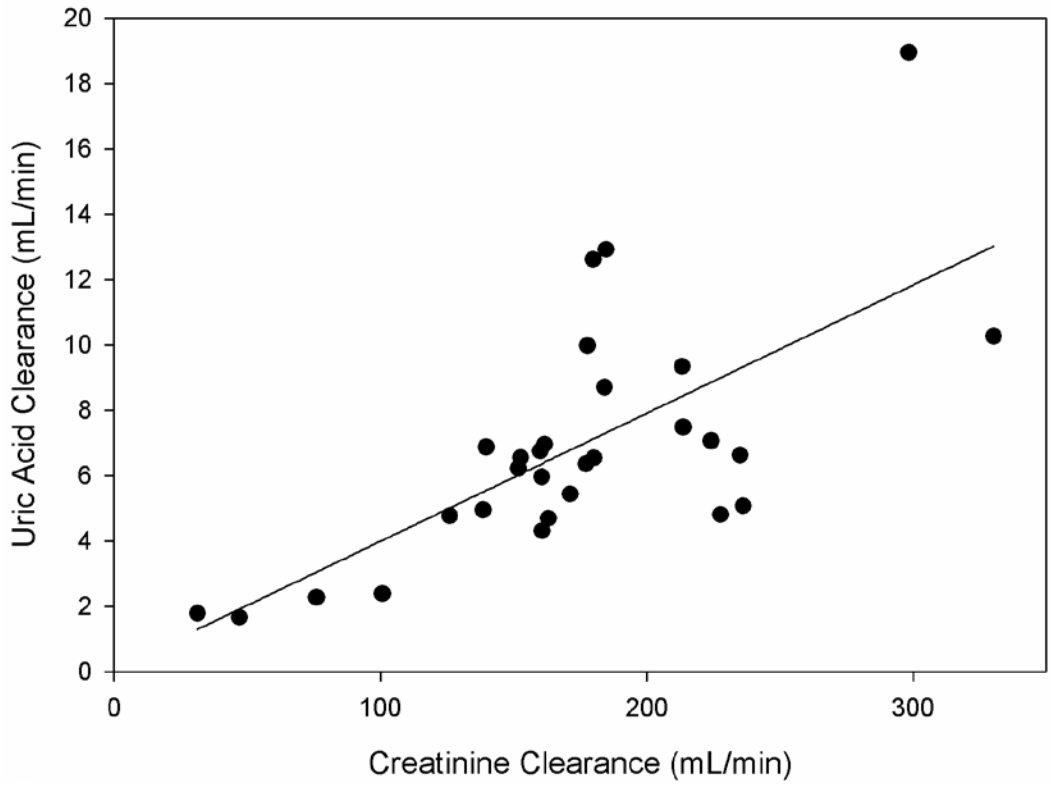

Linear regression analysis was used to determine the association between uric acid clearance and creatinine clearance. $r^2 = 0.47$

Chapter V
Development and Optimization of Screening Assays for UDP-Glucuronosyltransferase Inhibition and Time-Dependent Inhibition of Cytochrome P450s in Hepatocytes

5.1 Introduction

Cytochrome P450s (CYPs) and glucuronosyltransferases (UGTs) are major families of oxidative and conjugative drug metabolizing enzymes. In vitro phenotyping with human liver microsomes (microsomes contain the endoplasmic reticulum of cells which that contain membrane-associated drug metabolizing enzymes) in conjunction with specific inhibitors of drug metabolizing enzymes is a common strategy to identify and determine the enzymes responsible for a drug's metabolism. For CYPs, there are many selective inhibitors available to probe specific CYP isozymes (table 5.1). However, with UGTs, only a few selective inhibitors have been identified; which makes the use of microsomes to identify the UGTs responsible for a drug's metabolism very difficult. Therefore, the primary objective of this project was to develop screening assays to identify specific inhibitors of UGTs. The first step in this process is to determine selective substrates for UGTs, which can then be used to identify inhibitors of UGTs. After that, optimization of UGT assays with the addition of alamethacin and albumin will be tested. UGTs are oriented towards the luminal side of the endoplasmic reticulum, and the membrane of the endoplasmic reticulum needs to be disrupted to increase the amount of substrate and uridine 5'-diphospho-glucuronic acid (UDPGA) that reaches the active site of UGTs.[143] Alamethacin can be used to disrupt the membrane of the endoplasmic reticulum because it is an antibiotic peptide that inserts into the membrane and forms pores/channels.[143] The effect of albumin addition to incubations will be tested because it has been found to alter the kinetics of some UGT substrates by sequestering fatty acids that can inhibit UGT activity.[144]

In addition to developing and optimizing screening assays for UGTs, inhibition of CYPs, specifically time-dependent inhibition (TDI) of CYPs, was also studied. TDI of CYPs occurs when a substrate is metabolized to a reactive intermediate that binds to and inactivates the enzyme that produced it. Most studies of TDI in CYPs have been done in microsomes, but we wanted to determine if there were differences in TDI in hepatocyte cell culture compared to human liver microsomes (HLMs). Cell culture, which uses liver cells from donors, is more similar to in vivo conditions than the more artificial HLM system, which may make it a more translatable system to study TDI. For example, cell culture is more similar to in vivo conditions due to the fact that it is a more complete system, in which all transporters are present, while they are not present in HLMs. Therefore, we studied TDI in cell culture to determine if established time-dependent inhibitors in HLMs had similar inhibition potential in cell culture.

Table 5.1: Substrates and Inhibitors of CYPs in humans:

Enzyme	Substrate	Inhibitor
1A2	Theophylline, Caffeine	Fluvoxamine, Furafylline
2B6	Efavirenz, Bupropion	Ticlopidine, Thiotepa
2C8	Repaglinide, Rosiglitazone	Gemfibrozil, Montelukast
2C9	S-Warfarin, Flurbiprofen	Fluconazole, Sulfaphenazole
2C19	Esomeprazole, Lansoprazole	Fluvoxamine, Moclobemide
2D6	Desipramine, Dextromethorphan	Paroxetine, Quinidine, Fluoxetine
2E1	Chlorzoxazone	Disulfiram
3A4/3A5	Midazolam, Triazolam	Atazanavir, Itraconazole, Azamulin

5.2 Methods

General Incubation Conditions

100mM Tris buffer pH 7.4 at 37˚C, 1mM MgCl, 5mM saccharolactone, 0.1mg/ml protein concentration for recombinant UGTs (rUGTs), and 0.2mg/mL protein concentration for HLMs.

Substrate selectivity

Five substrates were tested for substrate selectivity with 12 human recombinant UGTs. The five substrates tested were estradiol, trifluoperazine (TFP), 1-naphthol, propofol, and zidovudine (AZT); these substrates were selected based on a literature search for selective probe substrates for UGTs.[143,145-149] The 12 recombinant UGTs tested were UGTs 1A1, 1A3, 1A4, 1A6, 1A7, 1A8, 1A9, 1A10, 2B4, 2B7, 2B15, and 2B17. Substrate concentrations, incubation times, microsome concentrations, and alamethacin concentrations used are listed in Table 5.2. Total activity was calculated by adding up the production of glucuronide by each UGT isoform, and percentage of total activity was calculated by dividing the production of glucuronide by a single UGT isoform by the total activity.

Table 5.2: Substrates and Incubation Conditions used to Determine Substrate Selectivity

Substrates	Substrate concentration (µM)	Incubation time (min)	Microsome protein concentration (mg/mL)	Alamethacin (µg/mL)
Estradiol	6	20	0.1	25
Trifluoperazine	100	10	0.1	25
1-Naphthol	27	20	0.1	25
Propofol	30	20	0.1	25
Zidovudine	600	10	0.1	25

Effect of Alamethacin Addition and Pre-incubation Times

Incubations were done with or without the addition of 2.5 mg/mL alamethacin in 50% methanol (final concentration of 25 µg/mL). Zero, ten, and twenty minutes pre-

incubation times on ice were tested with the addition of alamethacin. Substrate concentrations used varied between substrates, but ranges included concentrations in the linear range as well as concentrations that were at saturation. Incubation times were the same as those listed in Table X. for each listed substrate. Microsomal protein concentrations were 0.2mg/mL for all incubations.

Effect of Albumin Addition

Incubations were done at 37°C for 20 minutes with or without the addition of bovine or human serum albumin (2% w/v). Substrate concentrations used varied between substrates, but ranges included concentrations in the linear range as well as concentrations that were at saturation (Supplemental table X.). Microsome concentrations and alamethacin concentrations were the same as those listed in Table X. for each listed substrate.

Screening for UGT Inhibition by Antibodies

Incubation conditions were the same as those listed in Table 5.1. Three antibodies were tested for UGT1A1 inhibition along with 2 chemical inhibitors as positive controls. 2 ratios (mg antibody: mg rUGT) or concentrations of inhibitors were used where possible. A ratio of 2:1 was used for antibody 1, 1:1 and 3:1 for antibody 2, and 1.25:1 and 2.5:1 for antibody 3. Concentrations of 50µM and 200µM were used for 4-nitrophenol and 5µM and 20µM silibinin were used as chemical inhibitors. Incubations were done at 37°C and stopped by addition of 2x volume acetonitrile containing internal standard.

TDI of CYPs in Hepatocytes

Four known time-dependent inhibitors of CYPs in HLMs were tested in hepatocyte suspensions and compared to literature values of K_I and k_{inact} in both HLMs and hepatocytes. Paroxetine was used as a time-dependent inhibitor of CYP2D6 and dextromethorphan was used as a probe substrate. Tienilic acid was used as an inhibitor of CYP2C9 and tolbutamide was used as a probe substrate. Mifepristone and troleandomycin were used as inhibitors of CYP3A4 and testosterone was used as a probe substrate. Incubations were done in duplicate for paroxetine and tienilic acid and as a single replicate for mifepristone and troleandomycin at saturating concentrations of probe substrates with 50,000 cells per incubation. Inhibitor pre-incubation times used for paroxetine and tienilic acid were 0, 15, 30, 60, and 120 minutes; and times used for mifepristone and troleandomycin were 0, 10, 20, 30, 45, 60, 90, and 120 minutes. K_{obs} was determined by calculating the slopes of linear regressions of the data, plotted with inhibitor pre-incubation times on the x-axis versus the natural log of the % remaining activity on the y-axis. K_{obs} was then plotted (y-axis) versus inhibitor concentration (x-axis) to determine K_I and k_{inact} which were used to determine inhibition potency (k_{inact}/ K_I).

5.3 Results

Substrate selectivity

As shown in Figure 5.1 the majority of the glucuronidation of estradiol was done by UGT1A1, 72% of total activity, while UGTs 1A3, 1A8, and 1A10 also contributed slightly to the glucuronidation of estradiol with 7.5%, 6.8%, and 11.4% of total activity respectively. If we look at only the UGTs that are expressed in the liver (Figure 5.2), then

only UGT1A1 and 1A3 have noticeable amounts of glucuronidation making up 88% and 9% of the total liver activity respectively. For 1-naphthol the majority of the glucuronidation was done by UGT1A6, 74% of total activity, while UGTs 1A7, 1A8, and 1A9 contributed slightly to the glucuronidation of 1-naphthol with 4%, 6.7%, and 5.4% of total activity respectively. For UGTs expressed in the liver, only UGT1A6 and 1A9 have substantial amounts of glucuronidation, making up 85.5% and 6.3% of the total liver activity respectively. The glucuronidation of propofol was mediated by UGTs 1A7 and 1A9, accounting for 37% and 60.2% of total activity respectively. When we only consider UGTs in the liver, UGT1A9 accounts for 99.5% of total liver activity. For AZT the only UGT that contributed to its glucuronidation was UGT2B7, accounting for 99% of total and liver activity. TFP was only glucuronidated by UGT1A4, accounting for 99% of both the total and liver activity.

Effect of Alamethacin Addition and Pre-incubation Times

For all substrates tested, the absence of alamethacin decreased activity, increased variability between replicates, and made fitting the data accurately not possible. When comparing pre-incubation times with alamethacin in estradiol glucuronidation, having no pre-incubation resulted in an intrinsic clearance (CL_{int}) of 65.1 µL/min/mg, a 10 minute pre-incubation resulted in a slightly increased CL_{int} of 70.6 µL/min/mg, and a 20 minute pre-incubation resulted in a slightly increased CL_{int} of 71.3 µL/min/mg.(Figure 5.3) When TFP glucuronidation is fitted to a substrate inhibition model, having no pre-incubation resulted in K_I of 0.11µM and a CL_{int} of 47.8 µL/min/mg, a 10 minute pre-incubation resulted in a K_I of 0.52µM and a CL_{int} of 44.0 µL/min/mg, and a 20 minute pre-

incubation resulted in an increased K_I of 72µM and a CL_{int} of 53.9 µL/min/mg. (Figure 5.4) When comparing pre-incubation times with alamethacin in 1-naphthol glucuronidation, having no pre-incubation resulted in an CL_{int} of 577 µL/min/mg, a 10 minute pre-incubation resulted in a slightly increased CL_{int} of 611 µL/min/mg, and a 20 minute pre-incubation resulted in a slightly increased CL_{int} of 822 µL/min/mg. (Figure 5.5) When comparing pre-incubation times with alamethacin in propofol glucuronidation, having no pre-incubation resulted in an CL_{int} of 94.3 µL/min/mg, a 10 minute pre-incubation resulted in a slightly increased CL_{int} of 98.7 µL/min/mg, and a 20 minute pre-incubation resulted in a slightly decreased CL_{int} of 71.9 µL/min/mg. (Figure 5.6) When comparing pre-incubation times with alamethacin in AZT glucuronidation, having no pre-incubation resulted in an CL_{int} of 1.00 µL/min/mg, a 10 minute pre-incubation resulted in a slightly increased CL_{int} of 1.17 µL/min/mg, and a 20 minute pre-incubation resulted in an increased CL_{int} of 1.50 µL/min/mg. (Figure 5.7)

Effect of Albumin Addition

For estradiol glucuronidation adding albumin to the incubations altered the kinetics fitting from a substrate activation model to a linear model. (Figure 5.8) The addition of either human or bovine serum albumin to the incubations with TFP decreased CL_{int} from 44.9 µL/min/mg to 20.4 µL/min/mg and 8.3 µL/min/mg respectively. (Figure 5.9) 1-Naphtol incubations with human or bovine serum albumin led to decreased CL_{int} from 957 µL/min/mg to 841 µL/min/mg and 582 µL/min/mg respectively. (Figure 5.10) For propofol incubations the addition of human or bovine serum albumin increased CL_{int} from 128 µL/min/mg to 172 µL/min/mg and 192 µL/min/mg respectively. (Figure 5.11)

AZT incubations with human or bovine serum albumin led to increased CL_{int} from 1.2 µL/min/mg to 6.3 µL/min/mg and 18.8 µL/min/mg respectively. (Figure 5.12)

Screening for UGT Inhibition by Antibodies

As shown in Figure 5.13, antibody 1 showed no inhibition capability of UGT1A1 when compared to control at a 2:1 ratio (97% activity remaining). Antibody 2 showed no inhibition capability at a 1:1 ratio (110% activity of control) or at a 3:1 ratio (110% activity of control). Antibody 3 did inhibit UGT 1A1 activity at both ratios of 1.25:1 (52% activity remaining) and 2.5:1 (20% activity remaining). 4-Nitrophenol showed no inhibition at 50µM (107% activity remaining) and a little inhibition at 200µM (80% activity remaining). Silibinin showed inhibition at both 5µM (48% activity remaining) and 20µM (6% activity remaining).

TDI of CYPs in Hepatocytes

Paroxetine had a maximal inhibition of 75%, k_{inact} = 0.009 min^{-1}, K_I= 0.33µM, and a inhibitory potency = 27 mL/µmol/min. (Figures 5.14-5.15) Tienilic acid had a maximal inhibition of 80%, k_{inact} = 0.03 min^{-1}, K_I= 0.65µM, and a inhibitory potency = 46 mL/µmol/min. (Figures 5.16-5.17) Mifepristone had a maximal inhibition of 55%, k_{inact} = 0.02 min^{-1}, K_I= 5.8µM, and a inhibitory potency = 3.4 mL/µmol/min. (Figures 5.18-5.19) Troleandomycin had a maximal inhibition of 55%, k_{inact} = 0.04 min^{-1}, K_I= 0.28µM, and a inhibitory potency = 143 mL/µmol/min. (Figures 5.20-5.21)

5.4 Discussion

All five of the UGT substrates tested are specific for one UGT in HLMs even though some of these substrates can be metabolized by extrahepatic UGTs. Estradiol is

selective for UGT1A1, TFP for UGT1A4, 1-naphthol for UGT1A6, propofol for UGT1A9, and AZT for UGT2B7 as had been previously reported for each of these substrates. Using these substrates as probes, one can screen for inhibitors of each of the five UGTs these substrates are probing.

The addition of alamethacin to UGT incubations increases activity, decreases variability between samples, and the data can be fitted more accurately. Pre-incubation with alamethacin on ice increased the CL_{int} and decreased km in most cases, but v_{max} varied with 2 substrates increasing with pre-incubation time and 3 substrates decreasing with pre-incubation time. The longer pre-incubation times likely increase the CL_{int} by affecting k_m, but longer pre-incubation times also decreases turnover/v_{max}, likely due to degradation of the microsomes. Therefore, a ten minute pre-incubation time with alamethacin is a good compromise to balance the increase in CL_{int} and decrease in overall turnover/ v_{max}.

The addition of albumin increased the CL_{int} for substrates glucuronidated by UGTs 1A9 and 2B7 as expected, but decreased CL_{int} for substrates glucuronidated for the other UGTs. The decreases in apparent k_m are likely due to increases in protein binding of substrate and lowering of the free fraction of substrate available as shown previously by Walsky et al.[143] Human serum albumin had a slightly smaller effect on propofol and AZT glucuronidation than bovine serum albumin and it is also more costly. Therefore, if albumin is added to incubations, bovine serum albumin should be used instead of human serum albumin. The addition of albumin to incubations has a large effect on substrate binding, which adds another step in order to counteract this effect, and its addition does

not benefit the majority of UGTs. Therefore, the addition of albumin should be reserved for UGTs 1A9 and 2B7, but the binding of all substrates and inhibitors should always be taken into account when adding in albumin.

The use of antibodies as selective inhibitors has been a strategy that has been used for CYP inhibition, but not for UGTs. More and more UGT antibodies are being developed and together with the use of UGT inhibition screening assays, selective UGT inhibitor antibodies can be discovered. Using an estradiol assay, we screened for UGT1A1 inhibitory antibodies. We discovered that UGT1A1 antibody 3 is indeed an inhibitor of estradiol glucuronidation, but much more needs to be done in order to see if it is a selective inhibitor for UGT1A1. The next steps to be taken are to test this UGT1A1 antibody for inhibition of other UGT isoforms to make sure that it does not have any cross-reactivity. Future studies can also use the assays for UGT1A4, UGT1A6, UGT1A9, and UGT2B7 to test for inhibitors of those isoforms.

The inhibition potency of time-dependent inhibitors of CYPs in hepatocytes was less than inhibition potencies in HLMs in all of the tested inhibitors. This lower inhibition potency may be due to efflux of the substrate by transporters in the hepatocytes that are not present in HLMs or that the substrate concentration in the cell at the enzyme active site is different than the concentration added to the media. Therefore, testing for TDI in HLMs may overestimate the inhibition potency of drugs in vivo, which would make testing for TDI in hepatocytes more accurate when translating findings to in vivo settings.

In conclusion, with the five substrates, namely estradiol, TFP, naphthol, propofol, and AZT as probes we can find inhibitors of each of the five UGTs selective for these

substrates. In addition, to optimize the UGT activity assays, the addition of alamethacin (25µg/mL) with a 10 minute pre-incubation time was ideal to increase activity and decrease variability between samples, and the addition of albumin was not needed as it may increase substrate binding and lower the free concentration of substrates which may confound data in inhibition studies, except for studies with UGT1A9 and UGT2B7. Lastly, the inhibition potency of time-dependent inhibitors is dependent on the assay method, with cell culture incubations exhibiting lower inhibition potency.

Figure 5.1

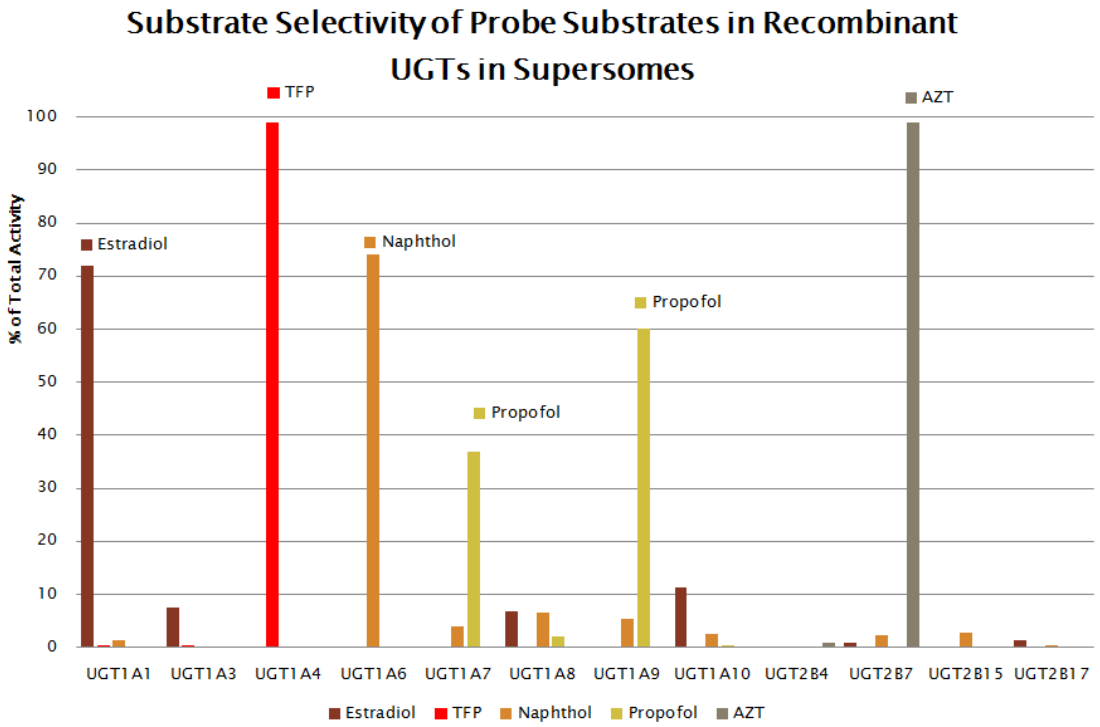

n=3, protein content=0.2mg/mL

Figure 5.2

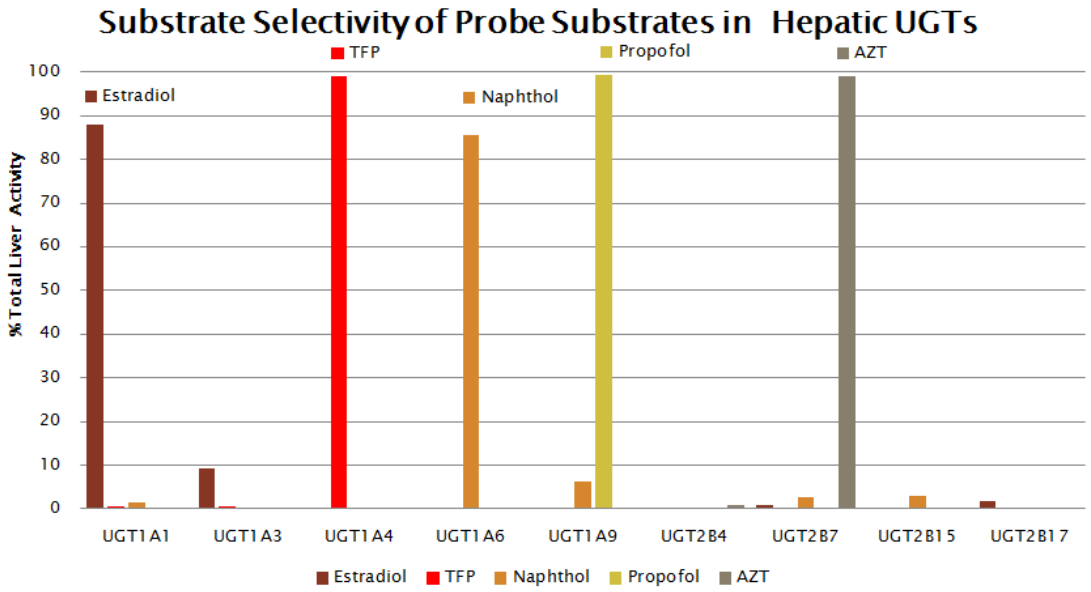

n=3, protein content=0.2mg/mL

Figure 5.3

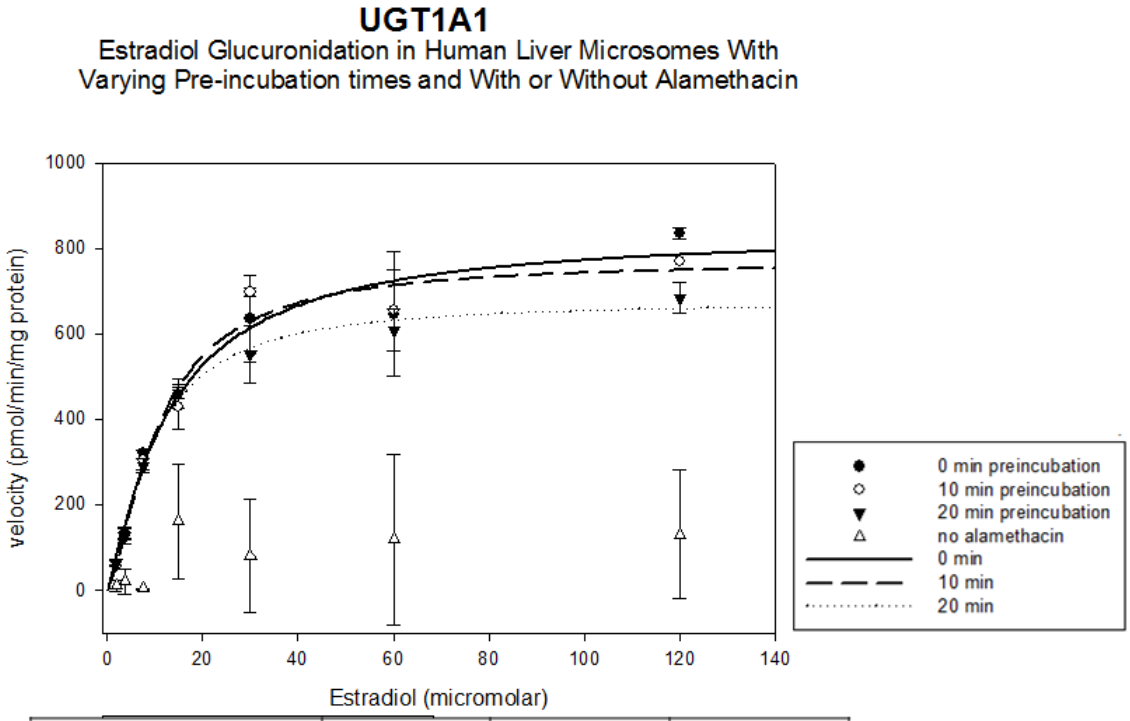

UGT1A1 Estradiol	0 min pre-incubation	10 min pre-incubation	20 min pre-incubation
v_{max} (pmol/min/mg)	840	770	677
S_{50} (μM)	12.9	10.9	9.5

n=3

Figure 5.4

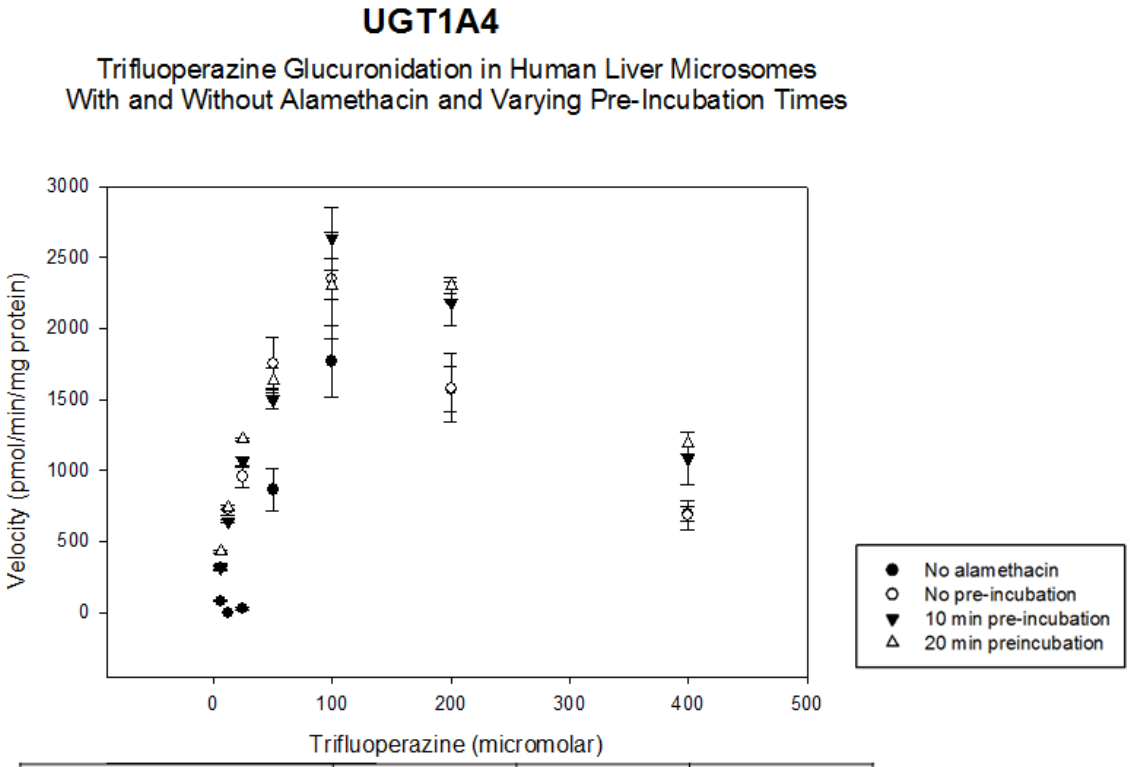

UGT1A4 Trifluoperazine	0 min pre-incubation	10 min pre-incubation	20 min pre-incubation
v_{max} (pmol/min/mg)	$3.3e^{6}$	$1.1e^{6}$	9,800
K_m (µM)	$6.9e^{4}$	$2.5e^{4}$	181.9
K_i (µM)	0.11	0.52	72

n=3

Figure 5.5

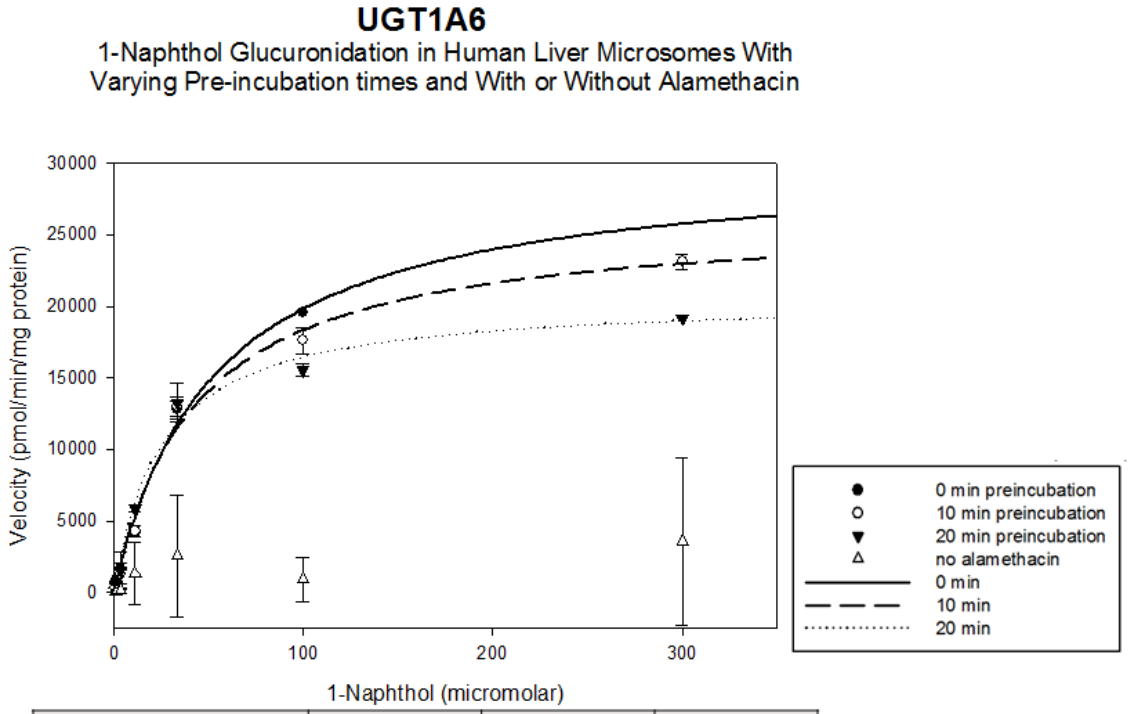

UGT1A6 1-Naphthol	0 min pre-incubation	10 min pre-incubation	20 min pre-incubation
v_{max} (pmol/min/mg)	30,272	26,260	20,561
K_m (µM)	52.5	43	25

n=3

Figure 5.6

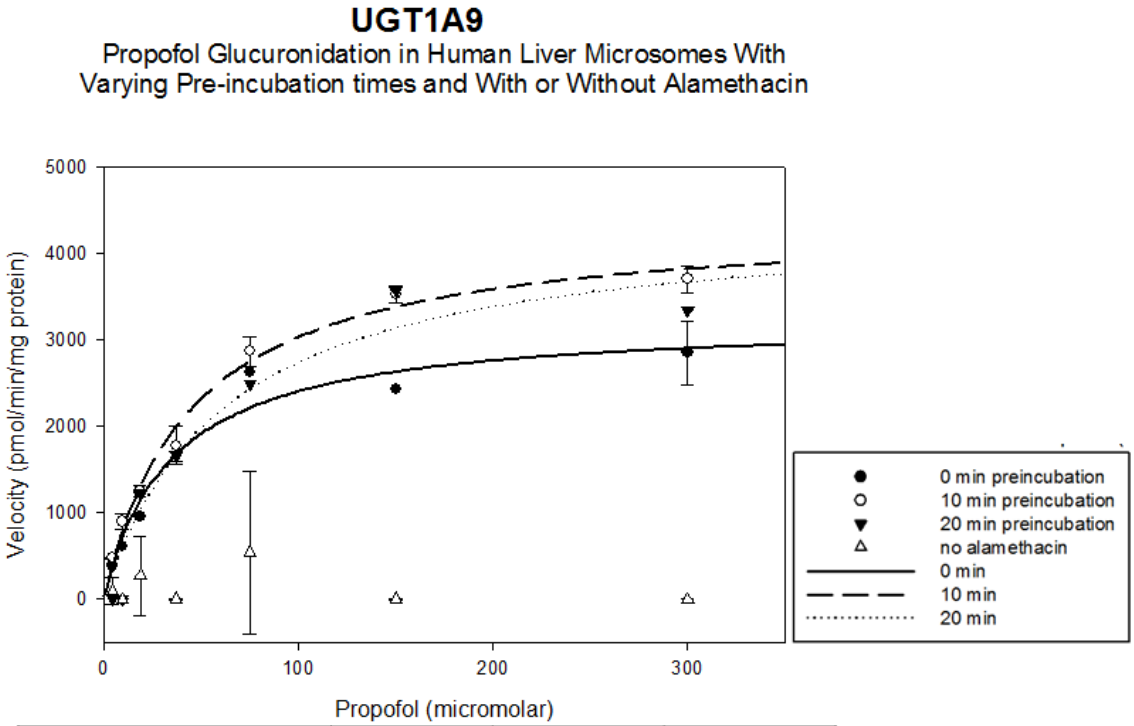

UGT1A9 Propofol	0 min pre-incubation	10 min pre-incubation	20 min pre-incubation
v_{max} (pmol/min/mg)	3,236	4,390	4,431
K_m (µM)	34.3	44.5	61.6

n=3

Figure 5.7

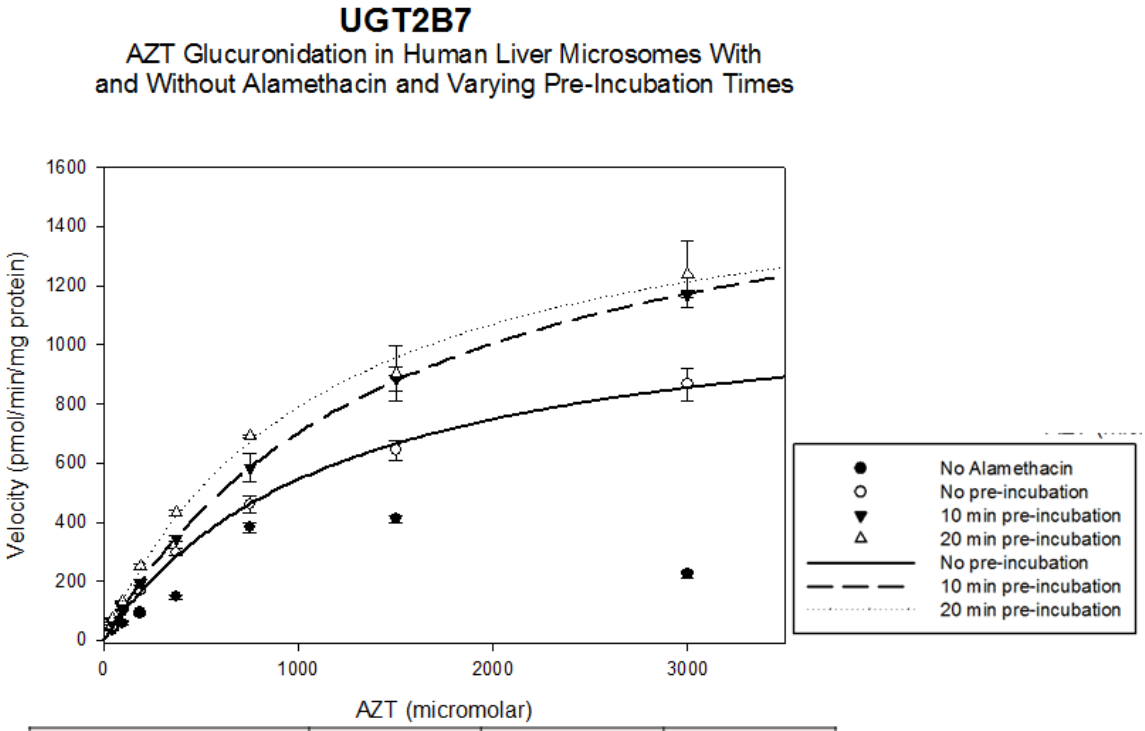

UGT2B7 AZT	0 min pre-incubation	10 min pre-incubation	20 min pre-incubation
v_{max} (pmol/min/mg)	1,193	1,765	1,661
K_m (µM)	1,190	1,514	1,104

n=3

Figure 5.8

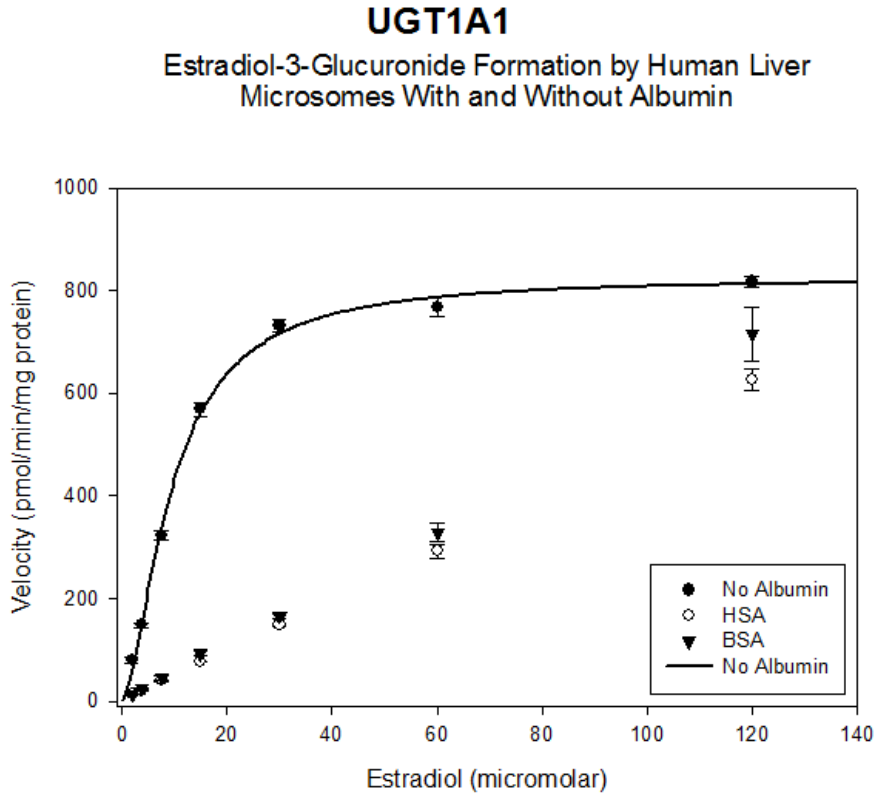

20 min incubation time		No Albumin	Human Serum Albumin	Bovine Serum Albumin
UGT1A1 Estradiol	V_{max} (pmol/min/mg)	825	-	-
	S_{50} (μM)	9.4	-	-

n=3

Figure 5.9

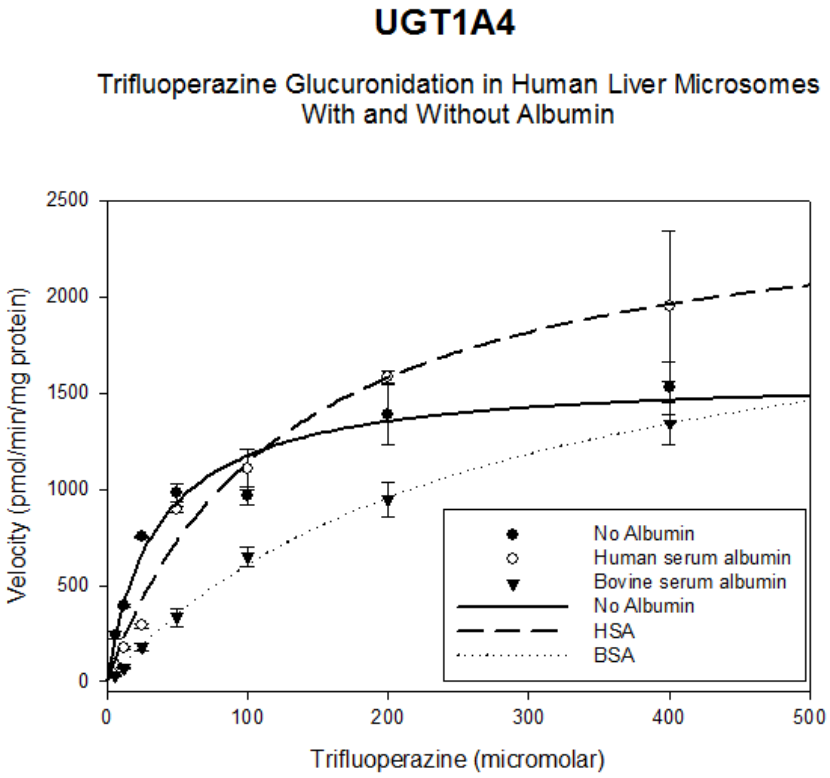

20 min incubation time		No Albumin	Human Serum Albumin	Bovine Serum Albumin
UGT1A4 TFP	V_{max} (pmol/min/mg)	1,590	2,581	2,245
	K_m (µM)	35.4	126.8	269.3

n=3

Figure 5.10

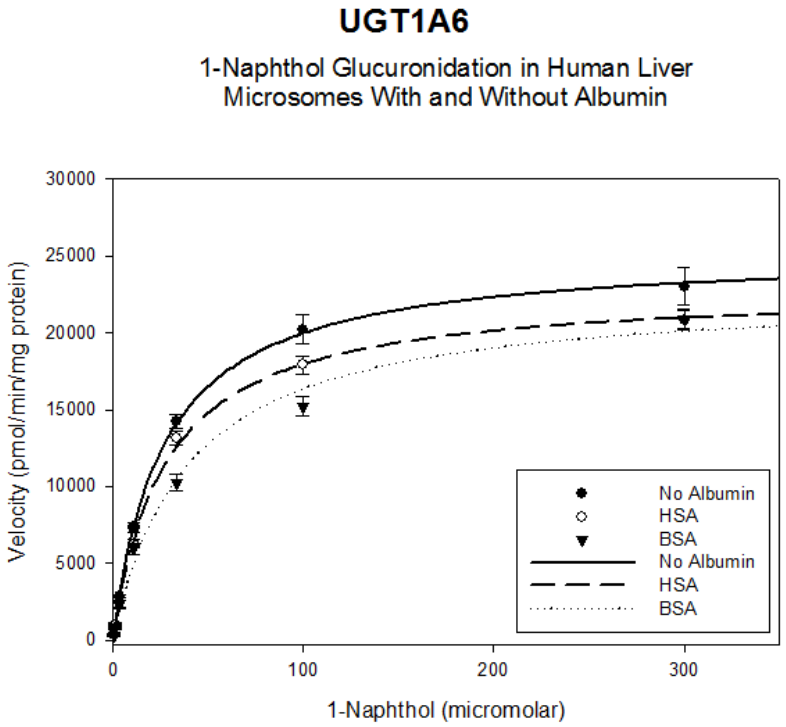

20 min incubation time		No Albumin	Human Serum Albumin	Bovine Serum Albumin
UGT1A6 1-Naphthol	v_{max} (pmol/min/mg)	25,272	22,876	22,728
	K_m (µM)	26.4	27.2	39.0

n=3

Figure 5.11

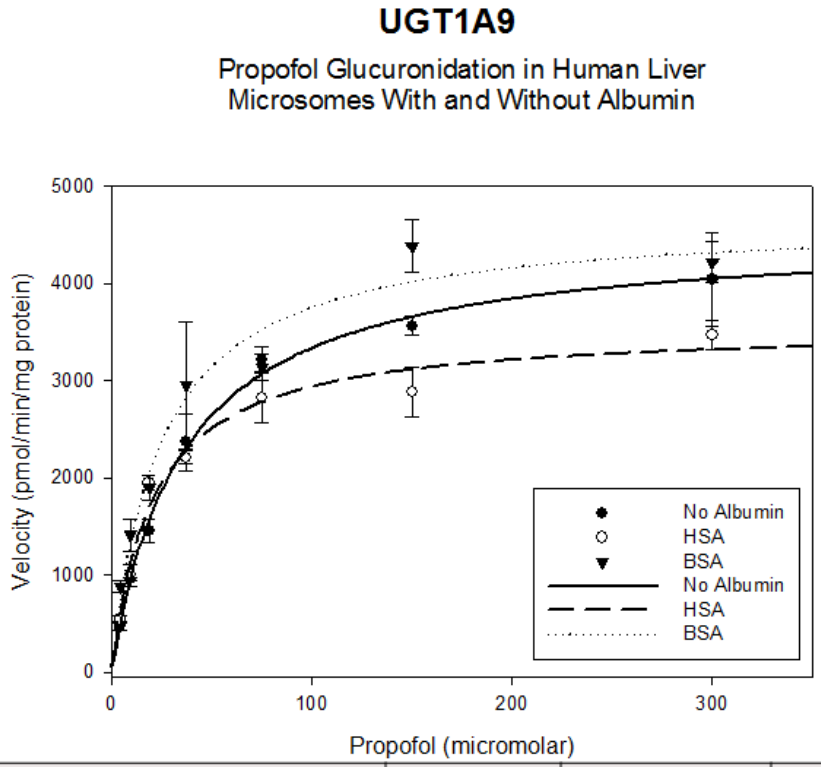

20 min incubation time		No Albumin	Human Serum Albumin	Bovine Serum Albumin
UGT1A9 Propofol	V_{max} (pmol/min/mg)	4,527	3,548	4,669
	K_m (µM)	35.5	20.6	24.3

n=3

Figure 5.12

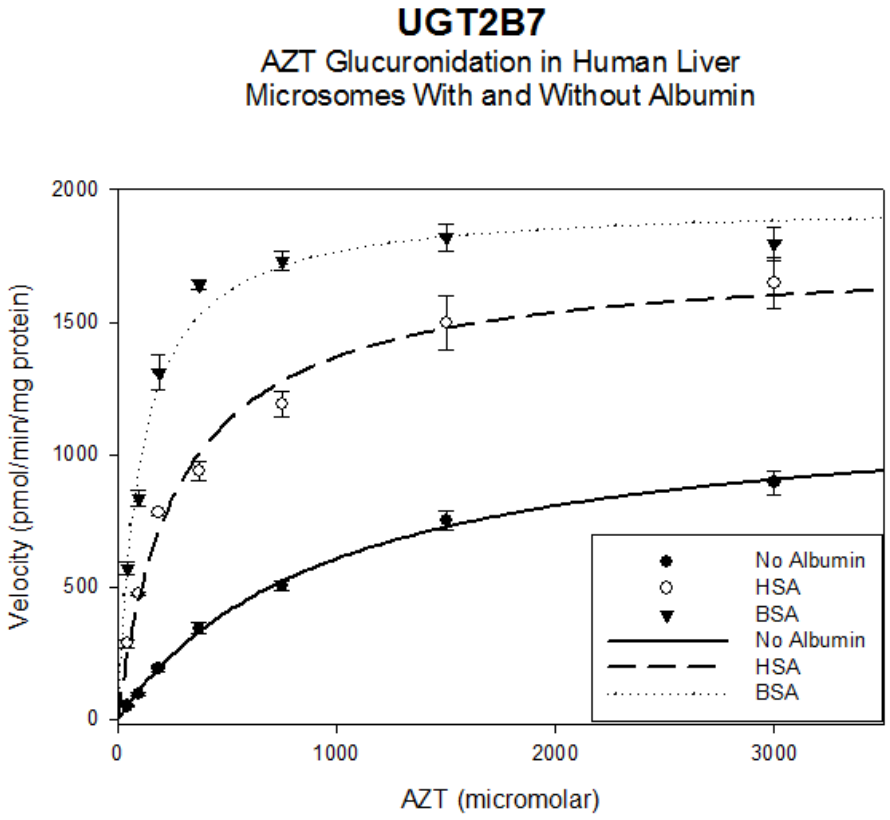

20 min incubation time		No Albumin	Human Serum Albumin	Bovine Serum Albumin
UGT2B7 AZT	V_{max} (pmol/min/mg)	1,199	1,748	1,948
	K_m (µM)	976.8	276.9	103.4

n=3

Figure 5.13

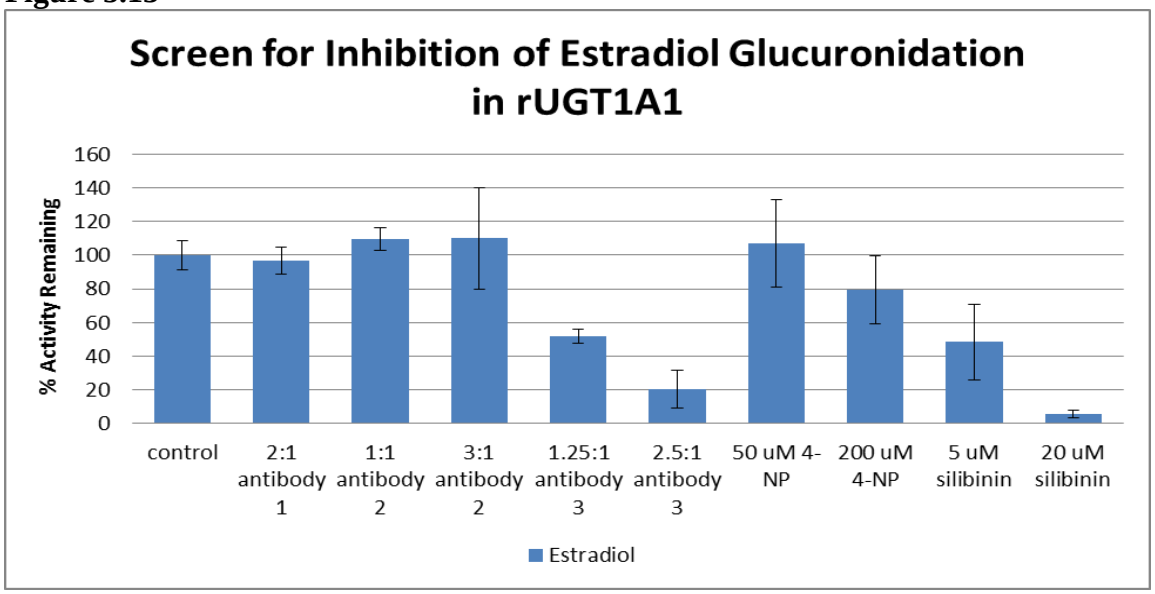

UGT protein content = 0.1mg/mL
n=2

Figure 5.14

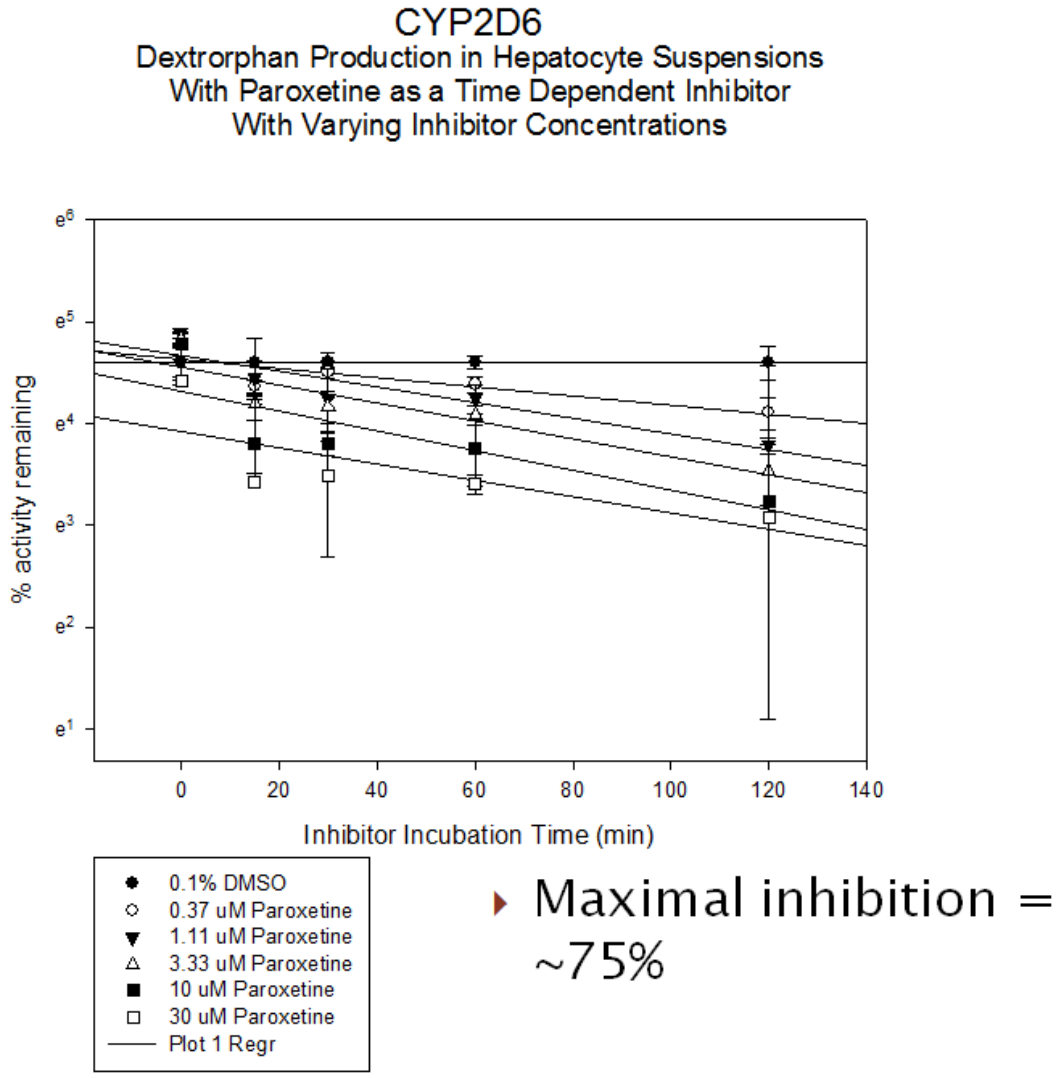

n=2

Figure 5.15

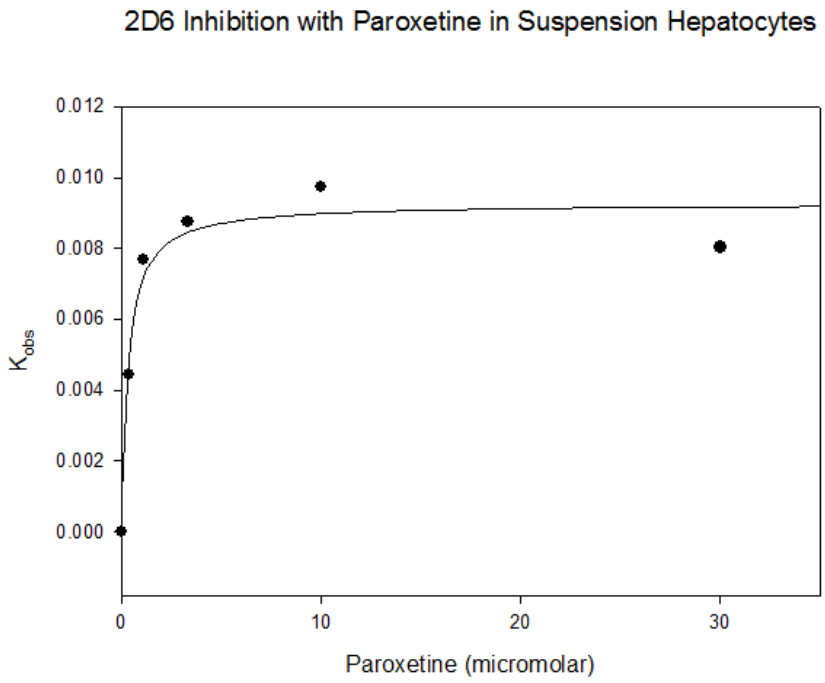

Paroxetine (CYP2D6)	Observed	Reported (hepatocytes)	Reported (HLMs)
k_{inact}	0.009 min^{-1}	-	0.17 min^{-1}
K_I	0.33 µM	0.3-0.5 µM	4.85 µM
k_{inact}/K_I	27 ml/µmol/min	-	35 ml/µmol/min

Figure 5.16

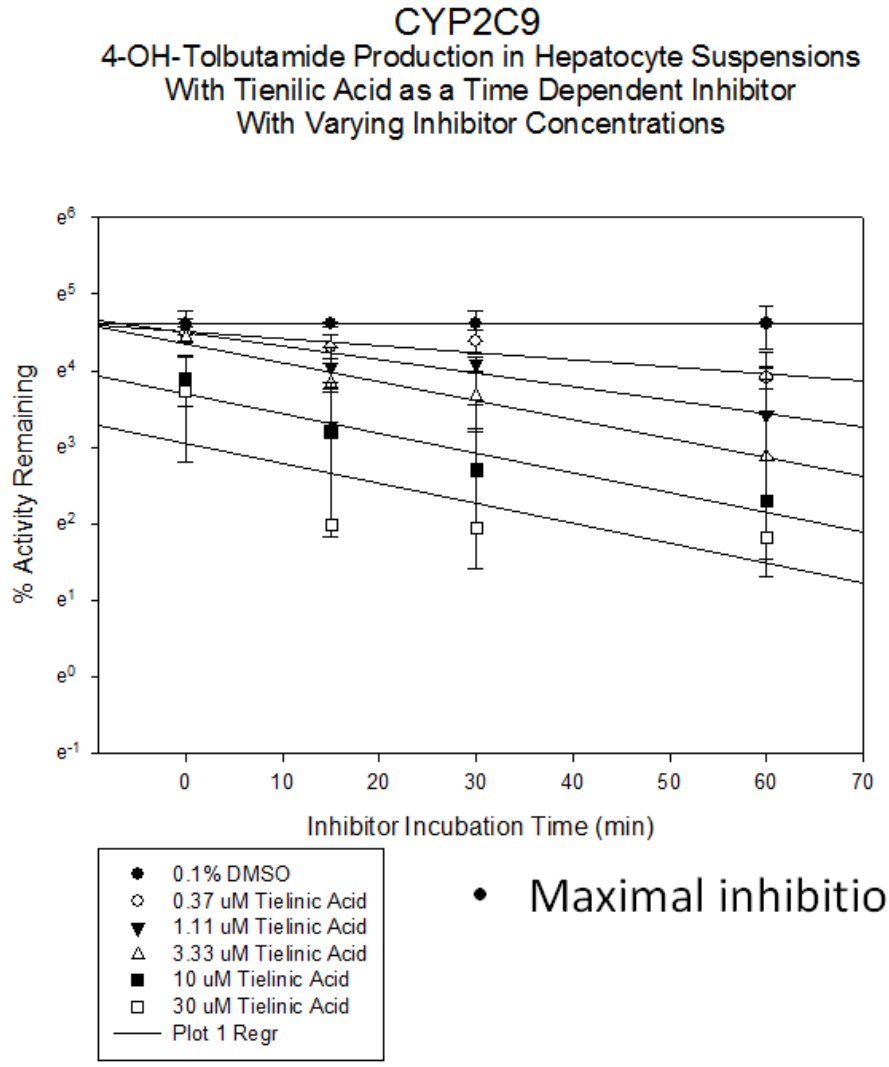

- Maximal inhibition = ~80%

n=2

Figure 5.17

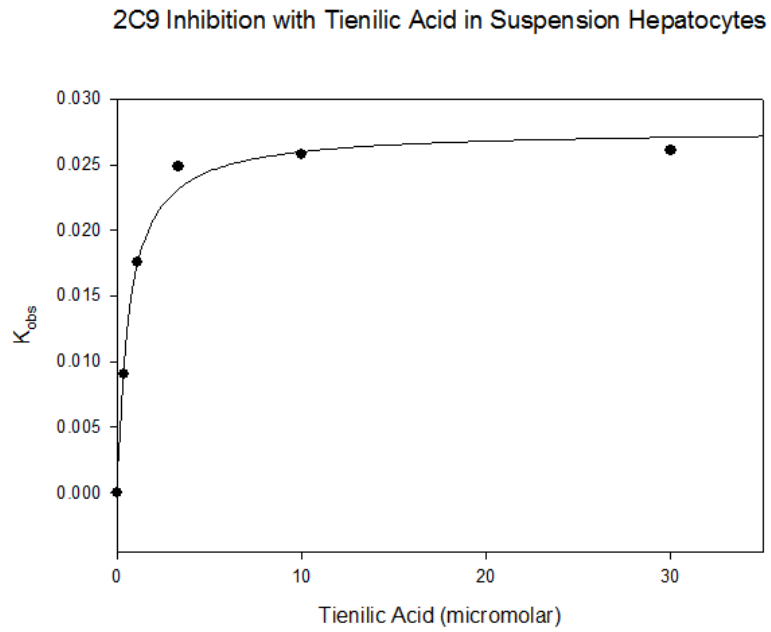

Tienilic Acid (CYP2C9)	Observed	Reported (hepatocytes)	Reported (HLMs)
k_{inact}	0.03 min^{-1}	0.05 min^{-1}	0.21 min^{-1}
K_I	0.65 µM	2 µM	1.8 µM
k_{inact}/K_I	46 ml/µmol/min	25 ml/µmol/min	117 ml/µmol/min

Figure 5.18

CYP3A4 Time-Dependent Inhibition by Troleandomycin in Hepatocyte Suspension With Differing Inhibitor Concentrations

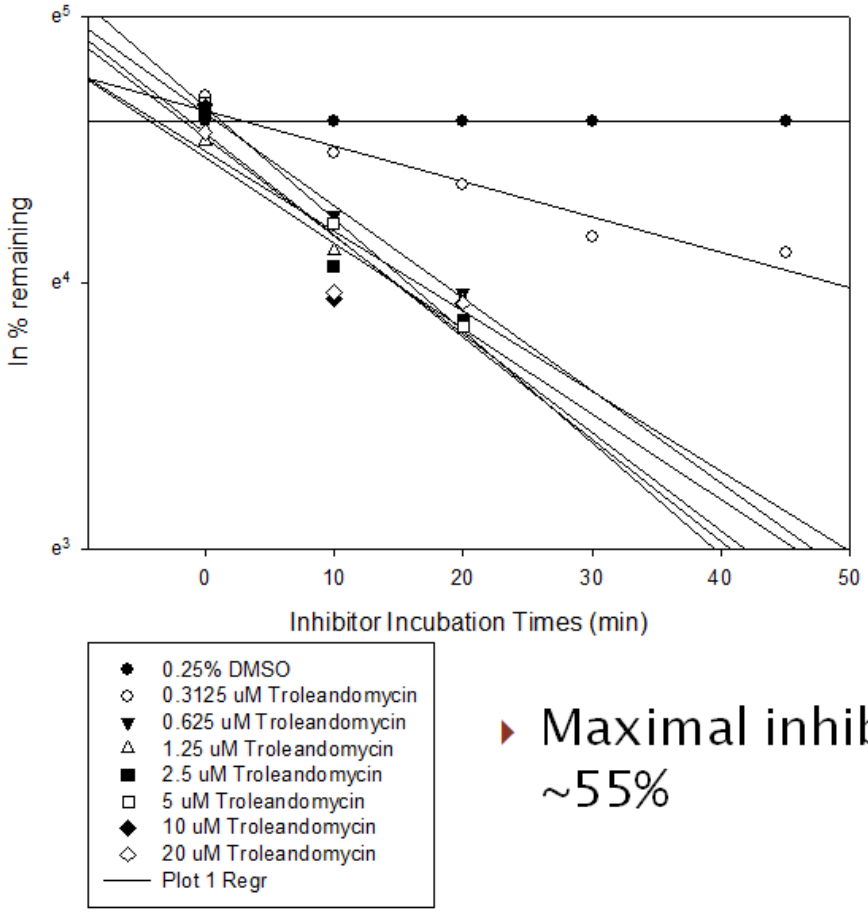

- Maximal inhibition = ~55%

n=1

Figure 5.19

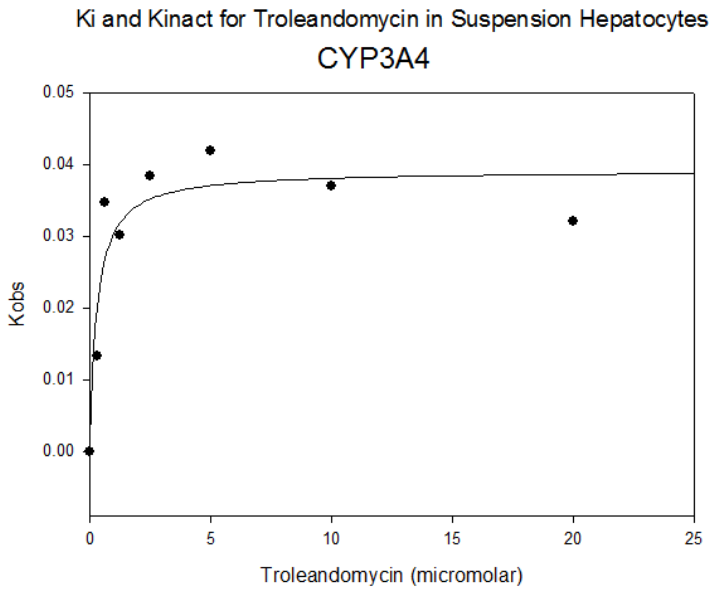

Troleandomycin (CYP3A4)	Observed	Reported (hepatocytes)	Reported (HLMs)
k_{inact}	0.04 min^{-1}	0.05 min^{-1}	0.171 min^{-1}
K_I	0.28 µM	0.4 µM	0.55 µM
k_{inact}/K_I	143 ml/µmol/min	125 ml/µmol/min	311 ml/µmol/min

Figure 5.20

CYP3A4 Time-Dependent Inhibition by Mifepristone in Hepatocyte Suspension With Differing Inhibitor Concentrations

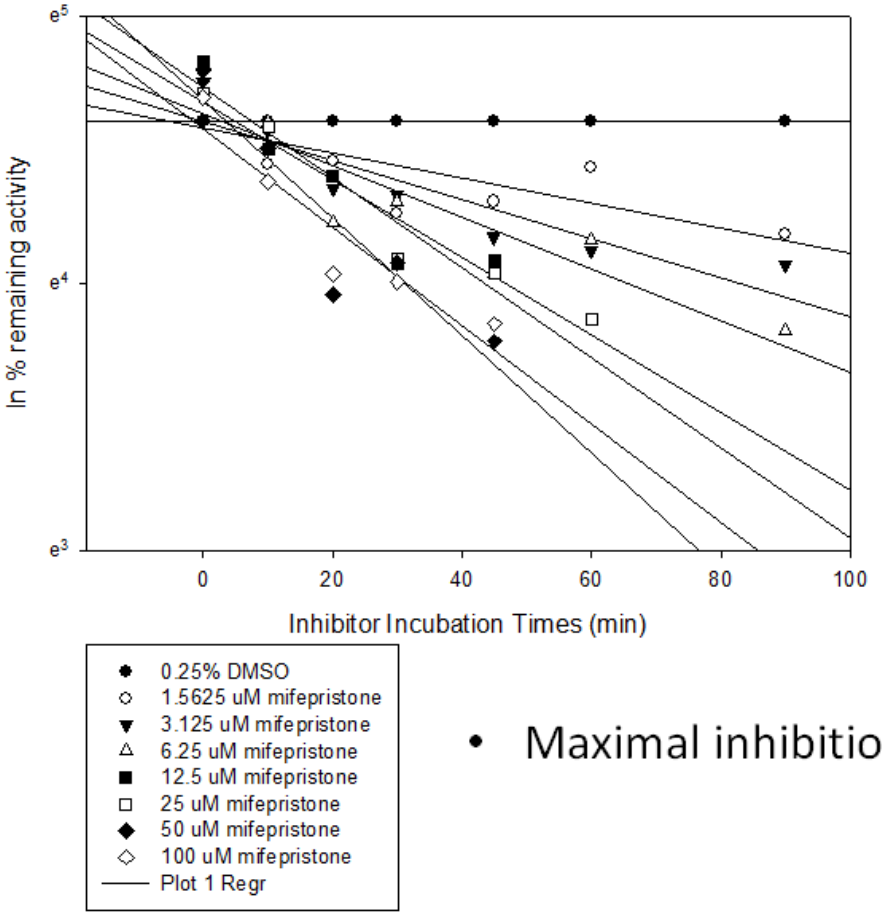

- Maximal inhibition = ~55%

n=1

Figure 5.21

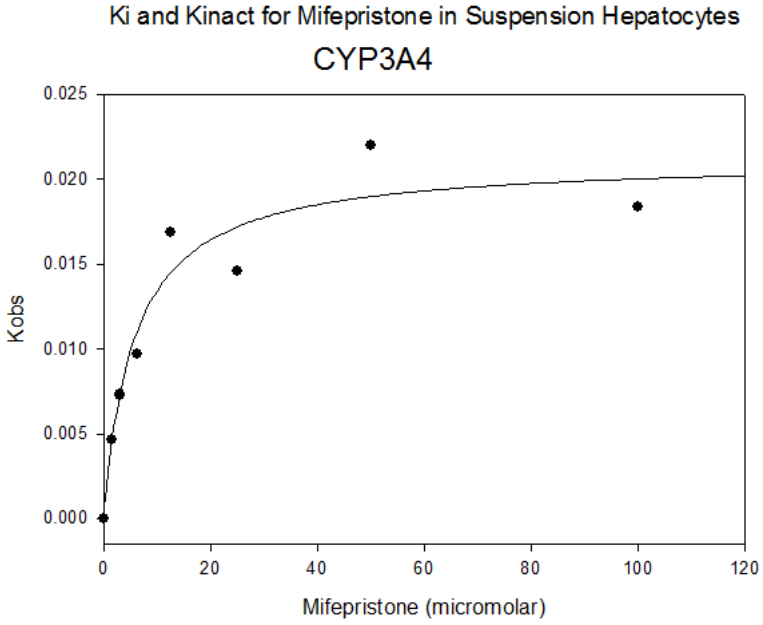

Mifepristone (CYP3A4)	Observed	Reported (hepatocytes)	Reported (HLMs)
k_{inact}	0.02 min^{-1}	0.1 min^{-1}	0.08 min^{-1}
K_I	5.8 µM	23 µM	0.61 µM
k_{inact}/K_I	3.4 ml/µmol/min	4.3 ml/µmol/min	131 ml/µmol/min

Chapter VI

The Effect of High-fat Diet on Intestinal Uridine Diphosphate Glucuronosyltransferase Activity

6.1 Introduction:

High fat diet (HFD) and obesity are known to alter the hepatic activity of oxidative and conjugative drug-metabolizing enzymes. Studies have shown that obesity and diet mediated changes in cytochrome P450s (CYPs) and uridine diphosphate glucuronosyltransferases (UGTs) result in to altered drug clearance.[31,150] Alterations in the expression and activity of CYPs have been reported in both animal models of obesity and in clinical studies in obese humans, while alterations in UGT expression and activity have only been studied in animal models of obesity. The animal models of obesity that are most prevalent are genetic models, which are caused by single point mutations leading to a loss of leptin or loss of leptin receptor activity; which leads animals to overeat and become overweight within weeks after birth. The major concern with studying obesity in models which lack leptin activity is that obesity in humans is rarely caused a loss in leptin activity, and in fact an increase in leptin is characteristic of human obesity.[84]

Diet induced models of obesity are more similar to human obesity than genetic models of obesity, and they lead to clinical symptoms that are also present in human obesity such as insulin resistance, elevated cholesterol, elevated triglycerides, and elevated plasma leptin levels when compared with controls on a standard diet. Diet-induced models of obesity are achieved by allowing normal-weight animals free access to high fat diets (HFDs), which contain similar amounts of fat content contained in modern western diets. Furthermore, animals may be selected for their resistance to developing

obesity or for their lack thereof by testing animals with a high-fat diet (HFD). Differentiation with a HFD to select for obesity resistance or proneness through multiple generations helps to mimic obesity that is seen in humans, in which polygenic obesity is most prevalent. The obesity resistant animal models do not gain significant amounts of weight whether they are fed a LFD or a HFD; while the obesity prone animal models will gain significant amounts of weight when fed a HFD. These animal models can be used to determine if there both are diet-mediated and weight/obesity-mediated changes in drug metabolism.

Alterations in drug metabolism have been extensively studied in hepatic tissue, but extrahepatic metabolism, specifically as it relates to the small intestine, also plays a major role in drug metabolism. There is limited knowledge on the effect of HFD or obesity on small intestinal drug metabolism. HFD and obesity have been shown to mediate many biological changes in the intestine including increased inflammation due to modified expression levels of cytokines and adipokines.[151] We hypothesize that modified levels of cytokines could lead to altered expression and activity of UGTs. Therefore, the aim of this study was to characterize the differences in activity of various intestinal isoforms of UGTs in a diet-induced model of obesity in obesity resistant rats and obesity prone rats.

6.2 Methods:

Sprague-Dawley rats were separated based on susceptibility to diet-induced obesity, with rats that were highly susceptible to weight gain being grouped into the obesity prone (OP) group and the rats with low susceptibility being grouped into the obesity resistant (OR) group. OP and OR rats were then bred within each group over multiple (>30)

generations before being used in the current study.

Whole intestinal tissue samples were isolated from 14 week-old rats (both OR and OP) fed either a standard low fat diet (LFD) or HFD. Pooled intestinal microsomes from these tissue samples (n=3 animals from each group) were isolated using previously described methods.[152] 4-methylumbelliferone (4-MU) was used to probe the general UGT activity while, estradiol 3-O-glucuronidation was used to probe for UGT1a1 activity, and acetaminophen (APAP) was used to probe UGT1a6 and UGT1a7. Incubations were carried out as listed in Table 1 at 37°C and terminated with methanol containing listed internal standards. Intrinsic clearance (CLint) of substrates was calculated by dividing its maximal velocity (V_{max}) by its binding affinity (k_m).

Table 6.1 Incubation conditions

Enzyme	Substrate	Incubation time (min)	Metabolite	Protein conc (mg/ml)	Internal standard	Analytical Method
UGT (general)	4-Methylumbelliferone	10	4-MU glucuronide	0.05	Umbelliferone	HPLC-Fluorescence
UGT 1A1	Estradiol	30	Estradiol 3-O-glucuronide	0.1	Dextromethorphan	HPLC-Fluorescence
UGT1A6	Acetaminophen	30	Acetaminophen -glucuronide	0.1	Caffeine	HPLC-UV

6.3 Results:

The overall intestinal UGT activity (4-MU glucuronidation) in rats was found to be higher in the obese group (Cl_{int} = 0.706 ± 0.02 ml/min/mg) as compared to the lean group (Cl_{int} = 0.113 ± 0.02 ml/min/mg) (p-value < 0.0001). UGT1a1 activity (estradiol 3-O-glucuronidation) in rats was found to be higher in the obese group (Cl_{int} = 41.04 ± 12

µl/min/mg) than the lean group (Cl_{int} = 4.51 ± 0.6 µl/min/mg) (p-value = 0.035). UGT1a6 and UGT1a7 activity (acetaminophen glucuronidation) in the rats was found to be higher in the obese group than the lean group (Cl_{int} = 0.29 ± 0.006 µl/min/mg vs. Cl_{int} = 0.06 ± 0.01 µl/min/mg, p-value = 0.0002).

6.4 Discussion:

The results from our study indicate that there is increased activity in all tested UGTs in the small intestinal microsomes of the rats that were fed a HFD, with a significant increase in UGT activity in rats fed a HFD regardless of being obesity resistant (OR) or obesity prone (OP). This indicates that there is an overall diet effect on glucuronidation enzyme activity. This increase in enzyme activity may be due to increases in the expression of UGTs, as transcriptional regulators of UGTs have endogenous ligands whose levels may be altered with a HFD, which would lead to changes to expression and activity levels of UGTs. Transcriptional regulators of UGT expression include the ligand activated nuclear receptors Farsenoid X receptor (FXR), peroxisome proliferator-activated receptor (PPARα), and nuclear factor (erythroid-derived 2)-like 2 (Nrf2). FXR activation is possibly increased in animals fed a HFD; as unsaturated fatty acids and bile acids are ligands for FXR and a HFD has been shown activate FXR likely due to enhanced enterohepatic flux of bile acids during HFD consumption.[153] Fatty acids are also ligands for PPARα, which may have increased activation due to a HFD increasing fatty acid levels in the blood. For example, Patsouris and others showed that certain CYPs in rats were upregulated due to PPARα activation by lipids from a HFD.[154] A HFD

has been shown to increase oxidative stress and cytokine production in the small intestine, and these increases in oxidative stress due to a HFD also increases Nrf2 activation, which may lead to changes in the expression of UGTs.[151]

The OR rats fed a HFD were not significantly heavier than the OR rats fed a LFD, but still exhibited increased UGT activity, which indicates that the change in UGT activity is diet-mediated and not obesity/weight-mediated. The OR rats also had higher overall clearance when compared to OP rats fed the same diet, which indicates that there may be genetic differences in the expression of UGTs between the two groups. More research must be done in order to determine if the resistance to obesity is correlated with the expression and activity of UGTs and how those two are related. In conclusion, our study shows that there are diet-mediated differences in UGT activity and that there are no weight/obesity-mediated differences. Because the effect of diet and obesity were studied only in a select few UGT isoforms, future studies should include other UGT isoforms in these models of obesity to determine if the increases in UGT activity reported in this study also apply to other isoforms.

Figure 6.1

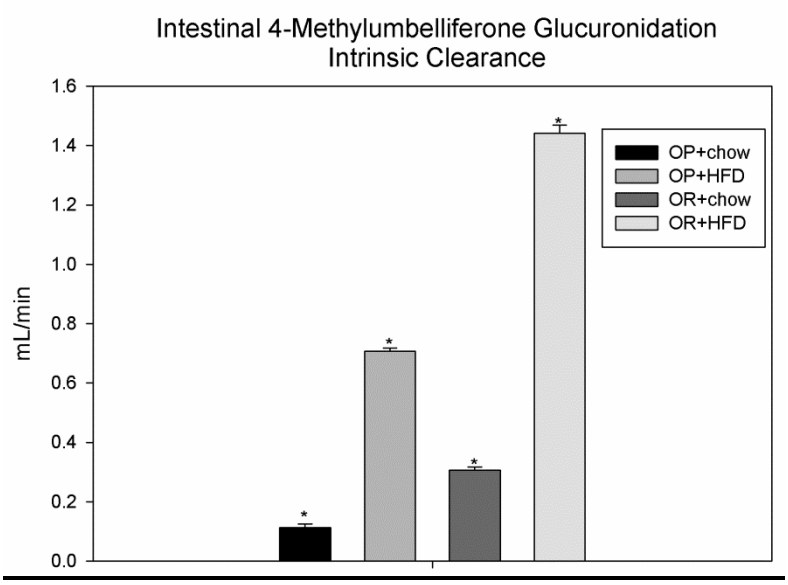

	4-methylumbelliferone		
Status	**Vmax (nmol/min/mg)**	**Km (µM)**	**CLint (mL/min/mg)**
OP	64 ± 2 [a]	582 ± 82 [a]	0.11 ± 0.01 [a]
OP + HFD	240 ± 7 [b]	340 ± 15 [a]	0.71 ± 0.01 [b]
OR	132 ± 6 [c]	433 ± 36 [a]	0.31 ± 0.01 [c]
OR + HFD	454 ± 4 [d]	315 ± 8 [a]	1.44 ± 0.03 [d]

n=3 for each group

Values with different letters in each column indicate a p-value ≤ 0.05, while values with the same letter are not significantly different from each other.

Figure 6.2

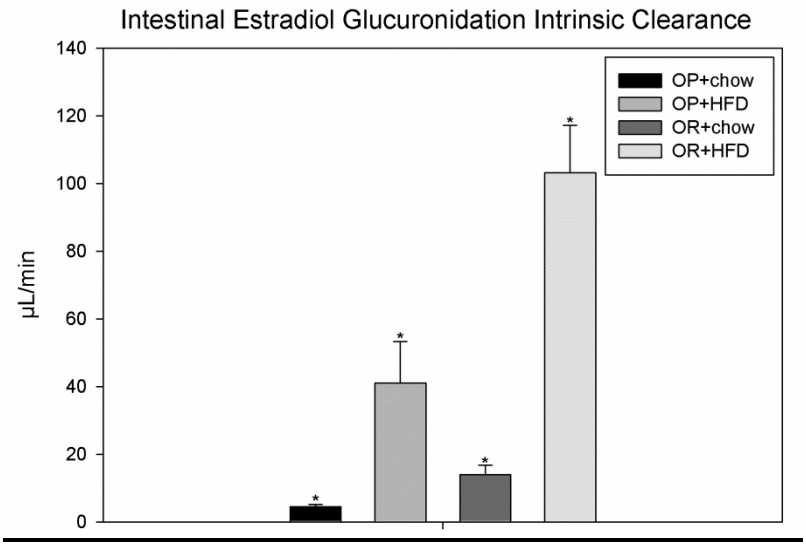

	Estradiol		
Status	**Vmax (nmol/min/mg)**	**Km (µM)**	**CLint (µL/min/mg)**
OP	0.213 ± 0.03 [a]	47 ± 3 [a]	4.5 ± 0.6 [a]
OP + HFD	1.28 ± 0.2 [b]	34 ± 16 [a]	41.0 ± 12 [b]
OR	0.629 ± 0.05 [c]	47 ± 14 [a]	13.9 ± 3 [c]
OR + HFD	10.6 ± 2 [d]	106 ± 40 [a]	103 ± 14 [d]

n=3 for each group

Values with different letters in each column indicate a p-value ≤ 0.05, while values with the same letter are not significantly different from each other.

Figure 6.3

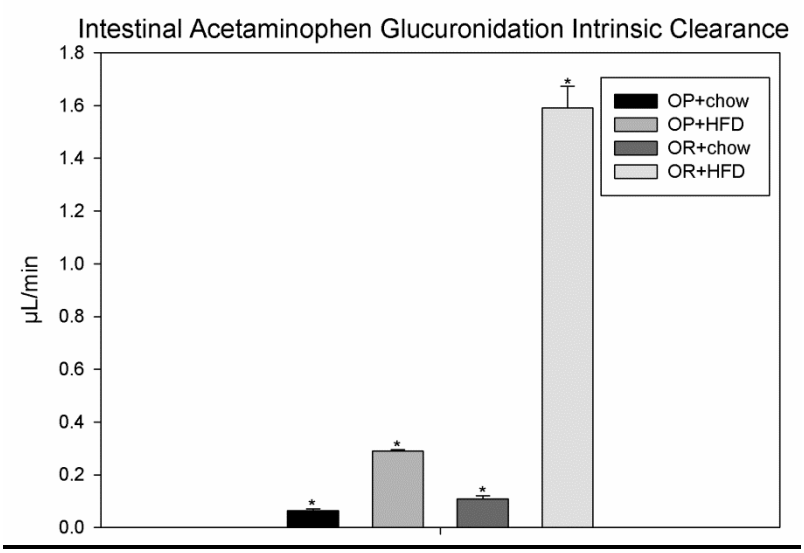

	Acetaminophen		
Status	**Vmax (nmol/min/mg)**	**Km (mM)**	**CLint (µL/min/mg)**
OP	0.072 ± 0.002 [a]	1.2 ± .1 [a]	0.063 ± 0.008 [a]
OP + HFD	2.8 ± 0.1 [b]	9.6 ± 0.5 [b]	0.29 ± 0.004 [b]
OR	0.39 ± 0.02 [c]	3.7 ± 0.5 [c]	0.11 ± 0.01 [c]
OR + HFD	14.5 ± 1 [d]	9.2 ± 1 [b]	1.6 ± 0.08 [d]

n=3 for each group
Values with different letters in each column indicate a p-value ≤ 0.05, while values with the same letter are not significantly different from each other.

Conclusion

The purpose of this thesis was to examine the effect of obesity and high fat diet on cardiovascular risk factors (e.g. xanthine oxidase activity and uric acid formation) and on small intestinal drug metabolism. In chapter II we developed an assay to measure the production of 7-hydroxy-lumazine to serve as more sensitive and accurate measure of plasma xanthine oxidase activity. This lumazine assay was then used to study xanthine oxidase as a risk factor for cardiovascular disease in obese children compared to normal-weight children (chapter III), and this assay was also utilized to study xanthine oxidase activity in obese adolescents before and after weight loss to determine xanthine oxidase's role in mediating changes in blood pressure due to weight loss (chapter IV). In order to study the effects of obesity and high fat diet on small intestinal drug metabolism, UGT activity was probed in a rat model of diet-induced obesity (chapter VI).

Using the lumazine assay that was developed to study the effect of obesity on cardiovascular risk and xanthine oxidase activity, it was discovered that plasma xanthine oxidase activity was increased in obese children. This increase in plasma xanthine oxidase activity was associated with BMI z-score and waist circumference, but was not associated with blood pressure. Therefore, in addition to the production of uric acid by xanthine oxidase, plasma uric acid levels and uric acid excretion was also measured in a follow-up study looking at the effects of weight loss in obese adolescents. Weight loss via meal replacement therapy led to decreases in both uric acid production and excretion, but no significant change in plasma levels. The change in diet in these subjects is hypothesized to be a factor in the decrease in xanthine oxidase activity. Plasma xanthine oxidase activity was also examined in adolescents that lost weight via bariatric surgery.

In the subjects with bariatric surgery, plasma xanthine oxidase activity was not significantly changed. The conflicting changes in xanthine oxidase activity between the weight loss methods may be explained by differing changes in the gut microbiota of the subjects; with the gut microbiota changing to produce less LPS in subjects losing weight via meal replacement therapy, and the gut microbiota changing to produce more LPS in subjects that lost weight via bariatric surgery. The changes in gut microbiota due to dietary fat content may also be responsible for the changes in intestinal UGT activity that is seen in our animal models of obesity. Increases in UGT activity were observed in both obesity resistant and obesity prone rats when they were fed a high fat diet, even though the obesity resistant rats didn't gain a significant amount of weight when fed a high fat diet.

In conclusion, a high fat diet and obesity lead to increases in xanthine oxidase activity and small intestinal UGT activity. The increase in xanthine oxidase activity due to obesity is not enough to predict changes in blood pressure, which makes it a poor measure of cardiovascular risk. The increases in small intestinal UGT activity due to obesity and high fat diet would lead to increased first pass metabolism, and may contribute to certain drugs, that are metabolized by UGTs, having lower efficacy in an obese population. The changes in xanthine oxidase activity and intestinal UGT activity due to obesity may be due to changes to diets and gut microbiota. High fat diets have been shown to alter the gut microbiota and increase plasma LPS levels, and in our animal models it was shown to alter UGT activity even in obesity resistant rats that were not obese. Therefore, a high fat diet and not obesity may be responsible for both the changes

in xanthine oxidase and UGT activities, and future studies on obesity and CVD risk or alterations in drug metabolizing enzymes should focus on monitoring diets and changes to the gut microbiota. Records of dietary fat intake, LPS levels in the plasma/blood, and the composition of the gut microbiota should all be studied in future studies, as these may be the keys to understanding the physiological mechanism of the changes in CVD risk and activity of drug metabolizing enzymes due to obesity and high fat diets.

Bibliography:

1. Ogden CL, Carroll MD, Curtin LR, Lamb MM, Flegal KM. Prevalence of high body mass index in US children and adolescents, 2007-2008. *JAMA*. 2010;303(3):242-249.

2. Centers for Disease Control and Prevention. Children's food environment state indicator report, 2011. . 2011.

3. Youth Risk Behavior Surveillance System. 2009 national YRBS overview. . 2010;http://www.cdc.gov/HealthyYouth/yrbs/pdf/us_physical_trend_yrbs.pdf.

4. U.S. Department of Health and Human Services. 2008 physical activity guidelines for americans. . 2008.

5. Institute of Medicine. Food marketing to children and youth: Threat or opportunity? *National Academies Press*. 2005.

6. Robinson TN. Television viewing and childhood obesity. *Pediatr Clin North Am*. 2001;48(4):1017—25.

7. Zimmerman FJ BJ. Associations of television content type and obesity in children. *Am J public health* 2010;100(2):334—40. *Am J Public Health*. 2010;100(2):334—40.

8. Larson NI, Story MT, Nelson MC. Neighborhood environments: Disparities in access to healthy foods in the U.S. *Am J Prev Med*. 2009;36(1):74-81.

9. Choquet H, Meyre D. Genetics of obesity: What have we learned? *Curr Genomics*. 2011;12(3):169-179.

10. Gerken T, Girard CA, Tung YC, et al. The obesity-associated FTO gene encodes a 2-oxoglutarate-dependent nucleic acid demethylase. *Science*. 2007;318(5855):1469-1472.

11. Frayling TM, Timpson NJ, Weedon MN, et al. A common variant in the FTO gene is associated with body mass index and predisposes to childhood and adult obesity. *Science*. 2007;316(5826):889-894.

12. Dina C, Meyre D, Gallina S, et al. Variation in FTO contributes to childhood obesity and severe adult obesity. *Nat Genet*. 2007;39(6):724-726.

13. Karra E, O'Daly OG, Choudhury AI, et al. A link between FTO, ghrelin, and impaired brain food-cue responsivity. *J Clin Invest*. 2013;123(8):3539-3551.

14. Stutzmann F, Tan K, Vatin V, et al. Prevalence of melanocortin-4 receptor deficiency in europeans and their age-dependent penetrance in multigenerational pedigrees. *Diabetes*. 2008;57(9):2511-2518.

15. Fantuzzi G. Adipose tissue, adipokines, and inflammation. *J Allergy Clin Immunol*. 2005;115(5):911-9; quiz 920.

16. Hansen D, Dendale P, Beelen M, et al. Plasma adipokine and inflammatory marker concentrations are altered in obese, as opposed to non-obese, type 2 diabetes patients. *Eur J Appl Physiol*. 2010;109(3):397-404.

17. Maffei M, Fei H, Lee GH, et al. Increased expression in adipocytes of ob RNA in mice with lesions of the hypothalamus and with mutations at the db locus. *Proc Natl Acad Sci U S A*. 1995;92(15):6957-6960.

18. Chandran M, Phillips SA, Ciaraldi T, Henry RR. Adiponectin: More than just another fat cell hormone? *Diabetes Care*. 2003;26(8):2442-2450.

19. Pannacciulli N, Vettor R, Milan G, et al. Anorexia nervosa is characterized by increased adiponectin plasma levels and reduced nonoxidative glucose metabolism. *J Clin Endocrinol Metab*. 2003;88(4):1748-1752.

20. Kappes A, Loffler G. Influences of ionomycin, dibutyryl-cycloAMP and tumour necrosis factor-alpha on intracellular amount and secretion of apM1 in differentiating primary human preadipocytes. *Horm Metab Res*. 2000;32(11-12):548-554.

21. Masaki T, Chiba S, Tatsukawa H, et al. Adiponectin protects LPS-induced liver injury through modulation of TNF-alpha in KK-ay obese mice. *Hepatology*. 2004;40(1):177-184.

22. Wulster-Radcliffe MC, Ajuwon KM, Wang J, Christian JA, Spurlock ME. Adiponectin differentially regulates cytokines in porcine macrophages. *Biochem Biophys Res Commun*. 2004;316(3):924-929.

23. Verbraecken J, Van de Heyning P, De Backer W, Van Gaal L. Body surface area in normal-weight, overweight, and obese adults. A comparison study. *Metabolism*. 2006;55(4):515-524.

24. Colles SL, Dixon JB, Marks P, Strauss BJ, O'Brien PE. Preoperative weight loss with a very-low-energy diet: Quantitation of changes in liver and abdominal fat by serial imaging. *Am J Clin Nutr*. 2006;84(2):304-311.

25. Vasan RS. Cardiac function and obesity. *Heart*. 2003;89(10):1127-1129.

26. Collis T, Devereux RB, Roman MJ, et al. Relations of stroke volume and cardiac output to body composition: The strong heart study. *Circulation*. 2001;103(6):820-825.

27. Demirovic JA, Pai AB, Pai MP. Estimation of creatinine clearance in morbidly obese patients. *Am J Health Syst Pharm*. 2009;66(7):642-648.

28. Ghobadi C, Johnson TN, Aarabi M, et al. Application of a systems approach to the bottom-up assessment of pharmacokinetics in obese patients: Expected variations in clearance. *Clin Pharmacokinet*. 2011;50(12):809-822.

29. Blouin RA, Kolpek JH, Mann HJ. Influence of obesity on drug disposition. *Clin Pharm*. 1987;6(9):706-714.

30. Messerli FH, Sundgaard-Riise K, Reisin E, Dreslinski G, Dunn FG, Frohlich E. Disparate cardiovascular effects of obesity and arterial hypertension. *Am J Med*. 1983;74(5):808-812.

31. Kotlyar M, Carson SW. Effects of obesity on the cytochrome P450 enzyme system. *Int J Clin Pharmacol Ther*. 1999;37(1):8-19.

32. Chiney MS, Schwarzenberg SJ, Johnson LA. Altered xanthine oxidase and N-acetyltransferase activity in obese children. *Br J Clin Pharmacol*. 2011;72(1):109-115.

33. Ritter JK. Intestinal UGTs as potential modifiers of pharmacokinetics and biological responses to drugs and xenobiotics. *Expert Opin Drug Metab Toxicol*. 2007;3(1):93-107.

34. Dietz WH. Health consequences of obesity in youth: Childhood predictors of adult disease. *Pediatrics*. 1998;101(3 Pt 2):518-525.

35. Freedman DS, Mei Z, Srinivasan SR, Berenson GS, Dietz WH. Cardiovascular risk factors and excess adiposity among overweight children and adolescents: The bogalusa heart study. *J Pediatr*. 2007;150(1):12-17.e2.

36. Han JC, Lawlor DA, Kimm SY. Childhood obesity. *Lancet*. 2010;375(9727):1737-1748.

37. Sutherland ER. Obesity and asthma. *Immunol Allergy Clin North Am*. 2008;28(3):589-602, ix.

38. Schwartz MB, Puhl R. Childhood obesity: A societal problem to solve. *Obes Rev*. 2003;4(1):57-71.

39. Taylor ED, Theim KR, Mirch MC, et al. Orthopedic complications of overweight in children and adolescents. *Pediatrics*. 2006;117(6):2167-2174.

40. Whitlock EP, Williams SB, Gold R, Smith PR, Shipman SA. Screening and interventions for childhood overweight: A summary of evidence for the US preventive services task force. *Pediatrics*. 2005;116(1):e125-44.

41. Freedman DS, Mei Z, Srinivasan SR, Berenson GS, Dietz WH. Cardiovascular risk factors and excess adiposity among overweight children and adolescents: The bogalusa heart study. *J Pediatr*. 2007;150(1):12-17.e2.

42. Saksela M, Lapatto R, Raivio KO. Xanthine oxidoreductase gene expression and enzyme activity in developing human tissues. *Biol Neonate*. 1998;74(4):274-280.

43. Feig DI. Hyperuricemia and hypertension. *Adv Chronic Kidney Dis*. 2012;19(6):377-385.

44. Kahn HA, Medalie JH, Neufeld HN, Riss E, Goldbourt U. The incidence of hypertension and associated factors: The israel ischemic heart disease study. *Am Heart J*. 1972;84(2):171-182.

45. Dyer AR, Liu K, Walsh M, Kiefe C, Jacobs DR,Jr, Bild DE. Ten-year incidence of elevated blood pressure and its predictors: The CARDIA study. coronary artery risk development in (young) adults. *J Hum Hypertens*. 1999;13(1):13-21.

46. Taniguchi Y, Hayashi T, Tsumura K, Endo G, Fujii S, Okada K. Serum uric acid and the risk for hypertension and type 2 diabetes in japanese men: The osaka health survey. *J Hypertens*. 2001;19(7):1209-1215.

47. Torok E, Gyarfas I, Csukas M. Factors associated with stable high blood pressure in adolescents. *J Hypertens Suppl*. 1985;3(3):S389-90.

48. Culleton BF, Larson MG, Kannel WB, Levy D. Serum uric acid and risk for cardiovascular disease and death: The framingham heart study. *Ann Intern Med*. 1999;131(1):7-13.

49. Staessen J. The determinants and prognostic significance of serum uric acid in elderly patients of the european working party on high blood pressure in the elderly trial. *Am J Med*. 1991;90(3A):50S-54S.

50. Stavric B, Johnson WJ, Grice HC. Uric acid nephropathy: An experimental model. *Proc Soc Exp Biol Med*. 1969;130(2):512-516.

51. Mazzali M, Hughes J, Kim YG, et al. Elevated uric acid increases blood pressure in the rat by a novel crystal-independent mechanism. *Hypertension*. 2001;38(5):1101-1106.

52. Mazzali M, Kanellis J, Han L, et al. Hyperuricemia induces a primary renal arteriolopathy in rats by a blood pressure-independent mechanism. *Am J Physiol Renal Physiol*. 2002;282(6):F991-7.

53. BRAY RC, Bray, Boyer PD. 6 molybdenum iron-sulfur flauin hydroxylases and related enzymes. *Enzymes*. 1975;12:299-419.

54. McCord JM, Fridovich I. The reduction of cytochrome c by milk xanthine oxidase. *J Biol Chem*. 1968;243(21):5753-5760.

55. Pritsos CA. Cellular distribution, metabolism and regulation of the xanthine oxidoreductase enzyme system. *Chem Biol Interact*. 2000;129(1-2):195-208.

56. Parks DA, Granger DN. Xanthine oxidase: Biochemistry, distribution and physiology. *Acta Physiol Scand Suppl*. 1986;548:87-99.

57. Kooij A, Schijns M, Frederiks WM, Van Noorden CJ, James J. Distribution of xanthine oxidoreductase activity in human tissues--a histochemical and biochemical study. *Virchows Arch B Cell Pathol Incl Mol Pathol*. 1992;63(1):17-23.

58. Al-Khalidi UA, Chaglassian TH. The species distribution of xanthine oxidase. *Biochem J*. 1965;97(1):318-320.

59. Kooij A, Schiller HJ, Schijns M, Van Noorden CJ, Frederiks WM. Conversion of xanthine dehydrogenase into xanthine oxidase in rat liver and plasma at the onset of reperfusion after ischemia. *Hepatology*. 1994;19(6):1488-1495.

60. Adachi T, Fukushima T, Usami Y, Hirano K. Binding of human xanthine oxidase to sulphated glycosaminoglycans on the endothelial-cell surface. *Biochem J*. 1993;289 (Pt 2)(Pt 2):523-527.

61. Berry CE, Hare JM. Xanthine oxidoreductase and cardiovascular disease: Molecular mechanisms and pathophysiological implications. *J Physiol*. 2004;555(Pt 3):589-606.

62. Hoidal JR, Xu P, Huecksteadt T, Sanders KA, Pfeffer K. Transcriptional regulation of human xanthine dehydrogenase/xanthine oxidase. *Biochem Soc Trans*. 1997;25(3):796-799.

63. Xu P, LaVallee P, Hoidal JR. Repressed expression of the human xanthine oxidoreductase gene. E-box and TATA-like elements restrict ground state transcriptional activity. *J Biol Chem*. 2000;275(8):5918-5926.

64. Schroder K, Vecchione C, Jung O, et al. Xanthine oxidase inhibitor tungsten prevents the development of atherosclerosis in ApoE knockout mice fed a western-type diet. *Free Radic Biol Med*. 2006;41(9):1353-1360.

65. Pfeffer KD, Huecksteadt TP, Hoidal JR. Xanthine dehydrogenase and xanthine oxidase activity and gene expression in renal epithelial cells. cytokine and steroid regulation. *J Immunol*. 1994;153(4):1789-1797.

66. Takeyama N, Shoji Y, Ohashi K, Tanaka T. Role of reactive oxygen intermediates in lipopolysaccharide-mediated hepatic injury in the rat. *J Surg Res*. 1996;60(1):258-262.

67. Kurosaki M, Li Calzi M, Scanziani E, Garattini E, Terao M. Tissue- and cell-specific expression of mouse xanthine oxidoreductase gene in vivo: Regulation by bacterial lipopolysaccharide. *Biochem J*. 1995;306 (Pt 1)(Pt 1):225-234.

68. Terada LS, Piermattei D, Shibao GN, McManaman JL, Wright RM. Hypoxia regulates xanthine dehydrogenase activity at pre- and posttranslational levels. *Arch Biochem Biophys*. 1997;348(1):163-168.

69. Lanzillo JJ, Yu FS, Stevens J, Hassoun PM. Determination of xanthine dehydrogenase mRNA by a reverse transcription-coupled competitive quantitative polymerase chain reaction assay: Regulation in rat endothelial cells by hypoxia and hyperoxia. *Arch Biochem Biophys*. 1996;335(2):377-380.

70. Lin J, Xu P, LaVallee P, Hoidal JR. Identification of proteins binding to E-box/Ku86 sites and function of the tumor suppressor SAFB1 in transcriptional regulation of the human xanthine oxidoreductase gene. *J Biol Chem*. 2008;283(44):29681-29689.

71. Erridge C, Attina T, Spickett CM, Webb DJ. A high-fat meal induces low-grade endotoxemia: Evidence of a novel mechanism of postprandial inflammation. *Am J Clin Nutr*. 2007;86(5):1286-1292.

72. Lakhan SE, Kirchgessner A. Gut microbiota and sirtuins in obesity-related inflammation and bowel dysfunction. *J Transl Med*. 2011;9:202-5876-9-202.

73. Acker T, Fandrey J, Acker H. The good, the bad and the ugly in oxygen-sensing: ROS, cytochromes and prolyl-hydroxylases. *Cardiovasc Res*. 2006;71(2):195-207.

74. Shin HJ, Takeda M, Enomoto A, et al. Interactions of urate transporter URAT1 in human kidney with uricosuric drugs. *Nephrology (Carlton)*. 2011;16(2):156-162.

75. GUTMAN AB, YU TF. Renal function in gout; with a commentary on the renal regulation of urate excretion, and the role of the kidney in the pathogenesis of gout. *Am J Med*. 1957;23(4):600-622.

76. Berkowitz RI, Wadden TA, Gehrman CA, et al. Meal replacements in the treatment of adolescent obesity: A randomized controlled trial. *Obesity (Silver Spring).* 2011;19(6):1193-1199.

77. Astrup A, Caterson I, Zelissen P, et al. Topiramate: Long-term maintenance of weight loss induced by a low-calorie diet in obese subjects. *Obes Res*. 2004;12(10):1658-1669.

78. DuCoin C, Moon RC, Mulatre M, Teixeira AF, Jawad MA. Safety and effectiveness of roux-en-Y gastric bypass in patients between the ages of 17 and 19. *Obes Surg*. 2014.

79. Santry HP, Gillen DL, Lauderdale DS. Trends in bariatric surgical procedures. *JAMA*. 2005;294(15):1909-1917.

80. Longitudinal Assessment of Bariatric Surgery (LABS) Consortium, Flum DR, Belle SH, et al. Perioperative safety in the longitudinal assessment of bariatric surgery. *N Engl J Med*. 2009;361(5):445-454.

81. Sweeney TE, Morton JM. Metabolic surgery: Action via hormonal milieu changes, changes in bile acids or gut microbiota? A summary of the literature. *Best Pract Res Clin Gastroenterol*. 2014;28(4):727-740.

82. David LA, Maurice CF, Carmody RN, et al. Diet rapidly and reproducibly alters the human gut microbiome. *Nature*. 2014;505(7484):559-563.

83. Kanasaki K, Koya D. Biology of obesity: Lessons from animal models of obesity. *J Biomed Biotechnol*. 2011;2011:197636.

84. Hansen D, Dendale P, Beelen M, et al. Plasma adipokine and inflammatory marker concentrations are altered in obese, as opposed to non-obese, type 2 diabetes patients. *Eur J Appl Physiol*. 2010;109(3):397-404.

85. Harrison R. Physiological roles of xanthine oxidoreductase. *Drug Metab Rev*. 2004;36(2):363-375.

86. Sanders SA, Eisenthal R, Harrison R. NADH oxidase activity of human xanthine oxidoreductase--generation of superoxide anion. *Eur J Biochem*. 1997;245(3):541-548.

87. Millar TM, Stevens CR, Benjamin N, Eisenthal R, Harrison R, Blake DR. Xanthine oxidoreductase catalyses the reduction of nitrates and nitrite to nitric oxide under hypoxic conditions. *FEBS Lett*. 1998;427(2):225-228.

88. Baker JF, Krishnan E, Chen L, Schumacher HR. Serum uric acid and cardiovascular disease: Recent developments, and where do they leave us? *Am J Med*. 2005;118(8):816-826.

89. Dawson J, Walters M. Uric acid and xanthine oxidase: Future therapeutic targets in the prevention of cardiovascular disease? *Br J Clin Pharmacol*. 2006;62(6):633-644.

90. Kang DH, Chen W. Uric acid and chronic kidney disease: New understanding of an old problem. *Semin Nephrol*. 2011;31(5):447-452.

91. McCord JM. Oxygen-derived free radicals in postischemic tissue injury. *N Engl J Med*. 1985;312(3):159-163.

92. Maulik N. Redox signaling of angiogenesis. *Antioxid Redox Signal*. 2002;4(5):805-815.

93. Linder N, Rapola J, Raivio KO. Cellular expression of xanthine oxidoreductase protein in normal human tissues. *Lab Invest*. 1999;79(8):967-974.

94. Moriwaki Y, Yamamoto T, Suda M, et al. Purification and immunohistochemical tissue localization of human xanthine oxidase. *Biochim Biophys Acta*. 1993;1164(3):327-330.

95. Wright RM, Vaitaitis GM, Wilson CM, Repine TB, Terada LS, Repine JE. cDNA cloning, characterization, and tissue-specific expression of human xanthine dehydrogenase/xanthine oxidase. *Proc Natl Acad Sci U S A*. 1993;90(22):10690-10694.

96. Chiney MS, Schwarzenberg SJ, Johnson LA. Altered xanthine oxidase and N-acetyltransferase activity in obese children. *Br J Clin Pharmacol*. 2011;72(1):109-115.

97. Djordjevic N, Carrillo JA, Roh HK, et al. Comparison of N-acetyltransferase-2 enzyme genotype-phenotype and xanthine oxidase enzyme activity between swedes and koreans. *J Clin Pharmacol*. 2012;52(10):1527-1534.

98. Partridge CA, Blumenstock FA, Malik AB. Pulmonary microvascular endothelial cells constitutively release xanthine oxidase. *Arch Biochem Biophys*. 1992;294(1):184-187.

99. McCarthy RD, Long CA. Bovine milk intake and xanthine oxidase activity in blood serum. *J Dairy Sci*. 1976;59(6):1059-1062.

100. Mousson B, Desjacques P, Baltassat P. Measurement of xanthine oxidase activity in some human tissues. an optimized method. *Enzyme*. 1983;29(1):32-43.

101. Davis MD, Olson JS, Palmer G. The reaction of xanthine oxidase with lumazine. characterization of the reductive half-reaction. *J Biol Chem*. 1984;259(6):3526-3533.

102. Bergmann F, Levene L, Tamir I, Rahat M. Oxidation of methyl derivatives of pteridin-4-one, lumazine and related pteridines by bovine milk xanthine oxidase. *Biochim Biophys Acta*. 1977;480(1):21-38.

103. Boomsma F, Bhaggoe UM, van der Houwen AM, van den Meiracker AH. Plasma semicarbazide-sensitive amine oxidase in human (patho)physiology. *Biochim Biophys Acta*. 2003;1647(1-2):48-54.

104. Boomsma F, van Dijk J, Bhaggoe UM, Bouhuizen AM, van den Meiracker AH. Variation in semicarbazide-sensitive amine oxidase activity in plasma and tissues of mammals. *Comp Biochem Physiol C Toxicol Pharmacol*. 2000;126(1):69-78.

105. Barr JT, Choughule KV, Nepal S, et al. Why do most human liver cytosol preparations lack xanthine oxidase activity? *Drug Metab Dispos*. 2014;42(4):695-699.

106. Dixon M, Thurlow S. Studies on xanthine oxidase: The dynamics of the oxidase system. *Biochem J*. 1924;18(5):976-988.

107. HOFSTEE BH. On the mechanism of inhibition of xanthine oxidase by the substrate xanthine. *J Biol Chem*. 1955;216(1):235-244.

108. Rajagopalan KV, Handler P. Purification and properties of chicken liver xanthine dehydrogenase. *J Biol Chem*. 1967;242(18):4097-4107.

109. Priest DG, Fisher JR. Substrate activation with a xanthine oxidase reaction. an alternative to dismutation as an explanation in the chicken liver system. *Eur J Biochem*. 1969;10(3):439-444.

110. Tan S, Radi R, Gaudier F, et al. Physiologic levels of uric acid inhibit xanthine oxidase in human plasma. *Pediatr Res*. 1993;34(3):303-307.

111. Ogden CL, Carroll MD, Kit BK, Flegal KM. Prevalence of obesity in the united states, 2009-2010. *NCHS Data Brief*. 2012;(82)(82):1-8.

112. Montezano A, Touyz R. Molecular mechanisms of hypertension--reactive oxygen species and antioxidants: A basic science update for the clinician. *Can J Cardiol*. 2012;28(3):288-295.

113. Paravicini T, Touyz R. NADPH oxidases, reactive oxygen species, and hypertension: Clinical implications and therapeutic possibilities. *Diabetes Care*. 2008;31 Suppl 2:S170-S180.

114. Guthikonda S, Sinkey C, Barenz T, Haynes W. Xanthine oxidase inhibition reverses endothelial dysfunction in heavy smokers. *Circulation*. 2003;107(3):416-421.

115. Butler R, Morris AD, Belch JJ, Hill A, Struthers AD. Allopurinol normalizes endothelial dysfunction in type 2 diabetics with mild hypertension. *Hypertension*. 2000;35(3):746-751.

116. Higgins P, Dawson J, Lees KR, McArthur K, Quinn TJ, Walters MR. Xanthine oxidase inhibition for the treatment of cardiovascular disease: A systematic review and meta-analysis. *Cardiovasc Ther*. 2012;30(4):217-226.

117. Kuczmarski RJ, Ogden CL, Guo SS, et al. 2000 CDC growth charts for the united states: Methods and development. *Vital Health Stat 11*. 2002;(246)(246):1-190.

118. Matthews DR, Hosker JP, Rudenski AS, Naylor BA, Treacher DF, Turner RC. Homeostasis model assessment: Insulin resistance and beta-cell function from fasting plasma glucose and insulin concentrations in man. *Diabetologia*. 1985;28(7):412-419.

119. Kelly A, Wetzsteon R, Kaiser D, Steinberger J, Bank A, Dengel D. Inflammation, insulin, and endothelial function in overweight children and adolescents: The role of exercise. *J Pediatr*. 2004;145(6):731-736.

120. Nyberg G, Ekelund U, Yucel Lindberg TL, Mode R T, Marcus C. Differences in metabolic risk factors between normal weight and overweight children. *International journal of pediatric obesity*. 2011;6(3-4):244-252.

121. Chedid R, Zoghbi F, Halaby G, GannagÃƒÂ©-Yared M. Serum uric acid in relation with the metabolic syndrome components and adiponectin levels in lebanese university students. *J Endocrinol Invest*. 2011;34(7):e153-e157.

122. Tsioufis C, Kyvelou S, Dimitriadis K, et al. The diverse associations of uric acid with low-grade inflammation, adiponectin and arterial stiffness in never-treated hypertensives. *J Hum Hypertens*. 2011;25(9):554-559.

123. Tamba S, Nishizawa H, Funahashi T, et al. Relationship between the serum uric acid level, visceral fat accumulation and serum adiponectin concentration in japanese men. *Internal medicine*. 2008;47(13):1175-1180.

124. Bo S, Gambino R, Durazzo M, et al. Associations between serum uric acid and adipokines, markers of inflammation, and endothelial dysfunction. *J Endocrinol Invest*. 2008;31(6):499-504.

125. Xing L, Remick DG. Mechanisms of oxidant regulation of monocyte chemotactic protein 1 production in human whole blood and isolated mononuclear cells. *Shock*. 2007;28(2):178-185.

126. Codoner-Franch P, Tavarez-Alonso S, Murria-Estal R, Megias-Vericat J, Tortajada-Girbes M, Alonso-Iglesias E. Nitric oxide production is increased in severely obese children and related to markers of oxidative stress and inflammation. *Atherosclerosis*. 2011;215(2):475-480.

127. Chander R, Kapoor NK. High density lipoprotein is a scavenger of superoxide anions. *Biochem Pharmacol*. 1990;40(7):1663-1665.

128. Norris A, Steinberger J, Steffen L, Metzig A, Schwarzenberg S, Kelly A. Circulating oxidized LDL and inflammation in extreme pediatric obesity. *Obesity*. 2011;19(7):1415-1419.

129. Kelly A, Jacobs D, Sinaiko A, Moran A, Steffen L, Steinberger J. Relation of circulating oxidized LDL to obesity and insulin resistance in children. *Pediatric diabetes*. 2010;11(8):552-555.

130. Kato R, Mori C, Kitazato K, et al. Transient increase in plasma oxidized LDL during the progression of atherosclerosis in apolipoprotein E knockout mice. *Arterioscler Thromb Vasc Biol*. 2009;29:33.

131. Tsimikas S, Aikawa M, Miller FJJ, et al. Increased plasma oxidized phospholipid:apolipoprotein B-100 ratio with concomitant depletion of oxidized phospholipids from atherosclerotic lesions after dietary lipid-lowering: A potential biomarker of early atherosclerosis regression. *Arterioscler Thromb Vasc Biol*. 2007;27:175.

132. Ogden CL, Carroll MD, Kit BK, Flegal KM. Prevalence of obesity in the united states, 2009-2010. *NCHS Data Brief*. 2012;(82)(82):1-8.

133. Tam HK, Kelly AS, Metzig AM, Steinberger J, Johnson LA. Xanthine oxidase and cardiovascular risk in obese children. *Child Obes*. 2014;10(2):175-180.

134. Zitsman JL, Inge TH, Reichard KW, Browne AF, Harmon CM, Michalsky MP. Pediatric and adolescent obesity: Management, options for surgery, and outcomes. *J Pediatr Surg*. 2014;49(3):491-494.

135. Lira FS, Rosa JC, Dos Santos RV, et al. Visceral fat decreased by long-term interdisciplinary lifestyle therapy correlated positively with interleukin-6 and tumor necrosis factor-alpha and negatively with adiponectin levels in obese adolescents. *Metabolism*. 2011;60(3):359-365.

136. Feig DI, Soletsky B, Johnson RJ. Effect of allopurinol on blood pressure of adolescents with newly diagnosed essential hypertension: A randomized trial. *JAMA*. 2008;300(8):924-932.

137. Ziccardi P, Nappo F, Giugliano G, et al. Reduction of inflammatory cytokine concentrations and improvement of endothelial functions in obese women after weight loss over one year. *Circulation*. 2002;105(7):804-809.

138. Jung SH, Park HS, Kim KS, et al. Effect of weight loss on some serum cytokines in human obesity: Increase in IL-10 after weight loss. *J Nutr Biochem*. 2008;19(6):371-375.

139. Lira FS, Rosa JC, Pimentel GD, et al. Long-term interdisciplinary therapy reduces endotoxin level and insulin resistance in obese adolescents. *Nutr J*. 2012;11:74-2891-11-74.

140. Ezequiel DG, Costa MB, Chaoubah A, de Paula RB. Weight loss improves renal hemodynamics in patients with metabolic syndrome. *J Bras Nefrol*. 2012;34(1):36-42.

141. Saiki A, Nagayama D, Ohhira M, et al. Effect of weight loss using formula diet on renal function in obese patients with diabetic nephropathy. *Int J Obes (Lond)*. 2005;29(9):1115-1120.

142. Agarwal V, Hans N, Messerli FH. Effect of allopurinol on blood pressure: A systematic review and meta-analysis. *J Clin Hypertens (Greenwich)*. 2013;15(6):435-442.

143. Walsky RL, Bauman JN, Bourcier K, et al. Optimized assays for human UDP-glucuronosyltransferase (UGT) activities: Altered alamethicin concentration and utility to screen for UGT inhibitors. *Drug Metab Dispos*. 2012;40(5):1051-1065.

144. Rowland A, Knights KM, Mackenzie PI, Miners JO. The "albumin effect" and drug glucuronidation: Bovine serum albumin and fatty acid-free human serum albumin enhance the glucuronidation of UDP-glucuronosyltransferase (UGT) 1A9 substrates but not UGT1A1 and UGT1A6 activities. *Drug Metab Dispos*. 2008;36(6):1056-1062.

145. Court MH, Krishnaswamy S, Hao Q, et al. Evaluation of 3'-azido-3'-deoxythymidine, morphine, and codeine as probe substrates for UDP-glucuronosyltransferase 2B7 (UGT2B7) in human liver microsomes: Specificity and influence of the UGT2B7*2 polymorphism. *Drug Metab Dispos*. 2003;31(9):1125-1133.

146. Court MH. Isoform-selective probe substrates for in vitro studies of human UDP-glucuronosyltransferases. *Methods Enzymol*. 2005;400:104-116.

147. Lepine J, Bernard O, Plante M, et al. Specificity and regioselectivity of the conjugation of estradiol, estrone, and their catecholestrogen and methoxyestrogen metabolites by human uridine diphospho-glucuronosyltransferases expressed in endometrium. *J Clin Endocrinol Metab*. 2004;89(10):5222-5232.

148. Uchaipichat V, Mackenzie PI, Elliot DJ, Miners JO. Selectivity of substrate (trifluoperazine) and inhibitor (amitriptyline, androsterone, canrenoic acid, hecogenin, phenylbutazone, quinidine, quinine, and sulfinpyrazone) "probes" for human udp-glucuronosyltransferases. *Drug Metab Dispos*. 2006;34(3):449-456.

149. Uchaipichat V, Mackenzie PI, Guo XH, et al. Human udp-glucuronosyltransferases: Isoform selectivity and kinetics of 4-methylumbelliferone and 1-naphthol glucuronidation, effects of organic solvents, and inhibition by diclofenac and probenecid. *Drug Metab Dispos*. 2004;32(4):413-423.

150. Xu J, Kulkarni SR, Li L, Slitt AL. UDP-glucuronosyltransferase expression in mouse liver is increased in obesity- and fasting-induced steatosis. *Drug Metab Dispos*. 2012;40(2):259-266.

151. Ding S, Chi MM, Scull BP, et al. High-fat diet: Bacteria interactions promote intestinal inflammation which precedes and correlates with obesity and insulin resistance in mouse. *PLoS One*. 2010;5(8):e12191.

152. Bruyere A, Decleves X, Bouzom F, et al. Development of an optimized procedure for the preparation of rat intestinal microsomes: Comparison of hepatic and intestinal microsomal cytochrome P450 enzyme activities in two rat strains. *Xenobiotica*. 2009;39(1):22-32.

153. Cyphert HA, Ge X, Kohan AB, Salati LM, Zhang Y, Hillgartner FB. Activation of the farnesoid X receptor induces hepatic expression and secretion of fibroblast growth factor 21. *J Biol Chem*. 2012;287(30):25123-25138.

154. Patsouris D, Reddy JK, Muller M, Kersten S. Peroxisome proliferator-activated receptor alpha mediates the effects of high-fat diet on hepatic gene expression. *Endocrinology*. 2006;147(3):1508-1516.